UNIVERSITÀ DEGLI STUDI DI TRIESTE

XXIX CICLO DEL DOTTORATO DI RICERCA IN
BIOMEDICINA MOLECOLARE

Cathelicidin host defence peptides in cetartiodactyls – identification and characterization of novel members and modification for exploitation as anti-infective agents

Settore scientifico-disciplinare: **BIO/10**

DOTTORANDO
STEFANO GAMBATO

COORDINATORE
PROF. GERMANA MERONI

SUPERVISORE DI TESI
PROF. ALESSANDRO TOSSI

ANNO ACCADEMICO 2016/2017

Università degli Studi di Trieste

XXIX CICLO DEL DOTTORATO DI RICERCA IN
BIOMEDICINA MOLECOLARE

Cathelicidin host defence peptides in cetartiodactyls – identification and characterization of novel members and modification for exploitation as anti-infective agents

Ph.D. student
STEFANO GAMBATO

Ph.D. Program Coordinator
Prof. **GERMANA MERONI**

Thesis Supervisor
Prof. **ALESSANDRO TOSSI**

ANNO ACCADEMICO 2016/2017

Ph.D THESIS SUPERVISOR	Prof. Alessandro Tossi University of Trieste, Department of Life Sciences Via Giorgieri, 1 - 34127 Trieste, Italy atossi@units.it
EXTERNAL ADVISOR	Prof. Olga Shamova Institute for Experimental medicine RAMS Department of General Pathology and Pathophysiology 19736 St. Petersburg, Russia oshamova@yandex.ru
OPPONENT	Prof. Barbara Skerlavaj University of Udine, Department of Medical Area Via Palladio 8 - 33100 Udine, Italy barbara.skerlavaj@uniud.it
Ph.D COURSE CORDINATOR	Prof. Germana Meroni University of Trieste, Department of Life Sciences Via Giorgieri, 1 - 34127 Trieste, Italy gmeroni@units.it

TABLE OF CONTENTS

Synopsis 6

List of abbreviations 8

1. INTRODUCTION 10

1.1 Antimicrobial peptides (AMPs) and innate immunity 11

1.2 AMPs - structure and mode of action 13

1.3 The cathelicidins family of vertebrate AMPs 17

1.4 α-helical AMPs 19

1.5 PR-AMPs - Proline-rich Antimicrobial Peptides 20

1.5.1 PR-AMPs and intracellular mechanisms of action 22

1.5.2 The bovine Pro-rich peptide Bac7 - structural and functional characteristics 23

1.5.3 The *E. coli* inner membrane protein SbmA 26

1.6 Expression of cathelicidin-related AMPs in the order of *Cetartiodactyla* 28

1.6.1 AMPs in the dolphin *Tursiops truncatus* 30

1.7 Use of AMPs as anti-infective agents 31

2. BOTTLENOSE DOLPHIN CATHELICIDINS 34

2.1 AIMS of the STUDY 35

2.2 MATERIALS and METHODS 37

2.2.1 Identification of *Tursiops truncatus* cathelicidin-derived AMPs 37

2.2.2 Peptide synthesis and purification 39

2.2.3 Folding of TUR4 42

2.2.4 BODIPY labelling of peptides 43

2.2.5 Antimicrobial activity assays 43

2.2.6 Bacterial strains 44

2.2.7 Minimum inhibitory concentration (MIC) 46

2.2.8 Inhibition of bacterial growth 46

2.2.9 Peptide internalization into bacterial cells 47

2.2.10 Permeabilization of bacterial membranes 47

2.2.11 Cytotoxicity assays 48

2.3 RESULTS and DISCUSSION 50

2.3.1 Identification of *Tursiops truncatus* cathelicidins 50

2.3.2 *Tursiops truncatus* cathelicidins selected for further characterization 55

2.3.3 Peptide synthesis and preparation 57

2.3.4 Peptide quantification 61

2.3.5 Antimicrobial activity: the bacteriostatic activity 62

2.3.6 Antimicrobial activity of TUR peptides against aquatic and terrestrial bacteria 66

2.3.7 Effect of TUR6 peptides on bacterial growth kinetics 69

2.3.8 Bacterial Growth kinetics of TUR1 orthologues 73

2.3.9 Cellular uptake of fluorescently labelled PR-AMPs 77

2.3.10 Flow cytometric studies of bacterial membrane permeabilization 78

2.3.11 Preliminary evaluation of cytotoxic activity on host cells 80

2.4 CONCLUSIONS 82

3. PRO-RICH PEPTIDES AS VEHICLES FOR ANTIBIOTIC CARGO 85

3.1 AIMS of the STUDY 86

3.2 MATERIALS and METHODS 89

3.2.1 Synthesis of $(Boc)_5$Tobramycin (Boc-T-OH) 89

3.2.2 Synthesis of $(Boc)_5$Tobramycin-Hemisuccinate (Boc-T-hS) 89

3.2.3 Synthesis of Tobramycin(Hemisuccinate)-Cys conjugate (T-hS-Cys) 90

3.2.4 Synthesis of Tobramycin-Cys-Thiopyridine (T-hS-Cys-TPy) 92

3.2.5 Synthesis of Bac7(1-35)[Cys^{36}] and Bac7(1-15)[Cys^{16}] 93

3.2.6 Bac7(1-35)[Cys^{36}] alkylation with iodoacetamide 93

3.2.7 Synthesis of Tobramycin-Bac7(1-35) and Tobramycin-Bac7(1-15) 94

3.2.8 Synthesis of $(Boc)_5$Tobramycin-OTibs (Boc-T-OTibs) 95

3.2.9 Synthesis of $(Boc)_5$Tobramycin-dioxaoctanethiol (Boc-T-DOT) 96

3.2.10 Synthesis of $(Boc)_5$Tobramycin-dioxaoctanethiol-thiopyridine (Boc-T-DOTTPy) 97

3.2.11 Antimicrobial activity assays 97

3.2.12 Bacterial strains 98

3.3 RESULTS and DISCUSSION 100

3.3.1 Purity check of the starting tobramycin compound 100

3.3.2 Synthesis of $(Boc)_5$-tobramycin (Boc-T) 101

3.3.3 Synthesis of $(Boc)_5$Tobramycin-Hemisuccinate (Boc-T-HS) 103

3.3.4 Synthesis of Tobramycin(Hemisuccinate)-Cys (T-HS-Cys) 104

3.3.5 Synthesis of Tobramycin-Cys-Thiopyridine (T-hS-Cys-TPy) 105

3.3.6 Synthesis of Bac7(1-35)[Cys^{36}] and Bac7(1-15)[Cys^{16}] 106

3.3.7 Synthesis of Tobramycin-Bac7(1-35) and Tobramycin-Bac7(1-15) 109

3.3.8 Overall reaction analysis 111

3.3.9 Synthesis of $(Boc)_5$Tobramycin-OTibs (Boc-T-OTibs) 112

3.3.10 Synthesis of $(Boc)_5$Tobramycin-dioxaoctanethiol (Boc-T-DOT) 113

3.3.11 Antibiotic/peptide Heterodimer and Peptide carrier quantification 115

3.3.12 Synergy assays (MIC checkerboard) 115

3.3.13 Activity of T-Bac7(n) against *E.coli* strains 116

3.3.14 Bacterial Growth kinetics 119

3.3.15 Investigating the potential of the Tobramycin/PR-AMP conjugate against other bacterial strains 120

3.4 CONCLUSIONS 123

4. REFERENCES 125

SYNOPSIS

Cathelicidins are a family of innate immunity effectors present in most vertebrates. Cathelicidin-derived antimicrobial peptides play an essential role in host defence, with a direct antimicrobial action as part of the innate immune responses and the capacity to modulate cellular immunity, affecting both innate and adaptive responses. Some can also have protective roles connected with wound healing, angiogenesis or sepsis. Cathelicidins are characterized by a conserved pro-region, known as 'cathelin-like' domain, carrying a highly variable, C-terminal antimicrobial domain. Many mammalian species express only one cathelicidin, but artiodactyles are known to express up to a dozen, bearing structurally and functionally very diverse AMPs. These including small disulfide-stabilized cyclic peptides, extended linear peptides rich in specific residues (e.g. proline, arginine, phenylalanine, tryptophan) and helical peptides of different sizes. Cetaceans are phylogenetic with artiodactyls, so are also expected to express this wide repertoire of cathelicidin-derived AMPs, whose functional characteristics may however have been shaped by the particular pathogenic microbiota they face in their aquatic lifestyle. With the known artiodactyl peptides, these might provide interesting leads for biomedical application.

My Ph.D. followed to two parallel lines of research:

i) the study of cathelicidin AMPs identified in the dolphin *Tursiops truncatus* (bottlenose dolphin), identified by searching genomic databases, to define their antimicrobial activities and obtain information on the modes-of-action, using different types of functional assays. These studies were carried out in parallel with selected orthologues from other artiodactyls, such as cow, sheep or pig, to screen for differences among them, and revealed both convergences and some interesting differences, especially relating to a proline-rich (PR-AMP) and an α-helical one. These studies established a potent antimicrobial activity for the helical peptide, with a remarkable capacity too inhibit bacterial growth also at sub-lethal concentrations. The PR-AMP instead showed an increased internalization capacity, due to its apparent efficient use of alternative transporters. These data provided interesting insights into specific aspects of Cetaceans cathelicidins in relation to those of other mammals, and lay the groundwork for the possible development of novel antimicrobial agents.

ii) the possible application of the bovine cathelicidin-derived PR-AMP Bac7(1-35) as a vehicle for delivering antibiotic cargo into susceptible bacterial cells. This peptide acts intracellularly, entering cells using specific transport systems. The aim was to conjugate it to

the antibiotic tobramycin and expand its capacity to penetrate into Gram-negative pathogens, possibly overcoming resistance mechanisms. I began to develop synthetic strategies for modifying the antibiotic and then linking it to the peptide vehicle. Functional assays showed that one type of construct had a broader spectrum of activity than the individual components, and in some cases was active against resistant strains. This new strategy may potentially be applied to other types or classes of currently available antibiotics, as long as they can be modified for conjugation without affecting activity.

LIST of ABBREVIATIONS

AMPD - antimicrobial peptide domain

AMPs - antimicrobial peptides

Boc - tert-butyloxycarbonyl

BODIPY-FL - N-(2-aminoethyl)maleimide

CFU - colony-forming units

CLD - cathelin-like domain

DCM - dichloromethane

DIPEA-N,N-diisopropylethylamine

DMAP - 4-dimethylaminopyridine

DMF - dimethylformamide

DMSO - dimethyl sulfoxide

DODT - 3,6-dioxa-1,8-octane-dihiol / 2,2′-(ethylenedioxy)diethanethiol

EDTA - 2,2',2",2'"-(ethane-1,2-diyldinitrilo)tetraacetic acid

ESI-MS - electrospray ionization mass spectrometry

EST - expressed sequence tag

FIC - fractional inhibitory concentration

Fmoc - fluorenylmethyloxycarbonyl

HDPs - host-defence peptides

IFN - interferon

LPS - lipopolysaccharide

LTA - lipoteichoic acid

MeOH - methanol

MDR - multidrug-resistant

MFI - mean fluorescence intensity

MH - Mueller-Hinton (microbiological medium)

MIC - minimal inhibitory concentration

MRSA - methicillin-resistant Staphylococcus aureus

MTT - 3-(4,5-dimethylthiazol-2-yl)-2,5-diphenyltetrazolium bromide

MW - molecular weight

NMP - N-methyl-2-pyrrolidone

OD - optical density

PAβN - phenylalanine-arginine β-naphthylamide

PAMPs - pathogen-associated molecular patterns

PBS – phosphate-buffered saline

PI - propidium iodide

PR-AMPs - proline-rich antimicrobial peptides

PRRs - pattern recognition receptors

PRSP - penicillin-resistant Streptococcus pneumoniae

PyBOP - benzotriazol-1-yl-oxytripyrrolidinophosphonium hexafluorophosphate

RND - resistance nodulation division

RP-HPLC - reverse phase high-performance liquid chromatography

SAR - structure–activity relationship

TB - trypan blue

TBME - tert-butyl methyl ether

TFA - trifluoroacetic acid

TIPS - tri-isopropylsilane

TLR - toll-like receptor

TPSCl - 2,4,6-triisopropylbenzenesulfonyl chloride

TRP - thyptophane

TSB - tryptic soy broth

WGS - whole genome sequence

VREF - vancomycin-resistant Enterococcus faecium

Chapter 1: Introduction

1. INTRODUCTION

1.1 Antimicrobial peptides (AMPs) and innate immunity

Some basic defence mechanisms that evolved in ancient eukaryotes still act today in their modern descendants, such as plant and invertebrate animals, including phagocytosis, host defence peptides (e.g. defensins) and the complement system. In vertebrates, the immune system shows a more complex organization, based on the two different systems of innate (or natural) immunity, based on these ancient mechanisms, and adaptive (or acquired) immunity.

The innate response is usually triggered when microorganisms are identified by 'pattern recognition receptors' (PRRs) expressed on the surface of immune cells, which are able to recognize specific components that are conserved among broad groups of microbes ('pathogen related molecular patterns' or PRAMPs) (Medzhitov, 2007), or when damaged, injured or stressed cells send out alarm signals (Matzinger, 2002). This type of response, which is the dominant host defence system in non-vertebrates, is mediated by both humoral and a cellular components. The cellular component of the innate immune system is represented by the so-called 'innate leukocytes' that includes phagocytes (macrophages, neutrophils and dendritic cells), mast cells, eosinophils, basophils and natural killer cells. These cells attack and engulf microorganism and, by releasing signal molecules, also mediate the activation of adaptive immune responses (Rus et al., 2005).

The humoral component of the innate response represents a first line of defence deployed to protect the organism continuously from infection by pathogens, and to keep commensal microorganisms under control. Exogenous molecules such as bacterial DNA, lipopolysaccharide (LPS) or peptidoglycan and other bacterial cell wall components (i.e. PRAMPs) activate PRRs such as the 'Toll-like' receptors (TLR). These transmembrane proteins are widely expressed in host immune cells like monocytes, macrophages and dendritic cells, as well as in epithelial cells, endothelial cells and fibroblasts (Janeway, 2001). They trigger two types of responses: *i)* production of pro-inflammatory cytokines and *ii)* release of antimicrobial (host defence) peptides, from specific cells. Both types of mechanism contribute to the overall antimicrobial and inflammatory response by the affected organism (Janeway and Medzhitov, 2002).

Host defence peptides (HDPs), often simply called 'antimicrobial peptides' (AMPs), are generally small, and are expressed in skin keratinocytes and mucosal epithelial cells, as well

as being secreted by circulating phagocytes. They represent an important defensive interface between microbes and the host, and their production, whether constitutive or induced by the engagement of TLRs, serves to limit the viability or growth of bacteria at the site of infection. AMPs are considered to be amongst the most ancient effector molecules of the defence system of microorganisms, plants and animals; and were discovered more than 30 years ago, in insect haemolymph, on the skin mucosa from frogs and in the granules of mammalian neutrophils. Several thousands of different antimicrobial peptides have since been reported in many species (effectively all species in which they have been searched for) and they have been isolated from numerous different tissues and organs (Mangoni, 2011).

AMPs have been found to display a broad spectrum of *in vitro* antimicrobial activity, being variously active against bacteria, fungi, parasites and viruses. This cidal capacity is most often, one could even say 'generally', due to their ability to interact with the microbial cell membrane; this includes principally the lipid bilayer but also other cell wall components and/or membrane bound protein machinery. The main result is irreparable damage to the barrier properties of the membrane, although inactivation of metabolic processes and further interaction with internal targets can also contribute to microbial killing. Moreover, many AMPs play a further antimicrobial role by modulating other types of immune responses. They can act as signal molecules, directly helping to recruit immune cells to the site of infection, or inducing the expression of chemokines, cytokines, and IFN-α and indirectly promoting the recruitment of effector cells such as neutrophils, monocytes, macrophages, immature dendritic cells and T cells (Hancock and Diamond, 2000), (Lai and Gallo, 2009). It is for this reason that vertebrate AMPs are referred to also as host defence peptides (HDP), as they serve to link innate and adaptive immunity and promote a concerted response. HDPs can therefor contribute to the resolution of inflammation and promote healing in different scenarios, as schematized in **Figure 1.1**. They can *i)* directly inactivate invading microorganisms; *ii)* they are able to sequester bacterial components such as LPS or LTA and thereby inhibit sepsis, and *iii)* they can aid in wound healing and angiogenesis by stimulating epithelial and endothelial cell growth (Cederlund et al., 2011).

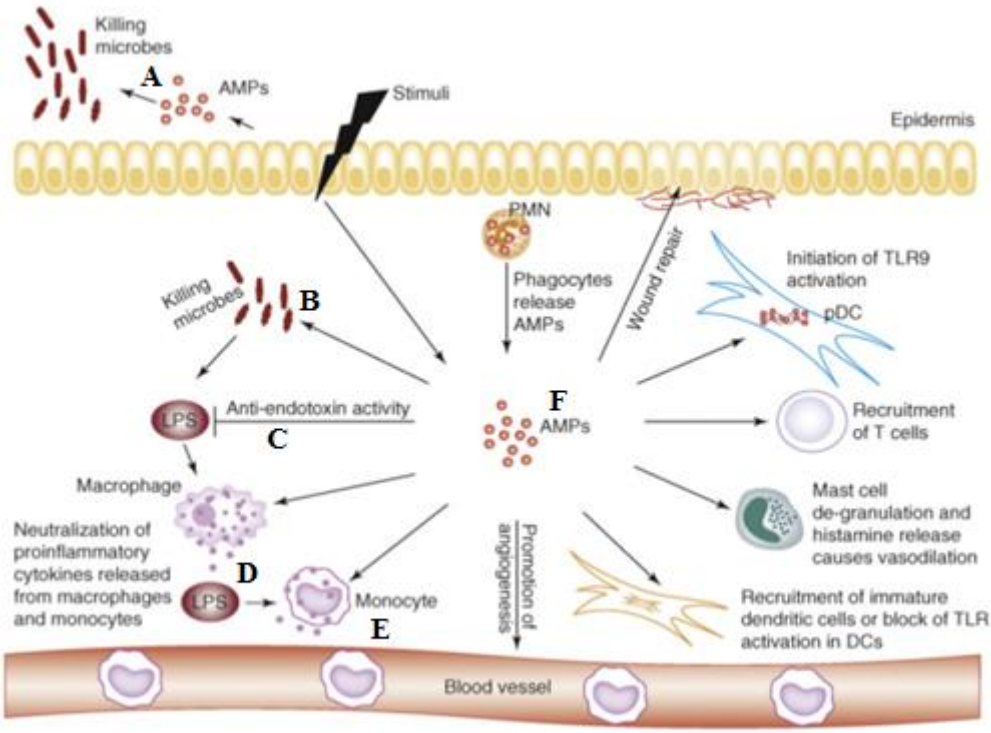

Figure 1.1. Multiple roles of AMPs in host defence. Host defence peptides can be released on the surface of barrier epithelia, helping to prevent infection (A). They are released in internal body fluids where they help contain invading pathogens and control the microbial biota (B). By interaction with bacterial components such as LPS (C) or with proinflammatory cytokines (D) they can inhibit sepsis. By stimulating the growth of different types of cells (E) they can promote wound healing and angiogenesis. By interacting with cellular components of innate or adaptive immunity, they can promote other defensive processes (F). Taken from (Lai and Gallo, 2009).

1.2 AMPs - structure and mode of action

AMPs from different species, and even within the same organism, can differ markedly in size, amino acid sequence, structure and biological functions. Nevertheless they have some common features, as they are generally relatively small (usually between 12-50 residues), cationic, amphipathic molecules with multiple cationic residues and are often stored in cytoplasmic granules of phagocytes as inactive pro-forms. In mammalian species these typically consist of an N-terminal signal region, a pro-segment which may serve to inhibit the mature peptides' activity until it is required, and a C-terminal antimicrobial peptide that becomes active after proteolytic release from the pro-region (Bals, 2000). The expression of functional AMPs can therefore depend on the presence and/or co-release of appropriate proteases. AMPs can also be constitutively released, but these are rarer, and their presence is

in any case influenced by age and sexual maturation. The expression and/or release of AMPs increases in case of injury or infection, and this often involves signalling cascades through pattern-recognition receptors such as TLRs, as indicated above, or induction by specific cytokines (Lai and Gallo, 2009).

As AMPs are so structurally highly variable (see **Figure 1.2**), they are rather difficult to categorize, but they are generally divided into to four broad classes based on their amino acid composition and/or conformational characteristics:

- The most abundant and widespread group is likely the linear, α-helical AMPs. These normally do not have a well-defined structure in aqueous solution, before coming into contact with microbial membranes, to which they are attracted, as these tend to be anionic. They adopt the amphipathic helical conformation only when they interact with the membrane, and this allows their insertion into the lipid bilayer. This type of AMP is often present in invertebrate animals (Hancock et al., 2006), for example the cecropins in *Hyalophora cecropia* moth (Steiner et al., 2009) or melittin in the honeybee (Dufourcq and Faucon, 1977), as well as in vertebrates, like pleurocidin from the winter flounder (Cole et al., 1997), magainins from Xenopus frogs (Zasloff, 1987), and cathelicidins from snakes (Wang et al., 2008), birds (Cheng et al., 2015), cetartiodactyla [myeloid antimicrobial peptides such as bovine BMAPs, (Skerlavaj et al., 1996), porcine PMAPs, (Storici et al., 1994) and ovine SMAP-29, (Skerlavaj et al., 1999)], and the CAP18-related peptides found in all placental mammals (Xhindoli et al., 2016), such as rabbit CAP-18 (Larrick et al., 1993) and human LL-37 (Agerberth et al., 1995).

- The second group of AMPS comprises cationic peptides rich in specific amino acid residues, such as proline, arginine, tryptophan or histidine etc. These are usually linear peptides with extended, not necessarily helical, conformations. The best known examples are *a)* proline-rich AMPs (PR-AMPs) such as apidaecin and abaecin from honeybees (Casteels et al., 1990), drosocin from Drosophila (Bulet et al., 1993), and bactenecins from cows, sheep and goats (e.g. Bac7 and Bac5), (Gennaro et al., 1989); (Shamova et al., 1999) or PR-39 and prophenins from pigs (Agerberth et al., 1991) (Harwig et al., 1995); *b)* histidine-rich salivary histatins (Kavanagh and Dowd, 2004) found in human and other primates, *c)* the tryptophan-rich indolicidin from cattle

(Selsted et al., 1992) and *d)* serine/glycine-rich cathelicidins in some fish species (Scocchi et al., 2009), (D'Este et al., 2016). Interestingly, several of these peptides (e.g. vertebrate Pro-rich, Trp-rich and Ser/Gly-rich peptides all belong to the cathelicidin family (Tossi et al., 2017).

- The third group of AMPs, which is large and widespread, includes cationic peptides that contain cysteine residues and form loops or β-hairpin structures, stabilized by one or two disulphide bonds. Examples of the first type are the anuran brevinins (Morikawa et al., 1992), while examples of the second are bovid dodecapeptide (Romeo et al., 1988a), porcine protegrins (Kokryakov et al., 1993) or tachyplesins from horseshoe crab (Nakamura et al., 1988).

- The last group of AMPs is formed by small but well-defined β-sheet structures stabilized by three or more disulfide bridges. One very broad class of such peptides are the fungal, plant, invertebrate and vertebrate defensins (Lehrer, 2007) (Zhu, 2008) (Antcheva et al., 2009).

Antimicrobial peptides having such different sequences and structures also tend to have different target sites and/or mechanisms of action. Nevertheless, they often show similar modes of action in the initial steps leading to microbial inactivation. As they are almost always cationic molecules, this includes electrostatic interaction with negatively charged components of microbial surfaces, such as for example the anionic phospholipids of bacterial cytoplasmic membranes, the phosphate groups on Gram-negative outer membrane lipopolysaccharide (LPS) or the teichoic acids of Gram-positive bacterial peptidoglycan (Brogden, 2005). During the subsequent steps, the peptides can show a multimodal mechanism of action. In most cases, they act to disrupt membrane integrity, leading to cellular inactivation. In less common cases, they cross the membrane using different mechanisms that do not necessarily require membrane permeabilization, and target intracellular components, thus blocking essential metabolic processes (Mookherjee and Hancock, 2007).

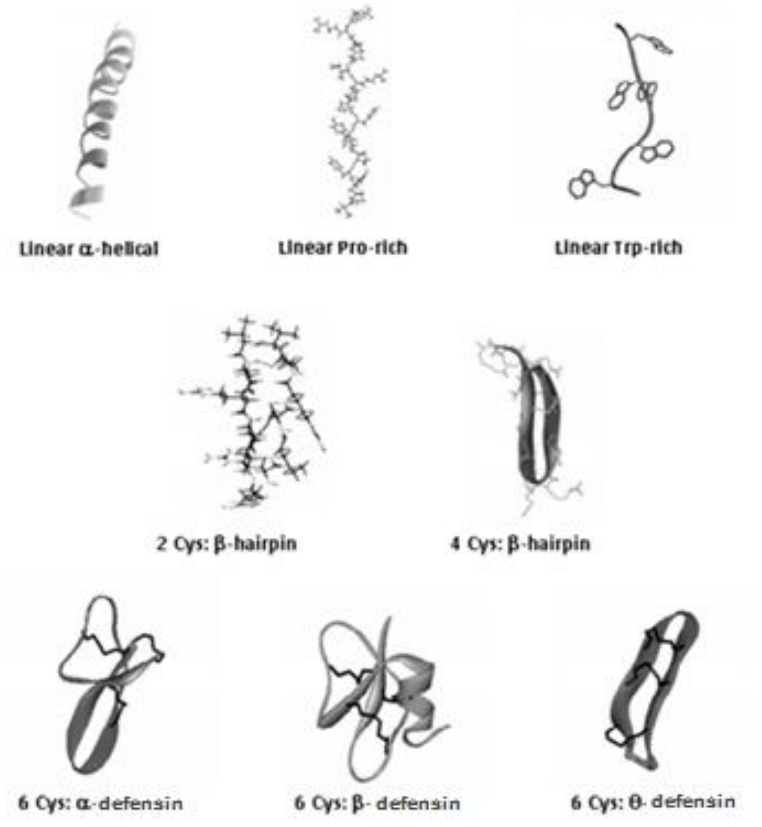

Figure 1.2. Common secondary structures of HDPs.
Adapted from Tossi & Sandri 2000.

With respect to the membranolytic activity, it was early proposed that AMPs could form "barrel-stave" pores, but this was not usually the case. The two principal mechanisms that are currently proposed, on the basis of the positioning of peptide relative to the membrane surface are the "carpet model" and "toroidal-pore model" (Yang et al., 2001), (Qian et al., 2008), (Fernandez et al., 2012)

The toroidal-pore model, which was initially developed to explain the mode of action of helical AMPs, proposes that these adsorb onto the membrane with their axes parallel to its surface, then forming a bundle that inserts into bilayer and induces the monolayers to continuously bend through the pore, meeting each other (Yang et al., 2001). Because of this 'cavitation', phospholipids remain intercalated among the peptides forming the pore, and the resulting depolarization and leakage of the cytoplasmic components may be a principal cause of cell death (Brogden, 2005).

According to the 'carpet model', the AMP molecules always remain positioned parallel to the membrane surface and cover it in a disordered manner. At a threshold concentration the membrane integrity is affected in a detergent-like manner, leading to cell lysis (Oren and Shai, 1998).

The term "barrel-stave" derives from the perpendicular structure that amphipathic peptides form when they orient themselves orthogonally to the membrane surface, joining to form a barrel-like structure. The hydrophobic side of peptides interacts with the lipid bilayer, while the hydrophilic side lines the central aqueous lumen, like in a classical protein pore. This requires both a certain flexibility and constraints on the size of the hydrophobic and hydrophilic faces of the helical structure (Giangaspero et al., 2001), (Christensen et al., 1988).

Despite many years of intensive studies, the exact mechanism of membrane perturbation is still unclear. In any case, lipid scrambling in the bilayer would alter the membrane stability and membrane-protein functions, and formation of pores, channels or less defined lesions would cause a leakage of essential cytoplasmic contents and membrane depolarization. Furthermore, once AMPs arrive at the membrane surface, or penetrate into the intracellular space, they can affect critical targets and for instance induce degradation of the cell wall by induction of hydrolases or inhibiting cell-wall synthesis apparatus, or interfere internally with nucleic-acid and protein synthesis or metabolic enzymatic activity, ultimately leading to microbial cell death (Zasloff, 2002), (Choi et al., 2012), (Brogden, 2005), (Hale and Hancock, 2007).

In the following sections I will concentrate on the cathelicidin family of host defence peptides, and two specific structural types, the α-helical AMPs and PR-AMPs (proline-rich peptides), as these are most pertinent to the peptides described in my thesis.

1.3 The cathelicidins family of vertebrate AMPs

The two main AMP families in mammals, and in many other vertebrates, are the defensins and cathelicidins. Defensins are cationic, non-glycosylated peptides with a molecular mass of 3.5 - 4.5 kDa, containing six conserved cysteine residues that form three defined intramolecular disulphide bonds (Lehrer, 2007), (Fellermann and Stange, 2001). On the basis of the position of the cysteine residues, their connectivity, and the resulting structure, the

defensins are classified into α-, β-defensins (with a further group, the θ-defensins being present only in primates), (Tang et al., 1999).

The cathelicidins are instead defined by the structure of the relatively well-conserved N-terminal pro-region, known as the 'cathelin-like' domain, rather than on that of the AMPs themselves, which can be structurally quite diverse (Tossi et al., 2017). In mammals, the pro-region is homologous to cathelin, a protein isolated from pig leukocytes, explaining their name cathelicidin (Cathelin-linked microbicidal peptide). The genes encoding cathelicidins are ~ 2 kb in size and share a common organization (see **Figure 1.3**), with four exons and three introns encoding the signal sequence and N-terminal cathelin-like domain in the first three exons, and the mature peptide in the fourth (Tomasinsig and Zanetti, 2005), (Hancock and Diamond, 2000). These peptides are expressed as "pre-pro" forms and in mammals and are usually stored as "pro-peptides" in the granules of neutrophils. The granule storage form requires further processing to unmask the antibacterial activity. The conserved N-terminal segment, corresponding to the cathelin-like domain, is cleaved upon stimulation, releasing the C-terminal domain as the mature antimicrobial peptide (Zanetti et al., 1995). The correct term for the AMPs is therefore cathelicidin-derived peptides, and the term cathelicidin should be reserved for the pro-form, but it has become usual to refer to the AMPs also as cathelicidins.

It has been proposed that the well conserved pro-sequence may play an important role in maintaining the peptide in an inactive form within the cell through the interaction between acidic residues and the basic ones of the C-terminal AMP region (Scocchi et al., 1992), (Zanetti et al., 1995). However, other possible roles have been proposed, ranging from biological functions such as protease inhibitor or antimicrobial protein, or presentation platform for the AMP on the leukocyte cellular surface (Xhindoli et al., 2016).

The most distant examples of cathelicidin peptides were isolated from the hagfish (*Myxine glutinosa*) (Uzzell et al., 2003). But they have been identified also in birds (Cheng et al., 2015), fish (Scocchi et al., 2009), amphibians (Hao et al., 2012) and reptiles (Wang et al., 2008)(Zhao et al., 2008), as well as in several mammals such as horse (Skerlavaj et al., 2001), rodents, carnivores and pigs and bovids (Zanetti, 2005), (Zarember et al., 2002), (Sang et al., 2007),confirming their role as ancient components of vertebrate immunity.

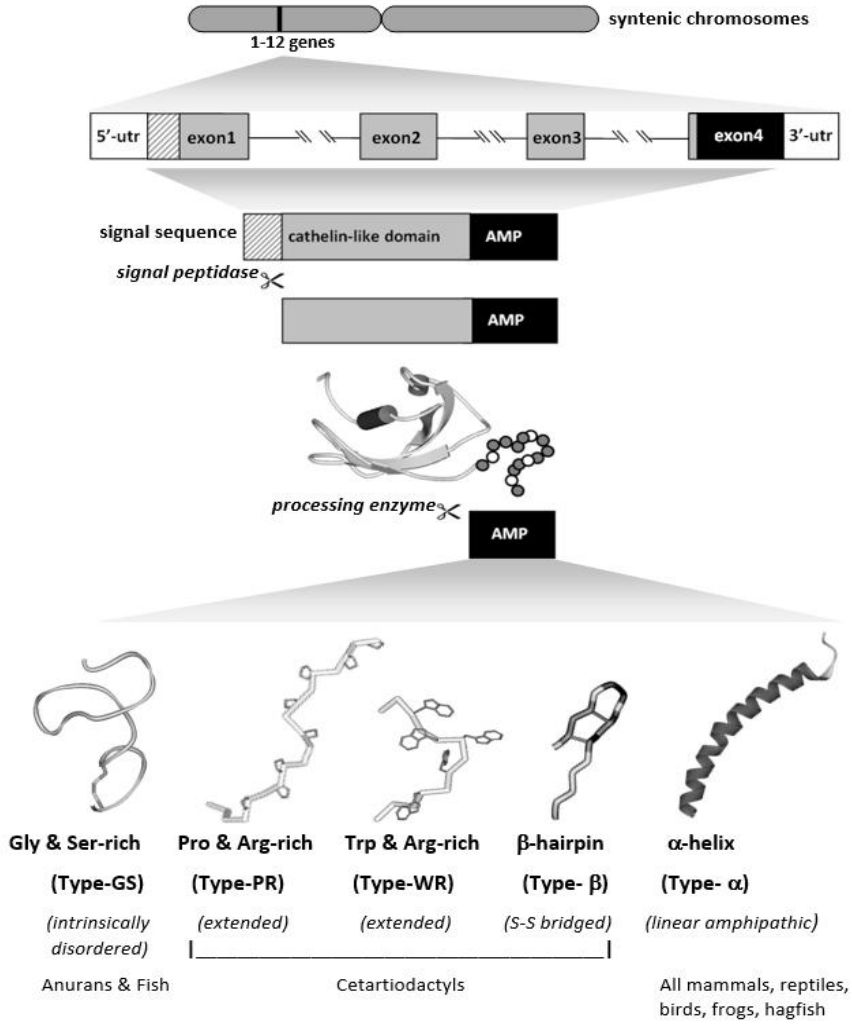

Figure 1.3. Schematic representation of the biosynthesis and structure of cathelicidins and cathelicidin-derived peptides. The cathelicidin genes are in syntenic chromosome positions and show a common organization. Many placental mammals (e.g. glires, carnivores and primates) express only one cathelicidin, while others express more than one (e.g. *perissodactyla*) and some express several (e.g. *cetartiodactyla*). Taken from (Xhindoli et al., 2016).

1.4 α-helical AMPs

The α-helical antimicrobial peptides are probably the most abundant and widespread in nature, so they represent a particularly successful structural strategy among host defence peptides. They generally have relatively short sequences (less than 40 residues – sometimes less than 20), which facilitates their chemical synthesis, and a relatively un-complicated structure that can be studied using simple spectroscopic techniques such as circular dichroism. They are also generally quite active against a broad spectrum of microorganisms, including Gram-negative, Gram-positive bacteria and fungi (Tossi et al 2000).

The net cationicity of these peptides, and their propensity for adopting an amphipathic, α-helical conformation in membrane-like environments, respectively promote their interaction with the anionic head groups of bacterial membrane phospholipids and insertion into the lipid bilayer of the bacterial membranes (Skerlavaj et al., 1996). The subsequent step in their mechanism of action typically involves membrane disruption by either (or both) the "carpet" or "pore-forming" processes (see above).

SAR studies have indicated at least seven parameters that can influence the potency and spectrum of activity of α-helical AMPs: *i)* the degree of structuring (% helical content) that is determined by the presence of amino acid residues that can stabilize (e.g. leucine, alanine, lysine) or destabilize (e.g. proline) the this conformation, *ii)* their size, *iii)* the sequence, *iv)* the charge, *v)* the overall hydrophobicity, *vi)* the amphipathicity, and *vii)* the respective widths of the hydrophobic and hydrophilic faces of the helix. These parameters are often closely interconnected, so the variation of one of them can affect the others (Tossi et al., 2000).

This structural group includes α-helical cathelicidin-derived peptides, such as the human LL37 and bovine BMAP-27 and BMAP-28 (Tomasinsig and Zanetti, 2005), but also cathelicidins from non-mammalian species (Zhang et al., 2015) (Yacoub et al., 2016), as well as many non-cathelicidin peptides from anurans (Coccia et al., 2011), fish (Cole et al., 2000) and insects (Chen et al., 2016) (Mylonakis et al., 2016). α-helical AMPs have also been found in very simple organisms, such as the placozoan *Trichoplax adhaerens* (Simunić et al., 2014)

The activity of this type of cathelicidin has been assayed against numerous pathogens, also in comparison to other types of AMPs, and in contexts such as bovine mastitis and human cystic fibrosis (Tomasinsig et al., 2010), (Pompilio et al., 2012) also with a view of developing effective antimicrobial therapeutic agent..

1.5 PR-AMPs - Proline-rich Antimicrobial Peptides

Among the cathelicidins, an important subgroup is represented by the proline-rich peptides, found in cetartiodactyls (see **Figure 1.4**). These show some structural similarity to proline-rich peptides found in invertebrates species, even though these are not phylogenetically related to cathelicidins (Scocchi et al., 2011). These linear peptides are characterized by an unusually high content of proline residues (often up to 50% of the whole sequence), as well as a large number of positive charges carried by arginine or, less commonly, lysine residues

(Gennaro et al., 2002). They are also quite unusual amongst AMPs as they act by a non-lytic mechanism of action.

Most AMPs, in fact, interact initially with microbial cell wall components and then insert into the bacterial membrane, leading to its disruption, but PR-AMPs translocate through the membrane without apparent damage to it. The membranolytic mechanism, for example that shown by helical AMPs, is due mostly to non-specific interaction of their amphipathic structure with the membrane, so that synthetic all- *D* enantiomers exert a similar antimicrobial activity to the natural all-L counterparts. Conversely, all-*D* PR-AMP analogues display a significant, if not a complete, loss of activity. This suggests a mechanism of action which involves, at some stage, a specific interaction of the peptides either with a membrane translocation system (as they are non-lytic), or with the internal targets that they interfere with. Quite possibly both processes require a stereospecific interaction by the peptides (Scocchi et al., 2011). On the other hand, the relative content and arrangement of proline residues can be quite varied.

The fact that PR-AMPs tend to display a quite narrow activity spectrum, centred on Gram-negative bacterial species, is presumably also due to the requirement that susceptible microorganism express both appropriate transport systems and internal target/s that can be recognized by them. This requirement likely also explains their unusually low toxicity towards host cells, which are unlikely to express transporter or target/s similar to the prokaryotic ones (Benincasa et al., 2010).

Several PR-AMPs have been isolated from mammals, to date restricted to cetartiodactyl species, and they are always cathelicidins. The first to be identified and isolated from bovine neutrophils were named bactenecins, and specifically Bac5 and Bac7 from their respective size (Gennaro et al., 1989). Later, a probable pseudogene containing for a third bovine PR-AMP, Bac4, was identified (Scocchi et al., 1998). Several orthologues of these PR-AMPs were later identified in sheep and goat (Shamova et al., 1999) and a porcine PR-AMP, called PR-39, is also orthologous to these bovine bactenecins (Agerberth et al., 1991). These mammalian PR-AMP sequences are characterized by tandem repeat motifs (see **Figure 1.4**); Bac5 consists of 43 residues and includes 9 tandem repeat of the tetramer XPPY, where X is most often an arginine residue and Y a hydrophobic residue (Frank et al., 1990). PR-39 shows 7 tandem repeats of the tetramer YPPX where again X is often Arg and Y is a hydrophobic residue (Agerberth et al., 1991). Bac7 comprises 60 residues containing 3 tandem repeats of a

tetradecamer made up of PRP triplets spaced by a hydrophobic residue (Frank et al., 1990), (Gennaro et al., 2002).

Porcine prophenins, quite long porcine PR-AMPs, present another variation on the theme, with sequences presenting several FPPPNFPGPR repeats. As indicated by their name, they are also quite rich in Phe residues.

Name	Origin	Sequence[a]	N° AA	Z[c]	Pro (%)	Repeated motifs
PR-39	pig	RRRPRPPYLPRPRPPPFFPPRLPPRIPPGFPPRFPPRFP-NH2	39	+11	49	PPRX (× 4)
PR-39[b]	pig	RLRRQAFPPPIFPGPGFRPPIFPPPPFRPAPFGPPRFP-NH2	(38)[d]	+7	42	PPRX (× 1)
prophenin	pig	AFPPPNFPGPRFPPPNFPGPRFPPPNFPGPRFPPPNFPGPRFPPPNFPG PPFPPPIFPGPWFPPPPPFPRPPPFGPPRFP-NH2	79	+7	53	PPPX (× 8)
Bac3.4	goat	RFRLPFRRPPIRIHPPPFYPPFRRFL-NH2	26	+8	31	PPXR (× 2)
Bac5	cow	RFRPPIRRPPIR---PPFYPPFRPPIRPPIFPPIRPPFRPPLGPFP-NH2	43	+10	47	PPXR (× 7)
Bac5	sheep	RFRPPIRRPPIR---PPFNPPFRPPVRPPFRPPFRPPFRPPIGPFP-NH2	43	+11	47	PPXR (× 7)
Bac5	goat	RFRPPIRRPPIR---PPFRPPFRPPVRPPIRPPFRPPFRPPIGPFP-NH2	43	+12	47	PPXR (× 8)
Bac4[b]	cow	RRLHPQHQRFPRER--PWPKPLSLPLPRPGPRPWPKPL-OH	(36)[d]	+6	33	PRPX (× 2)
Bac6	sheep	RRLRPRHQHFPSER-RPWPKPLPLPLPRPGPRPWPKPLPLPLPRPGLRPWPRPL-OH	53	+12	38	PRPX (×4)
Bac7	cow	RRIRPRPPRLPRPRPRPLPFFPRPGPRPIPRPLPFPRPGPRPIPRPLPFPRPGPRPIPRPL-OH	60	+17	47	PRPX (× 11)
Bac7	buffalo	RRFRPRRPRLPRPRPRPLPLPWPRPRPIPRPLPLPWPGPRPIPRPLPLPRPGPRPIPL-OH	58	+16	45	PRPX (× 8)
Bac7	sheep	RRLRPRRPRLPRPRPRPRPRPRSLPLPRPQPRRIPRPILLPWRPPRPIPRPQPQPIPRWL-OH	60	+20	38	PRPX (× 7)
Bac7	goat	RRLRPRRPRLPRPRPRPRPRPRSLPLPRPQPRRIPRPILLPWRPPRPIPRPQPQPIPRWL-OH	60	+20	38	PRPX (× 7)
Bac 11	sheep	RRLRPRRPRLPRPRPRPRPRPRSLPLPRPKPRPIPRPLPLPRPRPKPIPRPLPLPRPR PRRIPRPLPLPRPRPRPIPRPLPLPQPQPSPIPRPL-OH	94	+28	45	PRPX (× 15)
PRP-SP-B	pig	APPGARPPPGPPPPGPPPPGP-OH	21	+1	67	PPPGP (× 3)

Figure 1.4. Structure and amino acid sequences of PR-AMPs from artiodactyl species. *a)* Tandem repeats present in some sequences are underlined with alternating full or dashed lines. *b*) Sequence from a putative pseudogene. *c)* Net charge (His residues are considered neutral). *d)* Putative peptide size (charge and % proline residues are based on this sequence). Modified from (Scocchi et al., 2011).

1.5.1 PR-AMPs and intracellular mechanisms of action

The formation of ion channels and transmembrane pores, or other forms of bacterial membrane lysis, are often considered the preponderant mechanisms used by AMPs to kill pathogens. There is however increasing evidence that many AMPs, and not only PR-AMPs, are internalized into the bacterial cell via mechanisms other than membrane lysis, and then exert their antimicrobial action on intracellular targets. An example is the amphibian buforin II that is reported to accumulate in the bacterial cytoplasm and carry out its antimicrobial action by binding the nucleic acids (Park et al., 2000). AMPs, with quite different structures appear to interact with nucleic acids as part of their mechanism of action, including tachyplesin (β-hairpin) (Nakamura et al., 1988), pleurocidin (helical), PR-39 (PR-AMP) and

indolicidin (Trp-rich), subsequently inhibiting the synthesis of DNA, RNA and proteins (Selsted et al., 1992), (Boman et al., 1993), (Cole et al., 1997).

The histatins (primate, salivary, helical His-rich peptides) bind a specific receptor of fungal cell membranes, enter into the cytoplasm and induce a loss of ATP through a non-lytic mechanism of action, then leading to disruption of the cell cycle and formation of toxic ROS (Andreu and Rivas, 1998), (Kavanagh and Dowd, 2004).

The proline-rich apidaecin from honeybees (Casteels et al., 1990) and drosocin from fruit flies (Bulet et al., 1993) penetrate into susceptible bacterial cell and specifically bind to the protein DnaK (Scocchi et al., 2009) and non-specifically to bacterial chaperonin GroEL. These interactions are related with their antimicrobial activity (Otvos et al., 2000) and it was demonstrated that their killing action is much slower than the fast killing action of membranolytic peptides. The mechanism of inhibition is not yet clear, although it has been proposed that the binding of these peptides to DnaK prevents the movement of the lid over its peptide-binding pocket, permanently closing the cavity and thus inhibiting chaperone-assisted protein folding (Kragol et al., 2001). Alternatively, these peptides interact with the substrate-binding site of DnaK so that their antimicrobial activity is due to competitive inhibition (Chesnokova et al., 2004). A dual-mode of inhibition, based on competitive inhibition and interference with the lid-mediated regulation of the chaperone cycle, has also been proposed (Liebscher and Roujeinikova, 2009). Studies on mammalian PR-AMPs have shown that they also bind to other internal targets apart from DnaK, leading to a multimodal killing mechanism.

1.5.2 The bovine Pro-rich peptide Bac7: structural and functional characteristics

Bac7 is a linear, 60-residue proline-rich peptide of bovine origin, originally isolated from neutrophils, and a member of the cathelicidin family (see **Figure 1.5**) (Scocchi et al., 1994)(Gennaro et al., 1989). The sequence has a 46% content of proline and 31% of arginine residues with a particularly Arg-rich N-terminal region, followed by three 14 -residue tandem repeats of somewhat more hydrophobic residues (see **Figure 1.4**).

The antimicrobial activity of Bac7, or more particularly of its fully functional truncated form Bac7(1-35), has been extensively characterised and it has been shown to present a potent *in vitro* activity against several Gram-negative bacteria including *Enterobacteriaceae* (particularly *Salmonella)*, and the genera *Acinetobacter*, and *Sinorhizobium* (Benincasa et al.,

2004), and to a lesser extent *Pseudomonas* (Podda et al., 2006), (Marlow et al., 2009). It is instead inactive against most of the Gram-positive bacteria. Bac7(1-35) is active against clinical isolates that are multi-resistant to conventional antibiotics (Benincasa et al., 2004) and can furthermore neutralize endotoxin in experimental rat models of Gram-negative septic shock (Ghiselli et al., 2003). Like other PR-AMPs, the killing mechanism does not involve membrane lysis. This peptide is not toxic to mammalian cells at concentrations well above those effective against microbes (Tomasinsig et al., 2006), (Benincasa et al., 2010)

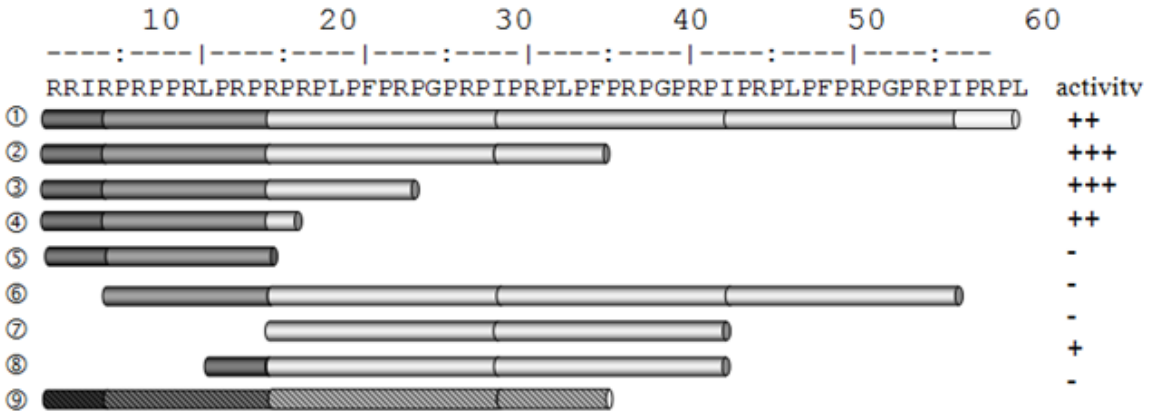

Figure 1.5. Sequence of Bac7 and schematic representation of active and inactive fragments. (1) The sequence comprises a cationic N-terminal stretch (darker grey region) followed by three tandem repeats. (2-4) The N-terminal fragments 1-35 and 1-23 are as active as the parent sequence, and fragment 1- 16 still maintains an appreciable activity, in the low micromolar range. All these peptides act via a non-membranolytic mechanism. (5) N-terminal fragments shorter than 15 residues are inactive. (6) The so-called 'N-cap' (RRIR, darkest grey cylinder) is required for activity and consequently (7) fragments from the central repeat region are inactive. (8) Some activity can however be recovered by grafting the N-cap onto central fragments. (9) All-*D* enantiomers of the active region (hashed cylinders), such as *D*-BAC7(1-35), are inactive at lower concentrations but act by a membranolytic mechanism at higher ones.

SAR studies on Bac7 have shown that the antimicrobially active domains correspond to specific segments of the peptide. A portion of the N-terminal region is required and sufficient for antimicrobial activity, as shortening from the C-terminus to Bac7(1-35) and Bac7(1-23) results in fragments with activities comparable to that of the native peptide (Benincasa et al., 2004) (Guida et al., 2015). The shortest active fragment includes 16 N-terminal residues, but shortening to 15 residues abrogates activity. Furthermore, removal of the first four N-terminal residues (sometimes called the N-cap) leads to a drastic decrease in activity irrespective of

fragment length, indicating that it exerts an essential role. Another crucial element for activity seemed to be the stereochemistry of the active region, as the all-*D* enantiomer of fully active fragment bac7(1-35) showed a significant loss of activity (Podda et al., 2006).

With respect to the mechanism of action, the minimum length requirements and necessity of the 'N-cap' for non-lytic activity, and the inactivity of the *D*-enantiomer, all argued for cytoplasmic translocation and inactivation of intracellular targets. The *in vitro* sensitivity of DnaK-deficient *E. coli* strains to Bac7(1-35), under growth permissive conditions, was not however significantly decreases compared to wild-type strains, so that this does not appear to be a principal target; other more vital targets for PR-AMPs are in fact present in susceptible bacteria (Scocchi et al., 2011).

The mechanism underlying the antibacterial activity of Bac7(1-35) was extensively investigated against several Gram-negative bacteria. At the MIC, it kills bacteria by a non-lytic, energy-dependent internalization mechanism into bacterial cells, while the all-*D* fragment is excluded, partly explaining its lack of activity. At significantly higher concentrations (>32-64 μM), both *L*- and *D*-enantiomers of Bac7(1-35) permeabilized the cytoplasmic membrane (Podda et al., 2006), leading to bacterial inactivation. This suggests that PR-AMPs such as Bac7 can inactivate bacteria with different modes of action, depending on the concentration: a mechanism based on uptake and internal target binding at concentrations near the MIC value, for which the stereochemistry is important, and an additional membranolytic mechanism acting only at higher concentrations, for which the stereochemistry is not important. The shortest active fragment, Bac7(1-16), still seems to act by a non-lytic mechanism even at a concentration 20 times its MIC value, so that the more hydrophobic tandem repeats may play a significant role in the lytic mechanism (Podda et al., 2006).

To better understand the non-lytic mechanism, a genetic approach was set up with the aim of identifying the proteins involved in membrane translocation. Bacterial mutants were selected by random mutagenesis with reduced susceptibility to the peptide's action (Scocchi et al., 2008). This allowed identification of a gene, *sbmA* that encode an inner membrane protein (SbmA), which based on homology could be part of an ABC transport system. Mutation or deletion of this protein conferred a partial resistance to Bac7 as well as other PR-AMPs, both cathelicidins (PR-39 and Bac5) and unrelated ones of invertebrate origin, such as apidaecin. On the other hand, the mutants remained susceptible to α-helical membranolytic AMPs

(Mattiuzzo et al., 2007), (Pränting et al., 2008). This suggested that SbmA was generally involved in PR-AMP internalization.

Regarding the internal targets, an attempt to identify these was carried out using affinity chromatography with either *L*- or *D*-Bac7(1-35) functionalized resin to search for specific bacterial cytoplasmic interactors in an *E. coli* lysate. It was quite striking that the only high affinity protein to be specifically retained by the *L*-Bac7(1-35) column was DnaK, while the all-*D* enantiomer failed to retain it. This confirmed the capacity of Bac7 to interact strongly with DnaK, and it was subsequently found to inhibit the protein refolding activity of the DnaK/DnaJ/GrpE/ATP molecular chaperone system, *in vitro*, in a concentration-dependent manner (Scocchi et al., 2009). Subsequently, it was shown that both insect-derived and cathelicidin-derived PR-AMPs were capable of inhibiting protein synthesis by bacterial ribosomes, interacting with the 70S subunit (Krizsan et al., 2014), (Mardirossian et al., 2014). Crystal structures have been obtained for these peptides bound to ribosomes, indicating that they bind to, and block, the ribosomal exit tunnel and destabilize the initiation complex, thus impeding polypeptide elongation in the ribosome (Seefeldt et al., 2015).

The exact mechanism of action of Bac7 is not yet fully characterized and several questions remain to be clarified, especially regarding its interaction with the outer and cytoplasmic bacterial membranes, the internalization mechanism and other possible internal targets. However, a quite detailed picture of the mode of action is emerging, as summarized schematically in **Figure 1.6.**

1.5.3 The E. coli inner membrane protein SbmA

SbmA appears to be a principal transporter for PR-AMPs from both mammalian and invertebrate animals. From an analysis of its 406 residue sequence it was deduced that it is an inner membrane protein with seven transmembrane spanning segments (Glazebrook et al., 1993), although the exact number of transmembrane helices is uncertain. The C-terminal part of the protein is highly hydrophobic and could form an eighth transmembrane segment, while cytoplasmic localization for this segment was suggested, on the other hand, by comparative analysis with other components of the *E. coli* inner membrane proteome (Daley et al., 2005). SbmA was initially predicted to be the transmembrane domain of an ABC-type peptide transporter, since it played a role in the uptake of structurally different such molecules (Laviña et al., 1986), (Yorgey et al., 1994), (Mattiuzzo et al., 2007).

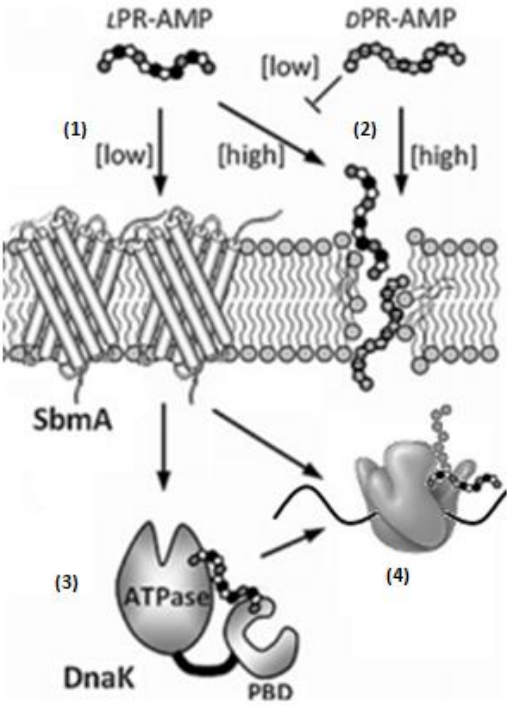

Figure 1.6. Model for the mode-of-action of PR-AMPs. PR-AMPs like Bac7 can penetrate into susceptible bacterial cells at micromolar concentrations, in a stereoselective manner, using a transport system involving the membrane protein SbmA (1). Other transporters may internalize these peptides at intermediate concentrations. At significantly higher concentrations, the peptides can lyse the bacterial membrane (2), irrespective of stereochemistry. Once internalized, PR-AMPs can interact with the bacterial chaperone DnaK (3), affecting its ATPase activity or its peptide-binding domain (PBD) or both. The principal target, however, appears to be the bacterial ribosome, in which they prevent initiation polypeptide synthesis and/or elongation (4). Adapted from (Scocchi et al., 2011).

It is, in fact, not specific for PR-AMPs as knocking out the *sbmA* gene results in a decreased susceptibility also to other types of antimicrobial agents, including microcins and antibiotics such as bleomycin (Yorgey et al., 1994), (Salomón and Farías, 1995).

Orthologues of SbmA have been identified in several Gram-negative bacterial species, including *Salmonella thyphimurium*, *Shigella flexneri* and *Klebsiella pneumoniae*, but it has not been found in Gram positive ones. Orthologues have also been identified in intracellular species such as *Sinorhizobium meliloti*, *Brucella abortus* and *Mycobacterium tuberculosis*, where it is known as BacA. SbmA/BacA has no close homologues in *Pseudomonas aeruginosa*, which consequently is less susceptible (in general) to Bac7 (Benincasa et al., 2004). While the function of SbmA in *E. coli* is not known, it can be inferred from its

homology with the BacA protein to have some function in assisting internalization of unknown substrate(s), triggering specialized functions that may be related to infection, so that it is necessary for the establishment of symbiosis or intracellular infection, (Runti et al., 2013).

1.6 Expression of cathelicidin-related AMPs in the order of *Cetartiodactyla*

The order of *Cetartiodactyla* includes two quite distinctive sub-orders of mammals: *i*) *Artiodactyla* (ungulates), of which cattle and sheep (*Bovidae*), pig (*Suidae*), camels and llamas (*Camelidae*), deer (*Cervidae*) and giraffes (*Giraffidae*) all form a part; and *ii*) *Cetacea* such as whales, dolphins and porpoises (see **Figure 1.7**). The evolutionary origin of whales, and the subsequent remarkable transformation that led to their adaptation to a fully aquatic existence, have fascinated biologists. Molecular biology studies had suggested for some time that the order *Cetacea* might be more closely related to cows or pigs in the order *Artiodactyla*, than to other orders of ungulates, such as *Perissodactyla* (horses, rhinoceros) or related orders such as *Hyracoidea* (hyraxes), *Proboscidea* (elephants), and *Sirenia* (sea cows). More recent studies indicate that the connecting species is likely that last common ancestor between Cetaceans and hippopotamus (Nikaido et al., 1999) (Price et al., 2005).

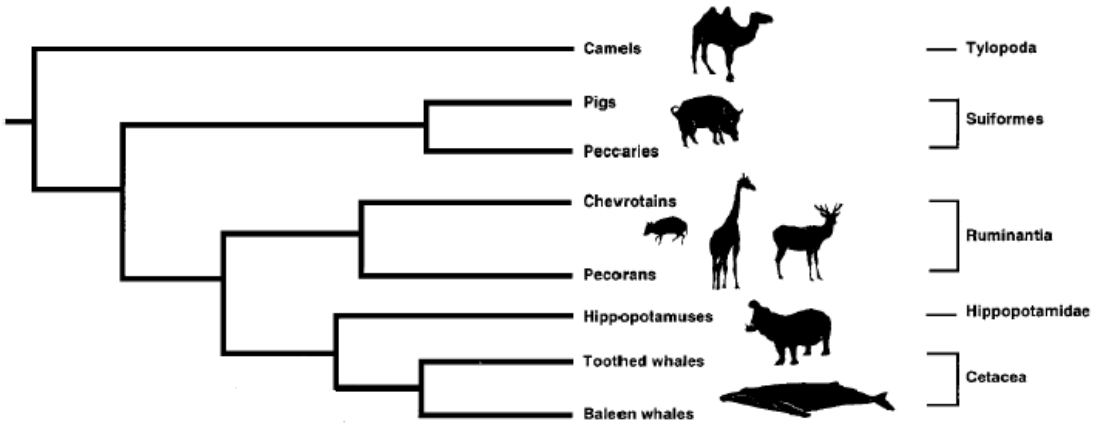

Figure 1.7. Phylogenetic relationships among the main subgroups of *Cetartiodactyla*. From (Nikaido et al., 1999).

Unlike primates and rodents, which express a single cathelicidin gene, cetartiodactyl species express a range of genes that express cathelicidins with quite diverse antimicrobial peptide domains (AMPD). This structural diversity likely results from a gene duplication mechanism followed by 'exon shuffling', by which a pre-existing and autonomous antimicrobial module presumably inserted downstream of the cathelin-like domain (CLD) of the duplicated gene by non-homologous recombination. This type of exon recombination cannot, however, be considered as a classical type of exon shuffling, as the shuffled AMPDs are not flanked by two introns with identical phases (Froy and Gurevitz, 2003), (Arguello et al., 2007). This mechanism has however been suggested to explain the remarkable diversity of the AMPD, considering the correspondence between these and their coding exons (Tomasinsig and Zanetti, 2005), (Yeaman and Yount, 2007). A high level of diversity is observed only at in the fourth exon, while the other three are generally well conserved The fact that the CLD in paralogous genes within some artiodactyl species are more conserved than in homologous genes from different species suggests they are actually subject to purifying selection by mechanisms such as gene conversion (Zanetti et al., 2000) .

Among *Cetartiodactyla,* cathelicidins from bovine *(Bos taurus)*, pig *(Sus scrofa)*, goat *(Capra hircus)* and sheep *(Ovis aries),* in that order, have been most extensively characterized. Bovine cathelicidins include PR-AMPs such as Bac5 and Bac7, (Gennaro et al., 1989), α-helical peptides such as BMAP-27 and -28, (Skerlavaj et al., 1996)], and quite unrelated peptides such as the Trp-rich indolicidin (Selsted et al., 1992) and β-hairpin cyclic dodecapeptide Bac1 (Romeo et al., 1988). The BMAPs (Bovine Myeloid Antimicrobial Peptide) rapidly permeabilize bacterial membranes *in vitro*, and kill a broad range of bacteria and fungi at micromolar and sub-micromolar concentrations (Skerlavaj et al., 1996), (Benincasa et al., 2003), (Benincasa et al., 2006). They are cytotoxic *in vitro* to host cells at concentrations that are not much higher than those necessary for antimicrobial activity, and this is linked to an appreciable permeabilising effect on host cell membranes that may also lead to mitochondrial damage, thus causing apoptosis (Risso et al., 1998).

Numerous porcine cathelicidins have also been isolated, including two types of PR-AMPs [prophenins and PR-39, (Agerberth et al., 1991), (Zhao et al., 1995)], several α-helical peptides [PMAP-23,-36 and -37 (Storici et al., 1994)], and several closely related β-sheet peptides known as protegrins (but with two disulphide bonds unlike the bovine dodecapeptide). PR-39 penetrates into bacterial cells without damaging the membrane, much like Bac7. It can also selectively translocate into host cells and bind to cytosolic signal

transduction factors and acts as a chemotactic agent for neutrophils (Huang et al., 1997), (Chan and Gallo, 1998).

A similar repertoire of cathelicidin-related AMPs have been identified in sheep and goat, such as the α-helical SMAP-29 and several PR-AMPs homologous to bovine Bac5 and Bac7 (Huttner et al., 1998), (Skerlavaj et al., 1999), (Shamova et al., 1999). This strongly suggests that numerous cathelicidins are expressed also in other cetartiodactyl species, and indeed sporadic reports of such peptides have appeared regarding buffalo and deer, so it was logical to search for these polypeptides also in cetacean species, exploiting the increasing genomic sequence data that is becoming available.

1.6.1 AMPs in the dolphin *Tursiops truncatus*

The bottlenose dolphin (*Tursiops truncatus*) is one of the best-known and most studied cetacean species worldwide. As part of the order *Cetartiodactyla*, being an aquatic animal it seemed particularly interesting to determine how its immune system has developed compared to that of its terrestrial counterparts, having diverged from these only relatively recently (~50 MY). In fact, although the immune system has evident similarities, there is evidence that dolphins have a somewhat higher resistance to external pathogens, being constantly exposed to them in the aquatic environment (Mancia et al., 2007).

Among bacterial species, those mainly responsible for infections in cetaceans are *Dermatophilus spp*., *Erysipelothrix rhusiopathiae*, *Mycobacterium marinum*, *Pseudomonas spp*., *Streptococcus iniae* and *Vibrio spp*. Concerning the bottlenose dolphin itself, it is subjected to frequent attacks by sharks and other predators, which cause injuries that expose internal tissues to infections (Zasloff, 2011). However, injured animals survive in a significant number of observed cases (~40%) and wounds heal without consequences. This is further evidence that dolphins have a highly developed and efficient immune system.

This, and its belonging to the order cetartiodactyla, suggests the presence of several antimicrobial peptides in the humoral component of its innate immune system, able to efficiently act against different pathogens, and partially explain the efficient wound repair system. It would be interesting to characterize these AMPs, on the one hand to gather more information on an important aspect of immunity, on the other hand to exploit this information for the development of new anti-infective strategies.

1.7 Use of AMPs as anti-infective agents

The rapid spread of the antibiotics resistance phenomenon is a major challenge to modern medicine. Soon after the introduction of antimicrobial drugs, bacteria began an accelerated evolutionary process towards resistant strains, which combined with the ability to transfer resistance mechanisms amongst species, has resulted in most, if not all, antibiotics available today being affected (Fernández et al., 2011). This is underlined by the ever more frequent cases of nosocomial infections caused, for example, by vancomycin-resistant *Enterococcus faecium* (VREF) (Top et al., 2008), methicillin-resistant *Staphylococcus aureus* (MRSA) (Purrello et al., 2016), penicillin-resistant *Streptococcus pneumoniae* (PRSP) (Mamishi et al., 2014), fluoroquinolone-resistant *Pseudomonas aeruginosa* (Sawa et al., 2014) and *Acinetobacter baumannii* resistant to other antibiotics (Ageitos et al., 2016). Unfortunately, the resistant pathogens can then make their way into the community.

There are a number of possible mechanisms that lead to antibiotic resistance, including *i)* a reduced permeability to, or uptake of, certain drugs; *ii)* increased efflux activity so that drugs are expelled from the membrane or cytoplasm; *iii)* enzymatic inactivation of drugs; *iv)* alteration to or over-expression of the drug's target/s and *v)* suppression of enzymes involved in pro-drug activation (Fernández et al., 2011). The origin of these resistance traits, in a given bacterial strain, can be diverse. They can evolve independently due to selective pressure on a given strain, especially when it is exposed to sub-optimal concentrations of the drug. Genes encoding resistance determinants can also be horizontally transferred between different strains, or even different species, via conjugation. This mechanism is common, for example, for drug-inactivating enzymes, whose genes are often carried as cassettes on mobile elements. Fortunately, mutations in genes leading to resistance usually result in lower fitness, and if costly to the bacterial cell can be reversed (Baquero, 2001).

A further problem related to drug resistance is the production of biofilms; often mixed communities of microorganisms that adhere to bio-surfaces and are encased in a matrix composed of polysaccharides, proteins and nucleic acids that protects them from the external environment. These communities are shielded from antimicrobial drugs and often have a slower metabolism due to nutrient or oxygen depletion, both of which reduce the effects of the drugs. Biofilms are linked to the formation of dental plaque (Kanwar et al., 2016), urinary tract infections (Delcaru et al., 2016), endocarditis (Elgharably et al., 2016), lung infections (Cai et al., 2016) among many other infections.

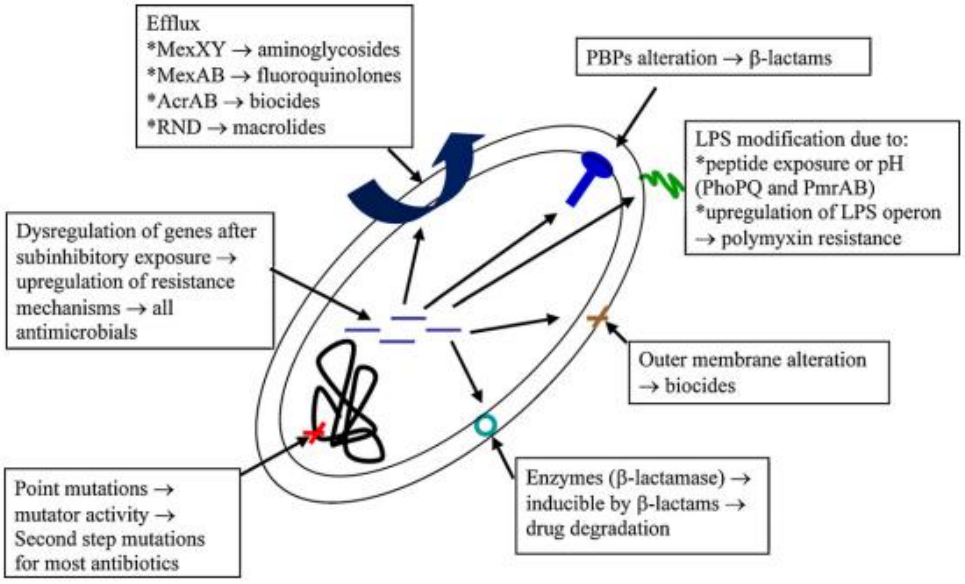

Figure 1.8. Schematic representation of some of the major known adaptive resistance mechanisms. RND, PBP and LPS stand for resistance-nodulation-cell division type efflux, penicillin binding protein and lipopolysaccharide, respectively. Taken from (Fernández et al., 2011).

AMPs are alternative anti-infective agents to antibiotics that could help to overcome these resistance mechanisms. SAR studies on AMPs have amply indicated that *i)* as direct antimicrobials the membranolytic AMPs combine a mode of action different to those of most conventional antibiotics, and therefore should not be susceptible to cross resistance; *ii)* this type of AMP often display a multi-modal mechanism of action, binding to different components of the cell membrane, so that it is more difficult for the bacterium to develop resistance, as this would require altering multiple targets; *iii)* cell penetrating AMPs tend to be more similar in their action to conventional antibiotics, but are non-toxic to the host, and might be capable of internalising useful molecular cargo into either bacterial or host cells. However, AMPs suffer from all the disadvantages of peptide drugs: *a)* production difficulties and high costs; *b)* therapeutic windows that may be too narrow, *c)* reduced bioavailability due to sequestration or renal clearance; *d)* susceptibility to proteolytic degradation (by either host or bacterial secreted enzymes); *e)* possible antigenicity. Attempts to improve their potential have therefore mostly been aimed at increasing serum stability without affecting their antimicrobial or cell-penetrating properties (Scocchi et al., 2011).

Helical peptides, being membranolytic, generally display a broader and more potent antimicrobial activity that is less sensitive to medium conditions than other types of AMPS. A

disadvantage is their relatively higher toxicity towards host cells, which makes them more suitable for topical rather than systemic uses. PR-AMPs have a significantly narrower activity spectrum, due to their non-membranolytic mechanism requiring transmembrane transport (see above), but are relatively facile to synthesize and may be more amenable to chemical modifications required to improve stability and bioavailability. They also tend to have low toxicities. An interesting potential application of PR-AMPs is their use as cell-penetrating peptides (CPPs) for the intracellular delivery of normally impermeant drugs into bacteria (e.g. conventional antibiotics or resistance-factor inactivating drugs) or even into eukaryotic cells.

In this thesis, I describe some studies that I have carried out to explore the potential of cathelicidin-derived peptides as possible anti-infective agents. These studies are conceptually quite different, so I have written separate Materials and Methods and Results sections for each. In chapter 2, I describe the characterisation of some novel cathelicidins that were identified in the bottlenose dolphin, *Tursiops truncatus*. These are structurally related to orthologous peptides from artiodactyl species, some of which have already been extensively characterized and display significant therapeutic potential. It was interesting to determine if and how the aquatic life-style of the dolphin could have modulated the activity of these peptides. In chapter 3, I instead explore the possibility of using the very well characterized PR-AMP fragment Bac7(1-35) to internalize antibiotic cargo into bacterial cells. This involved finding strategies for modifying the antibiotic, without impairing its activity, so that it could be covalently linked to the peptide and allow its transport, but also allow its release so that it could explicate its activity.

Chapter 2: Bottlenose dolphin cathelicidins

2.1 AIMS OF THE STUDY

The World Health Organization has identified bacterial resistance to antibiotics as one of the three greatest threats for human health. Multi-drug resistant bacterial strains are currently one of the leading causes of infections in hospitals. In this respect, the most problematic pathogens are gathered in the so-called "**ESKAPE**" group (***E****nterococcus faecium*, ***S****taphylococcus aureus*, ***K****lebsiella pneumoniae*, ***A****cinetobacter baumannii*, ***P****seudomonas aeruginosa*, and ***E****nterobacteria* spp.). New drugs, acting via alternative mechanisms are therefore urgently needed.

Unfortunately, the discovery process for new antibiotics does not keep up with the development of new resistant bacterial strains/species. From this point of view, cathelicidin-derived AMPs could be suitable candidates as new potential anti-infective agents. These molecules are *i)* very widespread in vertebrate animals, ranging from basal ones such as hagfish and lampreys, to reptiles, birds, fish, amphibians and mammals, indicating they are ancient and successful antimicrobial agents; *ii)* they are a structurally very diverse family of AMPs, with at least 5 different conformational classes, each with its own mode of action (Tossi et al., 2017), *iii)* they are both 'multimodal' and 'multifunctional', in the first case because they have a direct antimicrobial action based on interaction with multiple targets, and in the second case, because they have the capacity to modulate the activities of host defence cells. This means that apart from acting as antibiotics, they can also modulate the host's innate and adaptive responses, as well as having other protective roles connected with protecting from sepsis and promoting wound healing (Cederlund et al., 2011). Moreover, their structures are normally relatively simple (either linear, or if cyclic quite short and with few disulfide bonds), allowing for relatively facile chemical synthesis. They naturally, however, present the disadvantages of peptides already mentioned previously, relating production costs, reduced bioavailability and imperfect therapeutic windows. To this, one could add a very significant possible disadvantage that makes their detailed study quite important; should resistance develop against a therapeutic agent based on their structures, it could result in cross-resistance to endogenous immune factors, with all the consequences that entails.

The first part of my PhD thesis work aimed to study novel cathelicidins identified in the dolphin *Tursiops truncatus*, and probe the antimicrobial characteristics of these peptides, also in view of potential exploitation for biomedical applications.

The main purposes were to:

i) Synthesise and characterise peptides from cathelicidin genes identified in the dolphin after exploring different types of nucleic acid databases.

ii) To test the antimicrobial activity, in terms of MIC and other parameters reflecting inhibition of bacterial growth", comparing these to data from the orthologous peptides present in other *Cetartiodactyla*.

iii) To begin to investigate their mechanism of action by monitoring their effects on bacterial membranes, and/or their capacity to internalize into susceptible bacterial cells, and cytotoxic activities against selected host cells.

2.2 MATERIALS and METHODS

2.2.1 Identification of Tursiops truncatus cathelicidin-derived AMPs

Tursiops truncatus is one of 29 mammals that have been selected for the *Mammalian Genome Project*, for the sequencing of the entire genome (Lindblad-Toh et al., 2011). Consequently, genomic data has been available for some time. The initial identification of Tursiops cathelicidin genes was carried out by prof. G. Manzini in the Dept. of Life Sciences, University of Trieste, who searched in the nucleotide, EST (expressed sequence tag), WGS (whole genome sequence) and traces (crude sequence data) archives in Genebank. More recently, it has been possible to confirm these sequences, and partly determine the gene organization, by blasting the Ensemble dolphin assembly (turTru1) provided by the Genome Project.

The sequences of seven different putative bottlenose dolphin cathelicidins, called Tur1 - Tur7 (see **Table 2.2.1,** top), were identified from the genomic databases by using the known sequences of artiodactyl cathelicidins (cow or pig) as *query,* in a standard nucleotide BLAST search of the abovementioned NCBI databases (https://blast.ncbi.nlm.nih.gov). For some of the sequences, less frequent variants differing in one or a few residues were also found. The same sequences were then identified in scaffolds from the ENSEMBL truTUR1 dolphin partial genome assembly using its BLAST tool (http://www.ensembl.org/Multi/Tools/Blast). The scaffold and contig entries for the sequences in Ensemble or the NCBI Nucleotide database are TUR1D + TUR4D + TUR5: Ensemble Genescaffold 2343; TUR1V (variant): Genebank locus JH490241; TUR2D: Genebank locus JH521985; TUR2D + TUR3D: Ensemble Scaffold 362; TUR3V: Genebank locus JH475206; TUR5V: Genebank locus JH481255; TUR6: Ensemble Scaffold17717; Ensemble Genescaffold 3424.

The bottlenose dolphin genome was sequenced using first generation methods (Sanger) at a relatively low coverage (2.6 ×, *see* http://www.ensembl.org/Tursiops_truncatus) so that there could be imprecision. This suggested the need to use primers based on the sequences of TUR1-7 to selectively amplify the cathelicidin genes from genomic DNA obtained from samples of dolphin tissue. This work was carried out M. Del Ben in the laboratory of prof. Alberto Pallavicini, starting from frozen tissue samples obtained from the Mediterranean marine mammal tissue bank, Dept. Veterinary Experimental Sciences, Univ. of Padova. Sequencing confirmed the correctness of TUR5 and 7, failed to find TUR1D while revealing a

new paralogue, and indicated slight differences in one or more positions of TUR2, 3, 4 and 6. For this reason, peptides mined from the database are indicated as TURnD, and those from direct sequencing as TURnS. These latter sequences are also shown in **Table 2.2.1**.

Table 2.2.1. Amino acid sequences of cathelicidins (TUR) found in the *Tursiops truncatus genome*

Peptide	Sequence	Residues	Charge
	from database searching		
TUR1D	RRIRFRPPYLPRPGRRPRFPPPFPIPRIPRIP-OH	32	+10
TUR2D	GRFRRLRHRIGRVLSKVGRIVGPLIRIL-NH_2	28	+9
TUR3D	GIFRWLRHIGRVLPKVGRIVGPLIGIW-NH_2	27	+5
TUR4D	QRCRIIVIRMCR-OH	12	+4
TUR5	GLFRWLGDFLQRGGRR-OH	16	+3
TUR6D	RGLRSLGRNILRGWKKYGPIIVPIIRLI-NH_2	28	+8
TUR7	GLFRRLGDFLRRGGEKTGKKIERIGQRIKDFFGIFQPSKQS-OH	41	+7
	from direct sequencing		
TUR1S	RRIPFWPPNWPGPWLPPWSPPDFRIPRILRKR-OH	32	+6
TUR3S	GRFRRLRHRIGRVLPKVGRIVGPLIGIW-NH_2	28	+8
TUR4S	QGCRIVVIRMCR-OH	12	+3
TUR6S	RGLRSLGRKILRGWKKYGPIIVPIIRLI-NH_2	28	+8
TUR5 & 7	*confirmed*		

With respect to the expression of the dolphin cathelicidin-derived peptides, a search of the EST archive in Genebank found only TUR1. Very recently, however, it has been possible to identify expressed RNA from the SRA database (Sequence Read Archive). In particular, bioproject PRJNA313464 provided an RNA-Seq analysis of seasonal and individual variation in dolphin blood transcriptomes (Morey et al., 2016) while bioproject PRJNA20367 provided RNA-Seq data from different tissues (kidney, spleen, muscle and liver) (Foote et al., 2015). The sequences of TUR1-7 were used as query in a BLAST search against entries from these bioprojects, and the number of hits was considered roughly proportional to the expression levels.

Having obtained the sequences of Tursiops cathelicidins, it was possible to use these to search for orthologous peptides with sequences present in GeneBank, such as the river dolphin (*Lipotes vexillifer*), the killer whale (*Orcinus orca*), the sperm whale (*Physeter macrocephalus*), and the minke whale (*Balaenoptera acutorastrata*).

2.2.2 Peptide synthesis and purification

Based on their different conformations and likely mechanisms of action, I concentrated my work on three dolphin cathelicidins, which I chemically synthesized:

1) both versions of the pro-rich peptide **TUR1** (TUR1D and S), as well as a version of TUR1D modified with a C-terminal cysteine;

2) the sequenced version of the cyclic dodecapeptide **TUR4S**

3) both versions of the helical peptide **TUR6** (D and S).

Syntheses were performed in the solid phase, using Fmoc chemistry and global protection of aminoacid side chain (Atherton, and Sheppard, 1989). They were carried out on a Biotage Initiator+ automated microwave peptide synthesizer, with a synthesis scale of 0.1 mmol for each peptide. For peptides containing proline or cysteine as C-terminal residue (TUR1 and TUR1[Cys^{33}]), the 2-chlorotrityl chloride resin (Novabiochem, substitution $\leq$ 0.2 mmol/g) was chosen, to respectively prevent diketopiperazine formation and cysteine racemisation. The resin was manually preloaded with 4 fold molar excess of either Fmoc-Pro-OH or Fmoc-Cys(Trt)-OH dissolved in DCM with added DIPEA (diisopropylethylamine). For the

dodecapeptide TUR4, a commercially available TGA resin preloaded with Fmoc-Arg(Pbf) was used (Novabiochem, substitution 0.23 mmol/g). For the TUR6 the NovaPEG Rink Amide Resin LL (Novabiochem, substitution 0.16 mmol/g) was used. A five-fold excess of Fmoc-amino acid/PyBOP/DIPEA (1:1:1.7 v/v) was normally used for each coupling step with NMP as solvent. In the case of 2-chlorotrityl chloride resin, the coupling temperature used was kept to 45°C to prevent premature detachment; otherwise, it was 75°C.

Before setting up the synthesis, potentially difficult points in the sequence were predicted using the *Peptide Companion* software (Coshi Soft, AZ, U.S.A) (see **Figure 2.2.1**). Based on these profiles, for couplings predicted to be difficult, and for the bulky and sterically hindered, Pbf-protected Arg residues, double coupling cycles were performed at appropriate points. For the TUR1 peptides, the presence of a number of proline residues in any case reduces the aggregation potential during the peptide chain elongation, so that synthesis was in general not problematic. Deprotection of the Fmoc group was carried out using a solution of 20% piperidine in NMP.

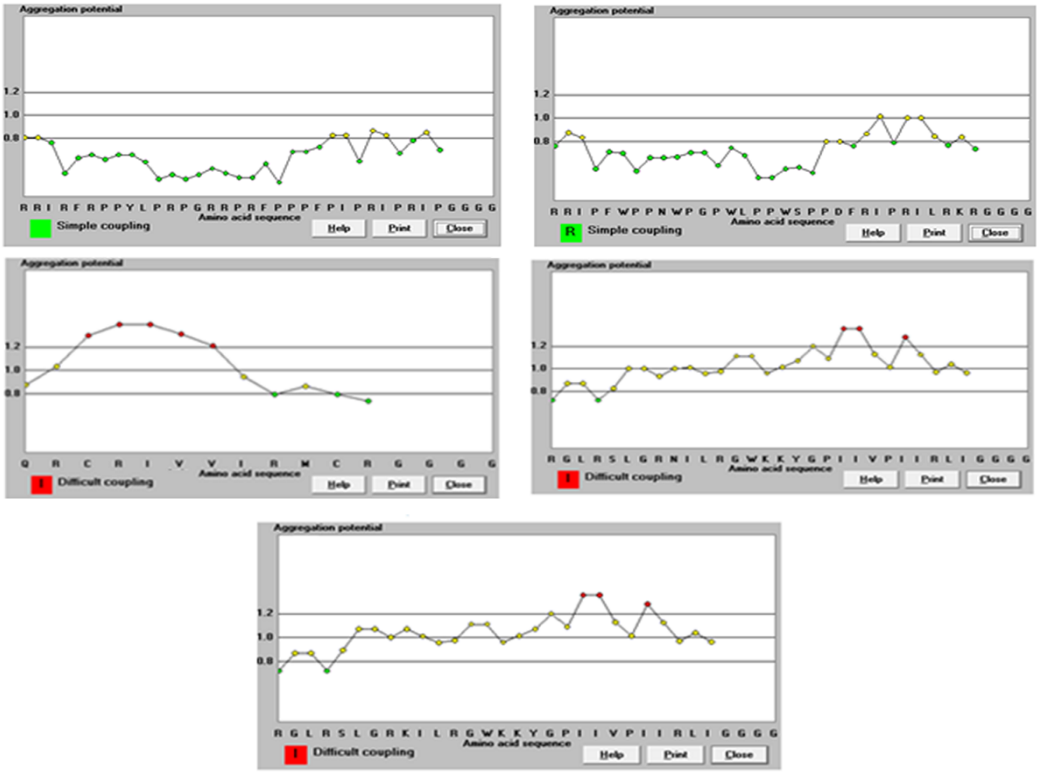

Figure 2.2.1. Prediction of difficult sequence. A) TUR1_DB; B) TUR1_SEQ; C) TUR4; D) TUR6_DB; E) TUR6_SEQ. The synthesis points with predicted high difficulty are in red, intermediate difficulty in yellow, while easy ones are in green. A stretch of Gly residues was added to the C-terminus as the program ignores residues close to the C-terminus.

The peptides were cleaved from the resin using a cocktail of trifluoroacetic acid (TFA), thioanisole, water, 3,6-dioxa-1,8-octane-dithiol (DODT), tri-isopropylsilane (TIPS) (85%,3%,2%,8%, 2% v/v) and then precipitated and washed several times with cold tert-butyl methyl ether (TBME) and dried under nitrogen. The crude peptides were analysed by ESI-MS [Brucker Daltonics Esquire 4000] (see **Figure 2.2.2** for an example). All peptides were purified by reverse-phase HPLC on a Phenomenex preparative column (Jupiter™, C18,10 µm, 90 Å, 250x21,20 mm) using a 5-35% CH_3CN in 50 min gradient with a 8 ml/min flow. The peptides, lyophilized several times from HCl to remove TFA as a counterion, were then accurately weighed and dissolved in Milli-Q water. Quality control was carried out by analytical RP-HPLC (Waters Symmetry 4.6 x 75 mm C18 column) followed by ESI-MS. The concentration of stock solutions was determined from the weight and by spectrophotometric determination of peptide bonds using ε214 calculated as described by (Kuipers and Gruppen, 2007), or by the method of Waddell, measuring the differential absorbance at 215nm and 225nm (Waddell, 1956). For those peptides with aromatic side-chains, absorbance at 280 nm was also used.

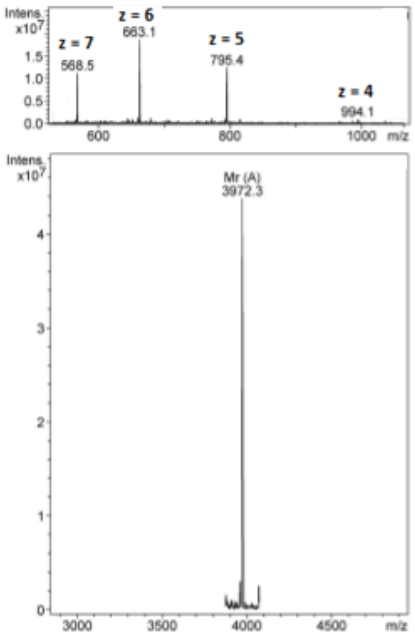

Figure 2.2.2. Mass spectrum of TUR1_DB. Top: ESI-MS spectrum of at Compound stability = 100; below: reconstructed spectrum based on m/z peaks.

2.2.3 Folding of TUR4

On completion of the synthesis, and after cleavage using protocols as described above, the quality of TUR4 crude reduced linear peptide (MW = 1433.8) (see **Figure 2.2.3A**) was found to be sufficiently high to undergo the folding procedure directly, without previous purification. Folding was carried out in oxidizing conditions by dissolving crude peptide in aqueous buffer consisting of 0.1M ammonium acetate, 2 mM EDTA and 0.5M guanidinium chloride, at a final pH 7.5-8, under nitrogen. Cysteine (100 fold excess) and cystine (10 fold excess) were also added immediately prior to use, to catalyse disulfide exchange and facilitate obtaining the correct connectivities. The folding reaction was conducted at room temperature for 48h and was monitored by analytical RP-HPLC (Kinetex C18, 3µm, 100 Å, 50 x 4.6 mm column from Phenomenex, USA) until complete oxidation of the peptide, exploiting the fact that unfolded and folded peptides have different and characteristic elution times. The folding solution was then acidified at pH = 2-3 and subjected directly to preparative RP-HPLC, and the peptide then lyophilized. ESI-MS showed that the peptide was both correctly folded and of high purity (**Figure 2.2.3B**), with a yield of about 50%. Quality control was carried out by analytical RP-HPLC (Waters Symmetry 4.6 x 75 mm C18 column) followed by ESI-MS.

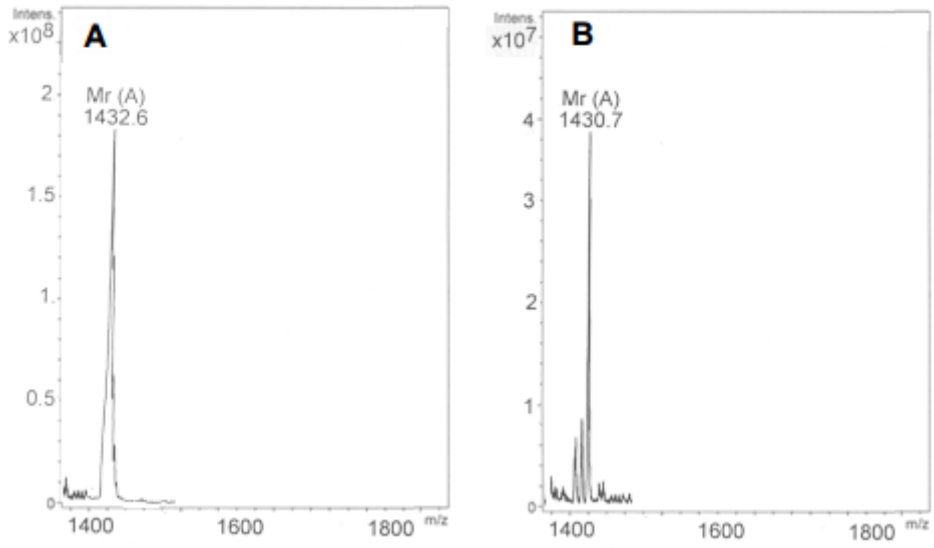

Figure 2.2.3. Mass spectrum of TUR4S. A) reduced crude peptide; B) oxidized and purified analogue. Spectra were deconvoluted from the ESI-MS spectra using the Esquire software.

2.2.4 BODIPY labelling of peptides

TUR1D and its bovine orthologue Bac7(1-35) were synthesized in the solid phase, as described above, but introducing a cysteine residue at the C-terminal. After cleavage, crude peptides were reacted with the fluorescent dye BODIPY-FL [N-(2-aminoethyl)maleimide] (1 eq. peptide/10 eq. dye) in 30% CH3CN, 10 mM sodium phosphate buffer at pH 7.4. The reaction (see **Figure 2.2.4**) was performed under nitrogen bubbling with stirring for 3 h at room temperature and subsequently overnight at 4°C. The SH group on the Cys residue reacts with maleimide group of BODIPY. The reaction was monitored periodically by analytical RP-HPLC (Kinetex C18, 3µm, 100 Å, 50 x 4.6 mm column from Phenomenex, USA) and ESI-MS. Upon completion (about 24h), a 10-fold excess of cysteine was added to the reaction mixture to quench unreacted dye. After 60 min quenching, the reaction mixture was diluted with 0.05% trifluoroacetic acid in water to a final concentration of 10% CH3CN and pH 2.5. This was necessary, as the crude peptide was relatively insoluble in water alone. The labelled peptide was purified by RP-HPLC on a Phenomenex semi-preparative column (Jupiter™, C18, 5 µm, 300 Å, 100x10 mm) with a linear gradient from 10% to 30% of CH3CN in 40 min and 2ml/min flow. The labelled peptides purity was confirmed by ESI-MS. After lyophilisation from 10 mM HCl, quality control was carried out by analytical RP-HPLC (Waters Symmetry 4.6 x 75 mm C18 column) followed by ESI-MS, and the concentration of labelled peptide stock solution was determined by spectrophotometric determination of BODIPY (ε_{504} = 79000 M^{-1} cm^{-1} in MeOH) (Invitrogen Molecular Probes Handbook, section 2.2).

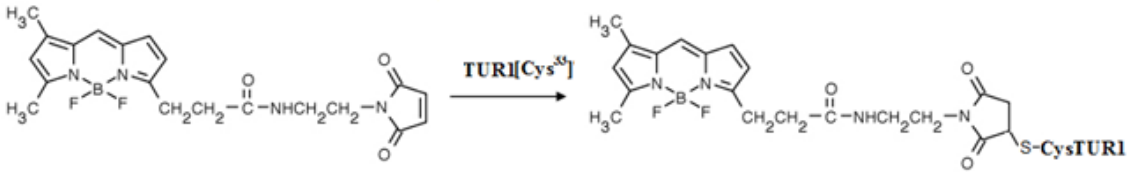

Figure 2.2.4. Schematic representation of peptide-BY reaction.

2.2.5 Antimicrobial activity assays

The antimicrobial activity of all synthesized peptides and their orthologues was tested in terms of Minimum Inhibitory Concentrations (MIC), as well as the more sensitive IC_{50} value

determined from inhibition of bacterial growth in the presence of peptides, for several bacteria strains. The MIC value was defined as the lowest peptide concentration that prevented visible bacterial growth after incubation for 20 hours at 37°. In the serial dilution method, bacterial loads were typically 5 x 10^5 cfu/ml, with 100 µl of medium per well, as described in section 2.2.7.

Bacterial growth curves were obtained using 10^6 cfu/ml bacteria in MH broth, with 200 µl of medium per well, in the presence of increasing peptide concentrations, monitoring the optical density at 600 nm at 37°C for 4 h, as described in section 2.2.8. IC_{50} values were determined from the degree of growth inhibition calculated as the relation between the absorbance of bacteria in presence and in absence of peptide, at 210 min. according to the formula $\%I = 1-(A^P/A^0) \times 100$, where A^0 is the absorption intensity in the absence of peptide at 210 min and A^P the absorption intensity in the presence of a given peptide concentration. By plotting the % inhibition at increasing [peptide] it is then possible to extrapolate the IC50 (see **Figure 2.2.5**).

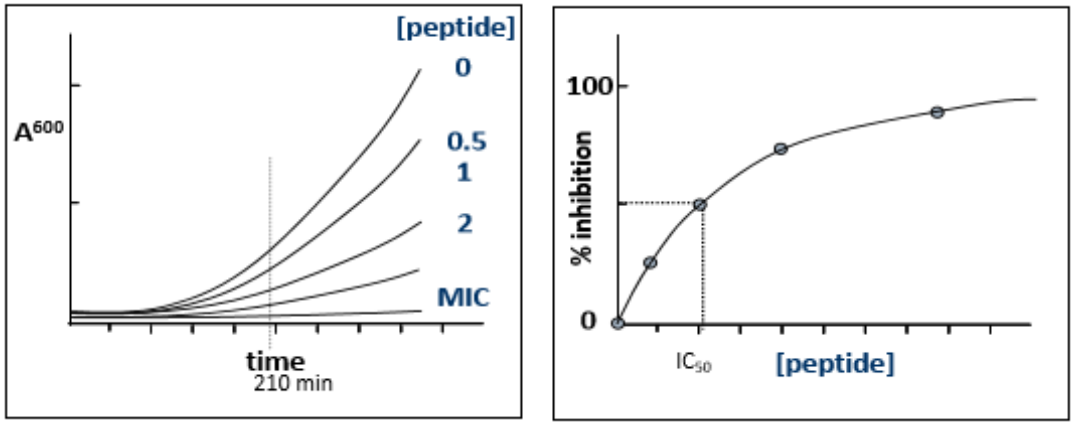

Figure 2.2.5. IC_{50} determination. Schematic representation of bacterial growth curve (left) and bacterial growth inhibition curve (right), from which the IC_{50} is determined as indicated by the dashed line.

2.2.6 Bacterial strains

The tested bacterial strains were chosen to reveal aspects of the different peptide's modes of action. In particular, previous studies have shown that the Pro-rich peptides penetrate into Gram negative bacteria principally using SbmA, an inner membrane transport protein (Mattiuzzo et al., 2007,) (Runti et al., 2013). Furthermore, recent work by our group has suggested that there may be a second transporter for proline-rich peptides (Guida et al., 2015)

and this was confirmed by Hoffmann's group, that has found a possible component of this transport system, the *YjiL* ATPase (Krizsan et al., 2015). For this reason, TUR1 and its orthologues peptides were tested against four different variants of *E. coli* strain: *a) E. coli* BW 25113, derived from the ATCC 25922 strain but lacking the O-antigen on its outer membrane LPS; *b) E. coli* BW 25311 *ΔsbmA,* a knock-out mutant that does not express the SbmA transporter; *c) E. coli* BW 25311 *ΔyjiL,* a knock-out mutant for YjiL transport system, both obtained from the Keio collection of *E. coli* single knockout mutants; *d) E. coli* BW 25311 *ΔyjiL / ΔsbmA* double knock-out mutant (kindly donated by the Hoffmann group).

The antimicrobial activity of TUR6 orthologues and TUR4 was instead determined, against the reference laboratory *E. coli* ATCC 25922 and *S. aureus* ATCC 25923 strains, in order to have a comparison between a Gram-negative and a Gram-positive strain, and with experiments previously carried out on other artiodactyl orthologues.

Furthermore, to probe for the effect of environment on the evolution of TUR peptides, the antimicrobial activity of TUR1, TUR4 and TUR6 was tested in terms of MIC against several aquatic and terrestrial bacteria, both Gram positive and Gram negative. The characteristics of each strain are indicated in **Table 2.2.2.**

Table 2.2.2. Bacterial strains used in antimicrobial activity assays.

	Strain	Characteristics or genotype[(a)]	Reference or source
	E. coli		
-	BW 25113	wild type	Genobase
-	Δ*sbmA* (JW0368)	BW25113 sbmA::Km^r mutant	Keio Collection[(b)]
-	Δ*yjiL* (JW5785)	BW25113 yjiL::Km^r mutant	Keio Collection[(b)]
-	Δ*yjiL* / Δ*sbmA* (BS-L)	BW25113 yjiL/sbmA::KmrTetr mutant	(Krizsan et al., 2015)
-	ATCC 25922	wild type	ATCC®
	S. aureus ATCC 25923	wild type	ATCC®
	A. hydrophila ATCC 7966	wild type	ATCC®
	A. salmonicida NCIMB 1102	wild type	NCIMB®
	V. anguillarum ATCC 43305	wild type	ATCC®
	Y. ruckeri NCIMB 1315	wild type	NCIMB®
	L. garviae ATCC 49156	wild type	ATCC®
	P. aeruginosa ATCC 27853	wild type	ATCC®
	A. baumannii ATCC 10606	wild type	ATCC®
	K. pneumoniae ATCC 700603	wild type	ATCC®

(a) Km^r, kanamycin resistant; Tet^r, tetracycline resistant; (b) Keio Collection of GenoBase (http://ecoli.aistnara.ac.jp/index.html)

2.2.7 Minimum inhibitory concentration (MIC)

The bacterial suspensions for MIC assays were prepared by inoculating a single bacterial colony into 5 ml of Muller-Hinton (MH) broth, then incubating at 37 °C with shaking overnight. The next morning, 300 µL of bacterial suspension were inoculated into 10 ml of fresh MH broth and incubated at 37 °C with shaking for 2 hours, to favour logarithmic growth of the bacteria. The optical density (OD) of the bacterial suspension at 600 nm (ULTROSPEC-2100 Pro Amersham Biosciences) was then measured using MH broth as reference, and the absorbance value compared with standard values previously measured for known cfu/ml suspensions of each strain of bacteria, to extrapolate the bacterial load.

The MIC assay was then based on serial dilutions in 96-well micro plates (Sarstedt), starting from a peptide concentration of 32 µM. The plates were prepared by putting 64 µM of peptide in 100 µl of MH broth in the first well, taking care not exceed 7% of the final volume with the added peptide stock solution. 50 µl of MH broth were placed in the following wells, to carry out serial 50% dilutions. To the resulting 50 µl of medium with precise dilutions of peptide 50 µl of fresh bacterial suspension in MH broth was added, with a concentration of $5*10^5$ CFU/ml; leading to final concentrations of peptide from 32 µM to 0.5 µM, and $2.5*10^5$ CFU/ml for bacteria, in a final volume of 100 µl medium. The last wells contained only untreated bacterial suspension in MH broth and were used as positive control. The plates were then incubated for ~18-20 hours at 37 °C and the next day the lowest peptide concentration able to completely inhibit bacterial growth was visually determined. The MIC value of the peptide corresponded to the last well in which there is a clear solution. Assays were typically carried out in duplicate in each plate, and repeated at least three times on different days.

2.2.8 Inhibition of bacterial growth

To determine the growth inhibition of the bacteria exposed to various peptide concentrations, an OD-based approach was used for measuring the cell density changes over a 4-hour incubation time in a microtiter plate. Mid-log phase bacterial cultures were diluted in MH broth to $2*10^6$ CFU/ml and 100 µl of each dilution were added to 100 µl of peptide solutions, previously prepared on a microtiter plate, or to 100 µl of medium with no peptide, as control. Thus, 200 µl suspensions with the peptide at half of the original concentration were placed inside a plate reader (Tecan Sunrise, Switzerland) and incubated at 37°C with intermittent shaking. The OD was measured at 620 nm at 10-min intervals for 25 cycles. The data,

performed in triplicate, were collected by Magellan 4 software (Tecan), transferred to an Excel sheet, where subtracted of the control, and then averaged and processed. These assays were carried out at least twice and usually 3 to 4 times, on separate days with freshly prepared bacterial suspensions.

2.2.9 Peptide internalization into bacterial cells

The uptake of BODIPY-labelled TUR1[Cys^{33}] in *E. coli* strains was determined and compared to that of the bovine ortholog Bac7(1-35)[Cys^{36}], prepared previously and well characterized (Benincasa et al., 2009), used as a positive control. A Cytomics FC 5000 instrument (Beckman-Coulter, Inc., Fullerton, CA) was used, equipped with an argon laser (488 nm, 5 mW) and a photomultiplier tube fluorescence detector for green (525 nm) filtered light. All detectors were set to logarithmic amplification. Optical and electronic noise were eliminated by setting the electronic gating threshold on the forward-scattering detector, while the data flow rate was kept below 300 events per second to avoid cell coincidence. At least 10,000 events were acquired for each sample. A standard bacterial culture was prepared in MH broth and then inoculated into 10 ml of fresh MH broth and left to grow two hours at 37°C into the logarithmic phase with shaking. After two hours the OD_{600} was measured, bacterial suspensions were diluted to 10^6 CFU/ml and 1 ml of the suspension was incubated with 0.1 μM TUR1-Cys-BY or Bac7(1-35)-Cys-BY for 10 or 60 minutes at 37°C. Note that the peptide concentrations used are below the MIC value, so that they should penetrate but not inactivate the bacteria. Bacteria were then collected by centrifuging at 10,000 rpm (RCF 16800g) for 5 minutes and the pellet was washed three times with Phosphate-Buffered-Saline, High Salt (PBS-HS, 400 mM NaCl; 10 mM $MgCl_2$ in 10 mM sodium phosphate buffer), to remove surface-bound peptide. Finally bacteria were resuspended in 1 ml of PBS-HS and assayed by flow cytometry according to the protocol established in (Benincasa et al., 2009). Data analysis was performed with the FCS express V3 software (De Novo Software, CA).

2.2.10 Permeabilization of bacterial membranes

Inner membrane permeabilization was determined by flow cytometry, measuring the uptake of propidium iodide (PI) by bacterial cells (Podda et al., 2006). Analyses were performed with the Cytomics FC 5000 instrument described in the previous section, but using a fluorescence detector for orange filtered light (620 nm). All detectors were set on logarithmic

amplification. Optical and electronic noise were eliminated by appropriately setting the electronic gating threshold and the flow rate kept to below 300 events/second and at least 10,000 events were acquired and stored as list mode files. For the analyses, samples of 10^6 CFU/ml were incubated in MH broth with the peptides at 37 °C for different times (5-60 min). PI (Sigma Aldrich) was then added to the peptide-treated bacteria to a final concentration of 10 μg/ml, and the cells were analysed in the flow cytometer after 4 min incubation at 37 °C. All experiments were conducted in triplicate. Data analysis was performed with the WinMDI software (Dr. J. Trotter, Scripps Research Institute, La Jolla, CA).

2.2.11 Cytotoxicity assays

The cytotoxic activity of TUR peptides against three different eukaryotic cell lines was determined by the 3-(4,5-dimethylthiazol-2-yl)-2,5-diphenyltetrazolium bromide (MTT) (Sigma-Aldrich) assay. This exploits the ability of metabolically active cells to reduce MTT, a yellow lipophilic molecule able to cross the cell membrane and reach the mitochondria, where it is reduced to formazan, a blue compound. This step allows discriminating viable and metabolically active cells, since the formazan crystals are observable by microscopy. These crystals are solubilised with Igepal-HCl and the absorption of the obtained solution can be quantified with a spectrophotometer, in order to correlate the optical density value with the amount of viable cells.

Toxicity of TUR6 and TUR1S were determined against U937 monocytic cells, deriving from a histiocytic lymphoma, growing in suspension. Toxicity of TUR1D was evaluated against A549 cells, deriving from basal alveolar epithelium of human lung cancer (growing in adhesion) and MEC-1, a lymphocyte cell line deriving from peripheral blood of a patient with chronic lymphocytic leukaemia (growing in suspension).

For MTT assays, U937 or MEC-1 cells were seeded in 90 μL complete medium in a 96-well plate, in the presence of different TUR concentrations (10 μl in PBS), and allowed to incubate for 24, 48 or 72 h. For A549 cells, after seeding in a 96-well plate in complete medium and allowing to adhere overnight, medium was replaced with TUR1D solutions at different concentrations in PBS (final volume 100 μl) and incubated for 1 hour. PBS was then replaced by complete medium and incubation allowed to proceed for 24 h. Alternatively, they were allowed to incubate for 24 h in the presence of different concentration of TUR1D in complete

medium. To perform the assay, 20 µl of 1:10-diluted MTT stock solution (5 mg/ml) was then added to each well, mixed, and incubated at 37°C in a humidified incubator (5% CO_2) for 4 hours. Igepal-HCl (100 µl) was added to each well to dissolve the purple formazan crystals, and absorbance was measured after overnight incubation with a Tecan plate reader at 550 nm. The viability index of treated cells was compared to that of untreated control (cells in medium without peptide). Experiments were performed at least in triplicate and repeated at least twice.

For the PI permeabilization assays, cells were twice washed with sterile PBS and centrifuged at 4°C for 5 min at 400g, and then $1x10^6$ cells/ml PBS were exposed to 10 µg/ml PI and 0-50 µM peptide. The cells were then analysed in the flow cytometer after 5-30 min incubation at 37 °C. For cell surface adhesion studies, $1x10^6$ cells/ml PBS were exposed to 0.25-10 µM

BODIPYlated peptide and incubated for up to 60 min at 37°C. Samples were run on the flow cytometer at 5, 15, 30 and 60 min, and % positive cells and MFI recorded. In parallel, at 30 and 60 min, cells were thoroughly washed to remove surface-bound peptide, and the MFI measured. The same sample was then treated with trypan blue quencher and a second MFI measurement obtained. This allowed determining fluorescence from only internalized peptide.

Flow cytometry was carried out with a FC500 Beckman Coulter instrument. Data analysis was performed with the FCS express V3 software (De Novo Software, CA). Statistical analysis was carried out using Graphpad software (Anova Student Newman Keuls post test)

2.3 RESULTS and DISCUSSION

2.3.1 Identification of *Tursiops truncatus* cathelicidins

The sequences of seven different bottlenose dolphin cathelicidins, named Tur1 - Tur7, were identified by prof. G. Manzini (Dept. Life Sciences, Univ. Trieste, private communication) from different genomic databases; mainly in the NCBI Nucleotide Collection, WGS and EST archives. More recently, it has been possible to identify the sequences also in the Ensemble partial assembly (turTru1) of the Tursiops genome. As direct amplification and sequencing (see below) in some cases resulted in residue differences, the database sequences are indicated with a "D" suffix (for database derived) (see **Table 2.3.1**).

TUR1D is a proline-rich sequence of 32 residues with a charge of +10. It is homologous to the bovine Bac7 N-terminal region and to porcine PR-39. **TUR2D** (28 residues) is a putatively amidated, α-helical peptide and shows a significant identity with **TUR3D** (27 residues). They appear to be orthologous to bovine BMAP-27 and porcine PMAP-36. **TUR4D** has 12 residues and is orthologous to bovine dodecapeptide, so is likely an S-S bridged loop. **TUR5** has a significant homology to the N-terminal part of bovine BMAP-34 and porcine PMAP-37, so is likely orthologous to the ubiquitous *CAMP* cathelicidin gene product (LL-37 in human). However, it seems to be truncated half way (see Table 2.3.1), due to a frame-shift deletion. Curiously, another highly homologous sequence was identified (**TUR7D**), that has the full CAMP peptide sequence, but seemed to consist of an isolated exon 4, which includes the proteolytic cleavage site (see **Figure 1.3**) but is not connected in any way to exons 1-3 corresponding to the CLD (pro-region). Finally, **TUR6D** (28-residues) is a putatively amidated, α-helical peptide with charge +8 and appears orthologous to bovine BMAP-28 and ovine SMAP-29.

Further searching of the databases revealed a variant of TUR1D with a three residue difference, which was named **TUR1V** (see **Table 2.3.1**). A 28-residue variant of TUR3D was also found that more closely resembled TUR2D (named **TUR3V**), suggesting multiple helical cathelicidin peptides.

The putative cathelicidin-derived peptide sequences showed some worrying anomalies.

i) There seemed to be multiple paralogues of the helical peptide corresponding to BMAP-27 (TUR2D, 3D and 3V).

Table 2.3.1. Tursiops cathelicidin-related peptides and their physico-chemical properties.

Peptide[1]	Sequence[2]	n[3]	q[4]	MW[5](Da) Predicted	MW (Da) Measured	<H>[6]	μH_{rel}[7]
TUR1D	RRIRFRPPYLPRPGRRPRFPPPFPIPRIPRIP-OH	32	+11	3972.9	3973.0	-0.86	n.a
TUR1V	RRIRFRPPYLPRPGLRPRFPPDFPIPRILRKR-OH	32	+11	4038.0	n.d.	-1.09	n.a.
TUR1S	RRIPFWPPNWPGPWLPPWSPPDFRIPRILRKR-OH	32	+7	4034.2	4033.2	0.32	n.a
TUR2D	GRFRRLRHRIGRVLSKVGRIVGPLIRIL-NH_2	28	+9	3294.2	3294.1	-0.42	0.66
TUR3D	GIFRWLRH-IGRVLPKVGRIVGPLIGIW-NH_2	27	+5	3108.9	3109.0	1.78	0.64
TUR3V	GIFRWLRHRIGRVLPKVGRIVGPLIGIW-NH_2	28	+7	3265.08	n.d.	1.36	0.56
TUR3S	GRFRRLRHRIGRVLPKVGRIVGPLIGIW-NH_2	28	+8	3278.08	n.d.	-0.01	0.60
TUR4D	QRCRIIVIRMCR-OH	12	+4	1545.0	n.d.	-1.31	0.24
TUR4S	QGCRIVVIRMCR-OH	12	+3	1433.8	1432.6	-1.06	n.a.
TUR6D	RGLRSLGRNILRGWKKYGPIIVPIIRLI-NH_2	28	+8	3258.1	3258.6	0.57	0.66
TUR6S	RGLRSLGRKILRGWKKYGPIIVPIIRLI-NH_2	28	+9	3272.1	3272.7	0.47	0.66
TUR5	GLFRWLGDFLQRGGRR-OH	16	+3	1934.2	1933.9	-0.31	0.67
TUR7	GLFRRLGDFLRRGGEKTGKKIERIGQRIKDFFGIFQPSKQS-OH	41	+7	4768.6	n.d.	-1.79	0.57

[1] In the peptide name, D indicates it is the main sequence found in the nucleotide databases, V indicates it is a less frequent variant, S indicates that the sequence was obtained by DNA sequencing.

[2]Sequence identity (grey shading) is relative to the first sequence in each series.

[3] n = N° of residues; [4]q = charge;

[5] MW calculated from sequence using Peptide Companion or measured for synthesized peptides on a Bruker Daltonics Esquire 4000 instrument;

[6]<H> = mean hydrophobicity; [7] μH_{rel}, mean relative hydrophobic moment, calculated using the HydroMCalc software.

ii) The ubiquitous CAMP gene, present in all placental mammals, carried a severely truncated peptide due to a frameshift deletion in the 4th exon, and furthermore, a +C frame-shift insertion in exon 3 of the CLD also leads to a premature stop codon. This suggested the sequence coding for TUR5D is a pseudogene.

iii) A sequence corresponding to complete CAMP-like peptide was in fact also present (TUR7), but completely devoid of the CLD (i.e. only an isolated sequence corresponding to exon 4 was present).

Given the relatively low coverage of the Tursiops sequence, these apparent anomalies could be due to sequencing errors, so this encouraged the isolation and direct sequencing of cathelicidin genes from genomic DNA obtained from a dolphin muscle tissue samples. The genes were in fact sequenced in the Pallavicini laboratory (Dept. Life Sciences, Univ. Trieste, private communication) using primers derived from the identified sequences for both selective amplification and sequencing via the Sanger method. The derived AMP sequences are shown in **Table 2.3.1** and are defined by the suffix 'S' (for sequenced).

Comparison with the database sequences confirmed the anomalies of the CAMP gene orthologues (TUR5 pseudogene with 2 premature stop codons, and isolated TUR7 sequence corresponding only to exon 4 of cathelicidins). On the other hand, it revealed unexpected structural difference in the other peptide sequences, which could lead to functional differences. TUR1D was not confirmed by sequencing, but a Pro-rich paralogue, curiously rich in Trp residues, was found (see **TUR1S** in **Table 2.3.1**). A sequence intermediate to TUR2D and TUR3V was found, similar but not identical to TUR3V. A version of TUR4D was found with an R→G variation reducing charge to +3 (**TUR4S**). Finally, the sequence of TUR6 showed an N→K variation, increasing charge increased to +9.

Confirmation of sequences would also derive from expression studies, but unfortunately, fresh dolphin blood or tissue were not available to extract RNA. Consequently, the peptides I selected to analyse in this thesis were based on informed guesses as to which could be most interesting. Only in 2016, data became available in the SRA archives that allowed checking which sequences were actually expressed. Morey et al. (2016) provided RNA-seq data from the blood of four individuals, taken over a period of a year. Foote et al. (2015) analysed RNA from multiple individuals and different tissues (kidney, spleen, muscle and liver). We carried out a preliminary evaluation of expression by BLASTing the sequence of exon 4 for each TUR peptide against the appropriate entries in the SRA database. The number of hits was considered to be roughly correlated to the expression level; high expression for >100 hits

(saturation of the BLAST search), intermediate expression for < 100 hits, and week expression for less than 10. Results are summarized in **Table 2.3.2**.

Preliminary results indicate that both TUR1D and S are differentially expressed at good levels, in blood and spleen, but not continuously. TUR2D, 3D and 3V were all also expressed differentially and not continuously. They have the widest tissue distribution, being found in blood, spleen and muscle. TUR4D was present in all individuals at all times at high levels, while TUR4S was sometimes found at quite low levels. TUR5 was apparently not present (which may confirm it is a pseudogene) and neither was TUR7. TUR6D was expressed at low levels and only in defined periods, while TUR6S was not found. Taken together, these results suggest that TUR4D is constitutively expressed and may be accompanied by a minor variant TUR4S. TUR1D and S are both strongly inducible. All of TUR2D, TUR3D and TUR3V are inducibly expressed at moderate levels, while TUR6D is inducibly expressed at low levels.

Table 2.3.2. Expression levels for dolphin cathelicidins based on BLAST hits in the SRA archives of *T. truncatus* RNA.

	TISSUE					
peptide	Blood	Liver	Kidney	Spleen	Muscle	Skin
TUR1D	++++	-	-	+	-	-
TUR2D	++	-	-	+	-	-
TUR3D	++	-	-	-	-	-
TUR3V	+++	-	-	+	+	-
TUR4D	+++++	-	-	-	-	-
TUR5	-	-	-	-	-	-
TUR6D	+	-	-	-	-	-
TUR7	-	-	-	-	-	-
TUR1S	+++	-	-	-	-	-
TUR3S	-	-	-	-	-	-
TUR4S	+	-	-	-	-	-
TUR6S	-	-	-	-	-	-

Finally, the TUR1-7 sequences were BLASTed against the Genebank databases selecting other cetacean species, and hits were collected for the river dolphin (*Lipotes vexillifer*), the

killer whale (*Orcinus orca*), the sperm whale (*Physeter macrocephalus*), and the minke whale (*Balaenoptera acutorastrata*). Orthologues corresponding most closely to each peptide are shown in **Table 2.3.3.** The genomes of these organisms are not complete or fully assembled, so some orthologues may be missing. Peptides corresponding to the complete TUR1 - TUR7 range were variously found in the other species, suggesting that this cathelicidin gene repertoire predates the differentiation of cetaceans from the land-based common ancestor. TUR5 is confirmed as a pseudogene in all species, and TUR7 is always present as an isolated exon. Otherwise, the pattern of ortologies is quite diverse, and curiously, TUR1D, 3D and 6D are not represented, as orthologues seem closer to V or S variants (based only on the mature peptide region). Furthermore, for all the other cetaceans only one representative of each cathelicidin was found. This may have two explanations; *i)* the repertoires for the other analysed cetacean species are incomplete or *ii)* the bottlenose dolphin has embarked on an evolutionary trajectory that has resulted in multiple gene duplications followed by diversification.

Table 2.3.3. Orthologues to *Tursiops truncatus* cathelicidins in other cetacean species[a].

T.t	*L.v*	*O.o*	*P.m*	*B.a*
TUR1D				
TUR1V	✓			✓
TUR1S		✓		
TUR2D	✓			✓
TUR3D				
TUR3V			✓	
TUR3S		✓		
TUR4D	✓	✓		
TUR4S			✓	
TUR5 (pseudogene)	✓	✓	✓	✓
TUR6D				
TUR6S	✓	✓	✓	✓
TUR7 (only exon 4)	✓	✓	✓	✓

a) *L.v*. river dolphin (*Lipotes vexillifer*); *O.o* the killer whale (*Orcinus orca*); *P.m*. the sperm whale (*Physeter macrocephalus*); *B.a*. minke whale (*Balaenoptera acutorastrata*).

2.3.2 *Tursiops truncatus* cathelicidins selected for further characterization

Faced with 7 cathelicidins to characterize, some present in multiple variants, I had to select a limited workable number. Based on their different conformations, I concentrated my work on three distinct structural types, one PR-AMP, one cyclic peptide, and one helical peptide. Within these three types, I selected particular peptides based on specific characteristics. Some of the other peptides have in any case been subject to preliminary characterization as part of student internships.

a) **PR-AMP**. I selected the **TUR1D** sequence for synthesis, which is structurally and functionally related to the bovine Bac7 and porcine PR-39, as shown in the alignment below, the genes likely being orthologous. The dolphin peptide is however significantly shorter, showing 53% identity to the equivalent stretch of Bac7 and 56% with PR-39.

```
TUR1D      RRIRFRPPYLPRPGRRPRFPPPFPIPRIPRIP                              32
TUR1S      RRIPFWPPNWPGPWLPPWSPPDFRIPRILRKR                              32
PR39       RR-RPRPPYLPRPRPPPFFPPRLPPRIPPGFPPRFPPRFP                      39
Bac7       RRIRPRPPRLPRPRPRPLPFPRPGPRPIPRPLPFPRPGPRPIPRPLPFPRPGPRP       55
```

Identity, in grey shading, assigned relative to the sequence of TUR1D

As PR-AMPs are known to have a potent activity against Gram-negative strains, but not against Gram-positives (Scocchi et al., 2011), and act internally, a peptide variant with a cysteine residue at the C-terminus, **TUR1D[Cys^{33}]**, was also synthesized separately for conjugation with the fluorescent probe BODIPY. This allowed evaluation of its internalization capacity into bacterial cells by using flow cytometry.

TUR1S has only 53% homology with TUR1D, so is an apparent paralogue, and has a lower identity with the pig and cow orthologues. It has a significantly lower charge and is particularly rich in Trp residues, so is likely have a somewhat different mode of action. The peptide was synthesised in a student internship and was available for characterization. The further presence of **TUR1V** (not synthesised) suggests that PRAMPs are present in multiple copies in cetaceans, like in other artiodactyls, although only one such gene was confirmed in the other cetacean species.

b) **Dodecapeptide**. **TUR4** has a high sequence homology with the cyclic dodecapeptides (also known as Bac1 or Bct1) of sheep and bovine, particularly concerning the position and spacing of the two cysteines that are essential for the formation of the intramolecular disulfide bond (see alignment below). The close homology to the bovine dodecapeptide, rather than to porcine protegrins, suggests a closer relationship to bovids than pig, in agreement with the accepted phylogenetic relationship (see **Figure 1.7** in Chapter 1)

```
TUR4D           QRCRIIVIRMCR
TUR4S           QGCRIVVIRMCR
Bac1 (sheep)    RICRIIFLRVCR
Bac1 (cow)      RLCRIVVIRVCR
```

Identity, in grey shading, assigned relative to the sequence of TUR4D

Synthesis of cyclic peptides is not facile, and even more so for dodecapeptide (see prediction in section 2.2.2, **Figure 2.2.1**) so it was decided to synthesise only one ortholog, TUR4S, as the most different from the other dodecapeptides, with a charge of only +3. This was before determining that TUR4D was constitutively expressed at high levels.

c) **Helical peptides. TUR6** variants are linear, helical peptides that appear to be orthologous to ovine SMAP-29 and bovine BMAP-28 (see alignment below). This orthologue is not present in pig, again confirming a closer relationship of dolphins to ruminants. The rather high level of identity (85% with BMAP-28) suggests that these peptides are quite conserved in cetartiodactyls and may be subject to purifying selection, further suggesting they may have an important defensive role.

```
TUR6D                   RGLRSLGRNILRGWKKYGPIIVPIIRLI-(am)
TUR6S                   RGLRSLGRKILRGWKKYGPIIVPIIRLI-(am)
SMAP-29(Ovis aries)     RGLRRLGRKIAHGVKKYGPTVLRIIRIA-(am)
BMAP-28(Bos taurus)     GGLRSLGRKILRAWKKYGPIIVPIIRI-(am)
```

Identity, in grey shading, assigned relative to the sequence of TUR6D

TUR6D and TUR6S differ by only an N→K substitution in position 9. Lysine in this position seems to be the more common, as it is conserved in cow, pig and all other analysed cetacean species. Indeed the orca sequence is identical to TUR6S. For this reason, it was deemed interesting to synthesize both TUR6 peptides. The variation results in a charge increased to +9, an important parameter for antimicrobial activity (Tossi et al., 2000).

2.3.3 Peptide synthesis and preparation

All peptides were synthesized in solid phase (SPPS) using the Fmoc chemistry. Before the synthesis, the peptide sequences were analysed with the program *Peptide Companion* in order to develop an appropriate synthesis protocol and obtain the maximum yield possible, by using double coupling cycles as requested. Curiously, it was the shortest peptide (TUR4S) that was predicted to be the most difficult to synthesize, followed by TUR6. The presence of multiple prolines instead facilitated the synthesis of TUR1 peptides. It was therefore decided to apply double-couplings at all positions for TUR4S and TUR6D while for TUR1 it was only applied for the C-terminal stretch, especially for the analogue with Cys^{33}

In this manner, the correct peptides were synthesized in good yields on a Biotage Alstra microwave machine (see **Table 2.3.4**) with temperature set to 75°C (see **section 2.2.2**). All peptides were then purified by reverse-phase HPLC on a Phenomenex preparative column (for an example see **Figure 2.3.2**), and high levels of purity (> 95%) were confirmed using a Waters Symmetry analytical column, followed by ESI-MS column. The elution profiles for the peptides (%CH_3CN at peak maximum) correlated well with the estimated peptide hydrophobicity shown in **Table 2.3.1** (see **Figure 2.3.1**). After purification, the correct structure and the purity of all peptides was also confirmed using ESI mass spectrometry (see **Figure 2.3.3**). All peptides were then lyophilized from HCL to remove TFA.

TUR4S was synthesized as the reduced linear peptide and then oxidised at low concentration in an ammonium acetate/EDTA/guanidinium HCl solution, in the presence of cystine and cysteine in order to catalyse the formation of the intramolecular disulfide bond (see **section 2.2.2**). The reaction was monitored by analytical RP-HPLC and ESI-MS (**Figure 2.3.4**), and after completion, the cyclic peptide was purified by exploiting the distinctly different elution times of folded and not-folded peptide.

Conjugation of the fluorescent dye BODIPY-FL [N-(2-aminoethyl)-maleimide] to TUR1D[Cys^{33}] was similarly monitored and observed to go to completion overnight. The product was then separated by semi-preparative RP-HPLC in good purity (see **Figure 2.3.5).**

Table 2.3.4. TUR peptide yields at different stages of preparation

Peptide	Yield [(a)]	MW (calculated) [(b)]	MW (ESI-MS) [(d)]
TUR1D	80 %	3972,9	3972,3
TUR1S	45 %	4032,8	4033,2
TUR1D[Cys^{33}]-BY	30 %	4489,8	4489,9
TUR4S	45 %	1429,8	1430,7
TUR6D	70 %	3259,1	3258,4
TUR6S	50 %	3273,1	3272,7

[(a)]Yield percentages of crude peptides; [(b)] Theoretical molecular weights calculated with *Peptide Companion;* [(c)] Molecular weights obtained by ESI-MS.

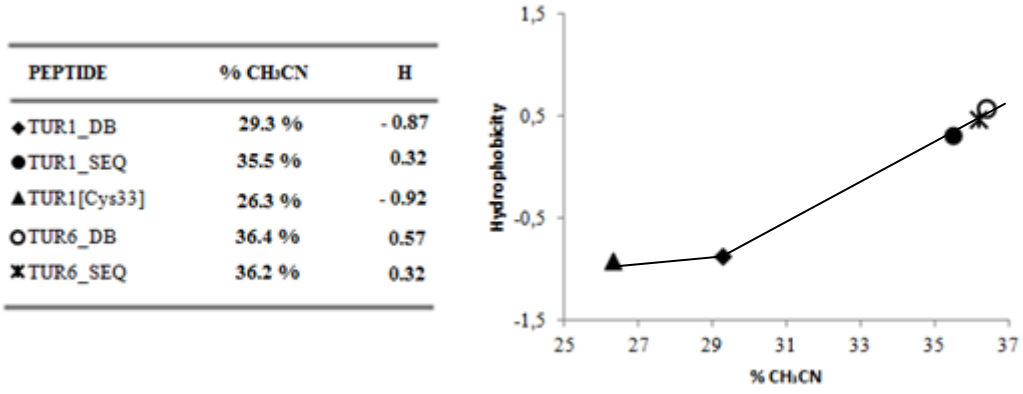

Figure 2.3.1. Correlation between elution and hydrophobicity for TUR peptides. [(a)] % acetonitrile at the elution peak maximum; [(b)] mean per residue hydrophobicity (HydroMcalc programme).

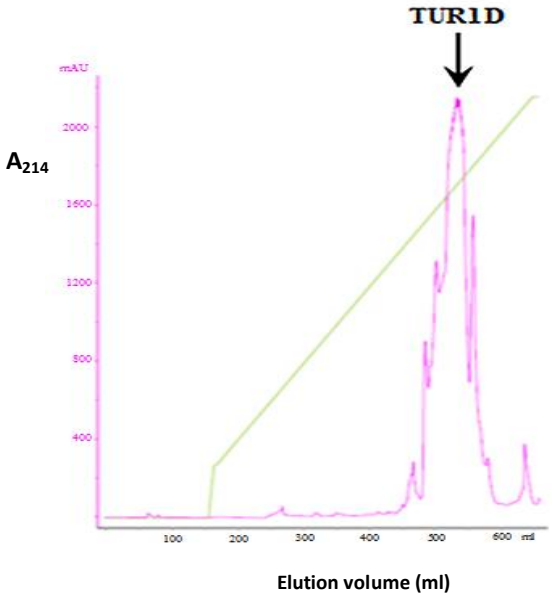

Figure 2.3.2. Example of preparative RP-HPLC chromatogram. TUR1D crude peptide. The peak corresponding to the correct peptide is indicated by the arrow (flow rate 8 ml/min, 5-35% CH_3CN in 60min).

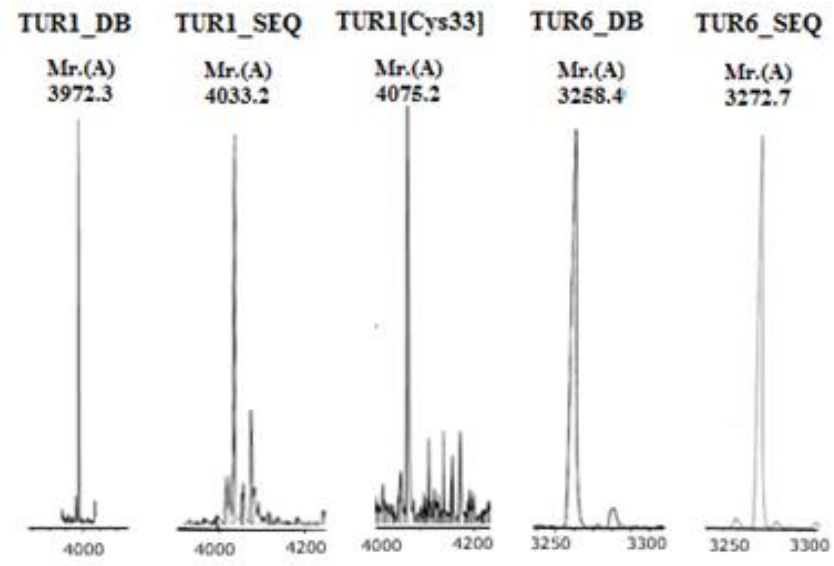

Figure 2.3.3. Mass spectral peaks for purified TUR peptides. Reconstructed spectra based on the m/z base spectra deconvoluted by the Bruker Daltonics DataAnalysis 3.3 software. Mr is the reconstructed average molecular weight.

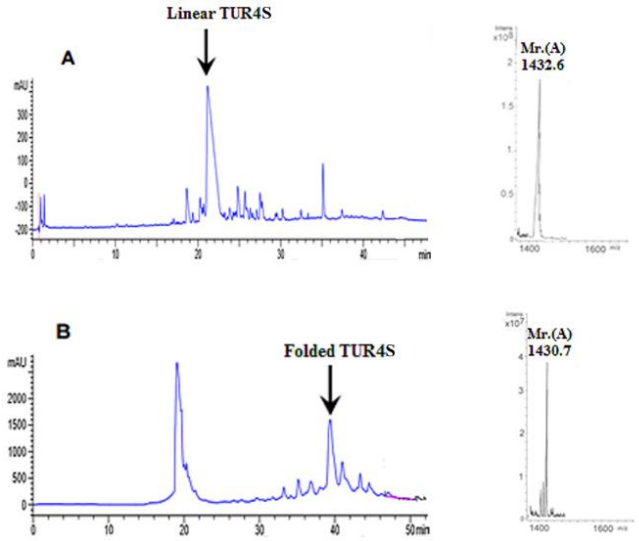

Figure 2.3.4. Folding reaction of TUR4S. A) analytical RP-HPLC spectra at 214 nm of crude, linear peptide and corresponding ESI-MS of the main peak; B) RP-HPLC after 4 hours folding reaction and corresponding ESI-MS of the reduced peptide. (flow rate 0.8 ml/min, 5-45% CH_3CN in 60min).

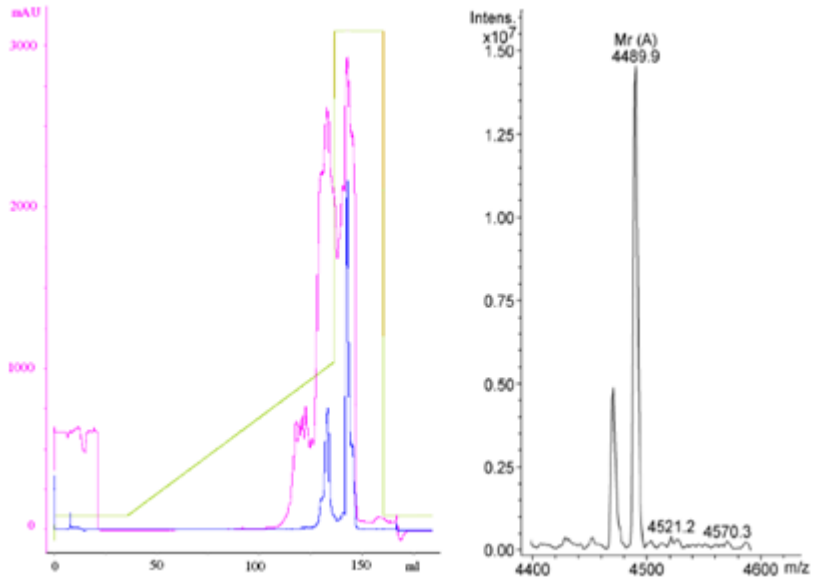

Figure 2.3.5. BODIPY labelling reaction of TUR1D[Cys^{33}]. Preparative RP-HPLC spectra (left) and ESI-MS of the main peak (right). The chromatogram shows the absorption at 214 nm (pink) and at 280 nm (blue) (flow rate 2 ml/min, 5-35% CH_3CN in 50 min).

2.3.4 Peptide quantification

Accurate quantification is necessary to perform rubust functional assays. However, is not easy to determining the correct peptide concentration by using spectrophotometric methods. It was therefore decided to compare the weight concentration of peptides with that obtained by measuring the absorbance at 214 nm and 280 nm, where the peptide bond and sidechains (especially tryptophan) respectively absorb. Since TUR4 peptide has no aromatic residues, the Waddell method was used for quantification instead. TUR1[Cys^{33}]-BY was quantified by measuring the absorbance at 504 nm, the absorption wavelenght of BODIPY. **Table 2.3.5** lists the calculated molar extinction coefficients for the peptides [according to (Kuipers and Gruppen, 2007)]. These measurements provided a final averaged concentration with an accetable error.

Table 2.3.5. Tables of concentration values obtained after the quantification. Concentrations were estimated using using several methods[a].

	Concentrations (mM)							
Peptide	**[Wt]**	**ε_{214} (M^{-1} cm^{-1})**	**[214]**	**ε_{280} (M^{-1} cm^{-1})**	**[280]**	**[Wad]**	**[504]**	**[Final]**
TUR1D	1.46	83850 ± 1160	1.38	1250 ± 150	1.04	-	-	1.3± 0.2
TUR1S	3.42	183450 ± 8050	3.39	22000 ± 300	3.32	-	-	3.4± 0.05
TUR1D-BY	1.16	84800 ± 1162	1.28	1250 ± 150	-	-	1.34	1.25± 0.1
TUR4S	3.49	12600 ± 180	3.28	125 ± 50	-	3.15	-	3,3± 0.15
TUR6D	2.10	65500 ± 4045	2.01	6750 ± 212	1.95	-	-	2.0± 0.05
TUR6S	3.89	65500 ± 4045	3.30	6750 ± 212	3.19	-	-	3.5± 0.4

Concentration by: [Wt] = by weight; [214] = by absorption at 214nm; [280] = by absorption at 280 nm (mainly Trp); [Wad] = by the Waddle 214nm/220nm absorption method; [214] = by absorption at 504nm (BODIPY); [Final] = average concentration with error.

2.3.5 Antimicrobial activity: the bacteriostatic activity

The bacteriostatic activity (MIC) of both TUR1 peptides was determined against *E.coli* ATCC 25922 and *S. aureus* ATCC 25923, representative respectively of a Gram-negative species susceptible to PR-AMPs and an unsusceptible Gram-positive one. The activity was also determined for the well-characterized characterized bovine Bac7(1-35), of comparable length, and an available fragment of porcine PR-39. TUR1D has a comparable activity to Bac7(1-35) against *E. coli* and is similarly inactive against *S. aureus*. TUR1S has a reduced but still appreciable activity which might, in part, result from the lower charge (see **Table 2.3.6).** However, this is likely not be the only significant parameter, considering that Bac7(1-15) and PR-39(1-18) fragments of comparable charge have significantly lower activities. The peptide did not show activity against *S. aureus*, despite being significantly more hydrophobic than the other PR-AMPS (see **Table 2.3.1**) due to several Trp residues. This suggests that it does not switch to a membranolytic mode (Podda et al., 2006).

Overall, the activity of TUR1D is consistent with that previously reported for the bovine and pig cathelicidin PR-AMPs, i.e. a spectrum of action limited to bacteria, which express the SbmA transport system, present in Gram-negative enterobacteria but not in Gram-positive species. It suggested that the TUR1 peptides might by a similar mechanism.

Table 2.3.6. MIC values for TUR peptides compared to Bac7 and PR-39 fragments.

		MIC (μM) [(a)]	
Peptide (charge)		***E.coli* ATCC 25922**	***S. aureus* ATCC 25923**
TUR1D	**+11**	1	>32
TUR1S	**+7**	8	>32
Bac7 (1-35)	**+11**	1	>32
PR-39 (1-18)	**+6**	>32	>32
Bac7(1-16) [(b)]	*+8*	*2*	*>32*
Bac7(1-15) [(b)]	*+7*	*>32*	*>32*

(a) Results reflect three separate experiments, carried out in duplicate, using the micro-dilution method, inoculating 2.5 * 10^5 cfu/ml in full Mueller-Hinton broth and incubating plates at 37 ° C for 20 hours. MIC values were evaluated visually by identifying the first well with no turbidity. (b) From (Benincasa et al., 2004)

To confirm this, the activity of the TUR peptides was determined against an *E. coli* deletion mutant lacking the SbmA transporter. This homodimeric inner membrane transporter is related to ABC transporters but powered by the membrane potential (Runti et al., 2013). The deletion mutant was obtained from the Keio Collection (see **Table 2.2.2**) and is derived from the BW25113 strain (see **Figure 2.3.6**). Besides SbmA, the wild type strain also expresses another possible transporter of PR-AMPS, the YjiL inner membrane protein. This is a putative ATPase associated with the multidrug transporter MtdM to form part of an efflux pump (Krizsan et al., 2015). It was also possible to obtain the *ΔyjiL* deletion mutant from the Keio collection, while the *ΔyjiL / ΔsbmA* double deletion mutant was kindly donated to us by the Hoffmann group. A differential activity of the TUR1 peptides against these strains should provide useful information on the mechanism of action, and reveal which transporter(s) are important for internalization, not forgetting that at higher concentrations PR-AMPs are known to switch to a membranolytic mode of action (Podda et al., 2006).

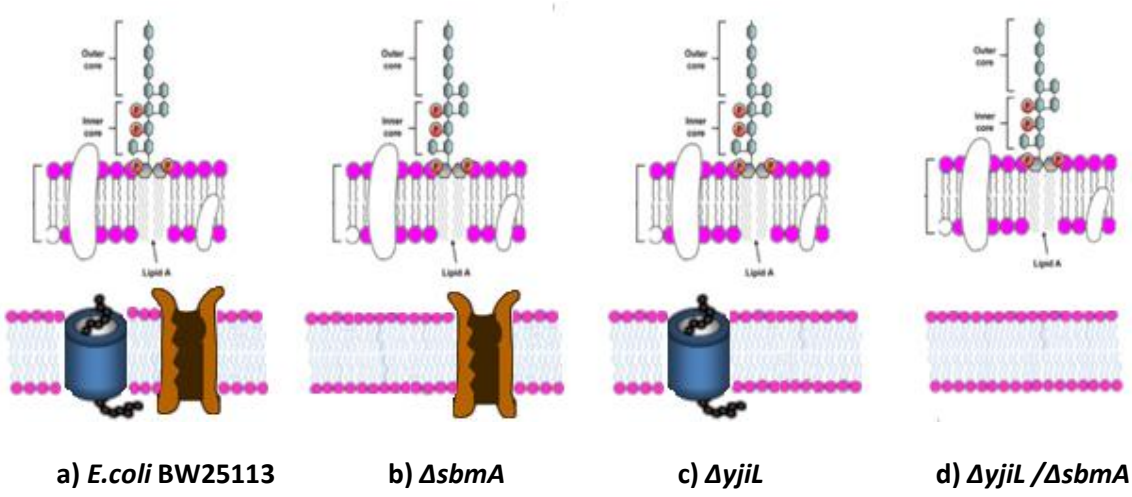

Figure 2.3.6. Schematic representation of *E.coli* strains used to test TUR1 orthologues. BW25113 is derived from the ATCC 25922 reference strain but is lacking the O-antigen in its outer membrane LPS. The blue cylinder represents YiJL/MdtM efflux transporter, while the brown channel represents the homodimeric SbmA transporter. The *ΔyjiL* and *ΔsbmA* knockout mutants were obtained from the Keio collection while the *ΔyjiL / ΔsbmA* double mutant was kindly provided by Hoffmann's group (see **Table 2.2.2**)

As summarized in **Table 2.3.7**, TUR1D and Bac7 (1-35) have a comparable activity, in the low micromolar range, against either the ATCC 25923 or the BW 25113 strain, so that the presence of the O-antigen is not an impediment to their action. However, while Bac7 lost activity against the *SbmA* KO mutant, TUR1D remained almost equally active. Both peptides were active against the *YjiL* KO mutant, but significantly less active against the double mutant. TUR1S maintained a comparable activity, with MIC of about 8 μM, against all tested strains. This generally lower activity is again conducible to the decreased cationicity, which could cause *a)* a less efficient passage through the bacterial outer membrane; *b)* decreased electrostatic interaction with the anionic surface of the bacterium, necessary to attract the peptide towards the transport system; *c)* decreased interaction with the transport systems and/or its internal target.

Overall, this data indicate: *i)* that both SbmA and YjiL are transport systems for PR-AMPs, but SbmA seems to be the principle one. *ii)* YjiL is an efficient accessory transport system for TUR1, that can use it in the absence of SbmA at comparable concentrations, but is less efficient in transporting Bac7; *iii)* TUR1S is either intrinsically less efficiently transported by either system, or has a different, and less efficient mechanism of action against this bacterium.

Table 2.3.7. MIC values for TUR1 peptides, Bac7 and a PR-39 fragments against selected knockout mutants of E. coli BW 25113.

	MIC (μM) [(a)]				
	E.coli **ATCC 25922**	***E.coli*** **BW 25113**	***E.coli*** **BW 25113 *ΔsbmA***	***E.coli*** **BW 25113 *ΔyjiL***	***E.coli*** **BW 25113 *ΔyjiL/ΔsbmA***
TUR1D	1	1	2	2	8
PR-39 (1-18)	>32	>32	>32	>32	>32
Bac7 (1-35)	1	2	8	2	16
TUR1S	8	8	4	8	8

a) Reflects three separate experiments carried out in duplicate, using the micro-dilution method, inoculating 2.5 * 10^5 cfu/ml in full Mueller-Hinton broth and incubating plates at 37 ° C for 20 hours. MIC values were evaluated visually by identifying the first well with no turbidity.

The antimicrobial activity of the helical TUR6 orthologues was determined against *E. coli* ATCC 25922 and *S. aureus* ATCC 25923 and is shown in **Table 2.3.8**. In this case, these activities were compared with those of with the bovine orthologue BMAP-28 and ovine SMAP-29. Both TUR6 peptides show a good antimicrobial activity towards both bacteria, which compared well with the bovid peptides. SMAP-29, with an average MIC value of 0.5 μM against *E.coli*, is the most potent, this value being one of the lowest found in a comparative analysis of a number of natural antimicrobial peptides. Comparing its activity to that of the other orthologues suggests this is likely due to its high positive charge (+10, over $^1/_3$ of residues are cationic), which may also explain the slightly better activity of TUR6S (+9) with respect to TUR6D and BMAP-28 (+8).

Table 2.3.8. MIC values for TUR6 peptides compared to bovine and ovine orthologues.

		MIC (μM) [(a)]	
	charge	***E.coli* ATCC 25922**	***S. aureus* ATCC 25923**
TUR6D	+8	2	2
TUR6S	+9	1	2
BMAP-28	+8	2	2
SMAP-29	+10	0.5-1	1

(a) Experiments were repeated three times in duplicate and the values were obtained using micro-dilution, inoculating 2.5 * 10^5 CFU / ml in 100% Mueller-Hinton broth and maintaining the plates at 37 ° C for 20 hours. The MIC values were then evaluated by observing the turbidity of the lowest concentration at which bacterial growth was inhibited.

Finally, the cyclic dodecapeptide orthologue, TUR4S, was tested, against both *E. coli* ATCC 25922 and *S. aureus* ATCC 25923 (see **Table 2.3.9**), as the bovine dodecapeptide is reported to be active against these species (Romeo et al., 1988), (Lee et al., 2008). As preliminary assays indicated a lack of activity, it was tested also under more permissive conditions, to take possible medium and salt effects into account (e.g. switching from 100% MH broth to 20% MH broth in 10 mM phosphate buffer), and using the helical TUR6D as positive control.

Nonetheless, the peptide showed no activity up to 64 μM against either strains irrespective of conditions, and this was confirmed by growth kinetics assays (data not shown).

This cast some doubt as to a direct antimicrobial function for this peptide. The fact that it is less active than reported for the bovine orthologue on these reference laboratory bacterial strains may again be the lower charge (+3), which could affect this type of activity. However, it might remain active against specific pathogens faced by the dolphin. To try to answer the first question, it was tested against a number of aquatic pathogens.

Table 2.3.9. MIC values for TUR4S.

	MIC (μM) [a]	
	***E. coli* ATCC 25922**	***S. aureus* ATCC 25923**
TUR4S (in 100 % MH)	>32	>32
TUR4S (in 20 % MH)	>32	>32
Bac1(LB broth)[b]	*1-2*	*4-8*
Bac1(MH broth)[c]	*4*	*4*
TUR6D (in 100 % MH)	2	2

(a) Experiments were repeated three times in duplicate and the values were obtained using micro-dilution, inoculating 2.5 * 10^5 CFU / ml in 20% or 100% Mueller-Hinton broth and maintaining the plates at 37 ° C for 20 hours. The MIC values were then evaluated by observing the turbidity of the lowest concentration at which bacterial growth was inhibited. (b) Measured against *S. aureus* KCTC 1621and *E. coli* KCTC 1682 in LB broth (Lee et al., 2008). (c) Measured against *S. aureus* ATCC25923 and *E. coli* ML-35 in full MH broth (Skrbec D, Degree Thesis 2002, Faculty of Pharmacy, University of Trieste).

2.3.6 Antimicrobial activity of TUR peptides against aquatic and terrestrial bacteria.

To evaluate if TUR peptides may have a selective activity against other bacterial strains than the standard laboratory ones, their bacteriostatic activity was determined against a wide range of aquatic and terrestrial bacteria. Some of these are reported to infect the bottlenose dolphin. (e.g. *Pseudomonas fluorescens*, *Aeromonas hydrophila*), while other species known to infect other aquatic organisms (*Aeromonas Salmonicida, Vibrio anguillarum, Yersinia ruckeri,*

Lactococcus garviae). All five TUR AMPs were used in order to test the activity with widely different conformations, and results are summarized in **Table 2.3.10.**

Table 2.3.10. MIC values for TUR peptides against bacterial species known to infect aquatic organisms.

	MIC (μM) [(a)]					
	Gram negative					*Gram positive*
	P.fluorescens **LMG 1794**	***A.hydrophila*** **ATCC 7966**	***A.salmonicida*** **NCIMB 1102**	***V.anguillarum*** **ATCC 43305**	***Y.ruckeri*** **NCIMB 1315**	***L.garviae*** **ATCC 49156**
TUR1D	>32	>32	>32	>32	>32	>32
TUR1S	>32	>32	>32	>32	>32	>32
TUR6D	4	>32	2	2	0.5	0.5
TUR6S	4	>32	2	1	0.5	0.5
TUR4S	>32	>32	>32	>32	>32	>32

(a) Experiments were repeated three times in duplicate and the values were obtained using micro-dilution, inoculating 2.5 * 10^5 CFU / ml in 100% Mueller-Hinton broth and maintaining the plates at 37 ° C for 20 hours. The MIC values were then evaluated by observing the turbidity of the lowest concentration at which bacterial growth was inhibited.

These assays were not always straightforward, as the growth conditions vary significantly for different bacterial species, with respect to the required medium, incubation temperatures etc. Overall, it could be observed that the proline-rich TUR1 peptides and cyclic TUR4 did not have an appreciable antimicrobial activity against the tested aquatic bacteria, in the assay. The TUR6 peptides were both instead broadly active and particularly potent against the Gram-positive *L. garviae* and Gram-negative *Y. ruckeri* species. Only *A. hydrophyla* was quite resistant to all tested peptides.

Interesting results were obtained using the TUR peptides against typically terrestrial bacteria, some of which are emerging pathogens. The species used were all Gram negative (*Pseudomonas aeruginosa*, *Acinetobacter baumannii* and *Klebsiella pneumoniae*) and are all implicated in several human diseases (Kharami et al., 1989), (Gasink et al., 2009), (McConnell et al., 2013) (see **Table 2.3.11**). The PR-AMPs have an appreciable antimicrobial activity, in particular towards *Acinetobacter baumannii* and *Klebsiella pneumoniae*, both of

which are known to be susceptible to PR-AMPs. In this case, TUR1S is almost as effective as TUR1D, so it could be an adaptation to target other Gram-negative species bearing the PR-AMP transporter(s), against which the presence of multiple Trp residues is useful. Again, the TUR6 peptides display a most potent activity, with TUR6S having the lowest MIC. Unfortunately, TUR4S continued to be inactive.

Overall, the TUR peptides display activities that are in line with those of their orthologues from terrestrial animals, but with some interesting peculiarities; *a)* the fact that TUR1D has the capacity to use either the principal SbmA and YjiL transporters; *b)* the presence of a Trp-rich PR-AMP paralogue with a somewhat diverse activity; *c)* the presence of a dodecapeptide paralogues that does not seem to be an AMP with direct antimicrobial activity. In this respect, MIC measurements of bacteriostatic activity are not particularly sensitive, so it was decided to also study the effect of the peptides on bacterial growth kinetics. These assays can sometimes reveal effects on bacteria at concentrations that are significantly below the MIC, and are therefore more sensitive.

Table 2.3.11. MIC values for TUR peptides against bacterial species known to infect humans.

	MIC (μM) [(a)]		
	P. aeruginosa **ATCC 27853**	***A. baumannii*** **ATCC 10606**	***K. pneumoniae*** **ATCC 700603**
TUR1D	8-16	1	2
TUR1S	16	1	16
TUR6D	2	1-2	2
TUR6S	1	1	1-2
TUR4S	>32	>32	>32

(a) Experiments were repeated three times in duplicate and the values were obtained using micro-dilution, inoculating 2.5 * 10^5 CFU / ml in 100% Mueller-Hinton broth and maintaining the plates at 37 ° C for 20 hours. The MIC values were then evaluated by observing the turbidity of the lowest concentration at which bacterial growth was inhibited.

2.3.7 Effect of TUR6 peptides on bacterial growth kinetics

The effect of TUR6 peptides on bacterial growth kinetics was determined at concentrations ranging from sub-toxic (significantly below the MIC), to toxic (in the range of the MIC), comparing to the effect of the bovine orthologue BMAP-28 and ovine SMAP-29. Note that it is difficult to directly compare results from growth kinetics assays to MIC as the bacterial loads are different (2.5×10^5 CFU/ml vs 2×10^6 CFU/ml, respectively). The effect of growth kinetics was determined against both the Gram positive and Gram-negative reference laboratory strains, and results are shown in **Figure 2.3.7.**

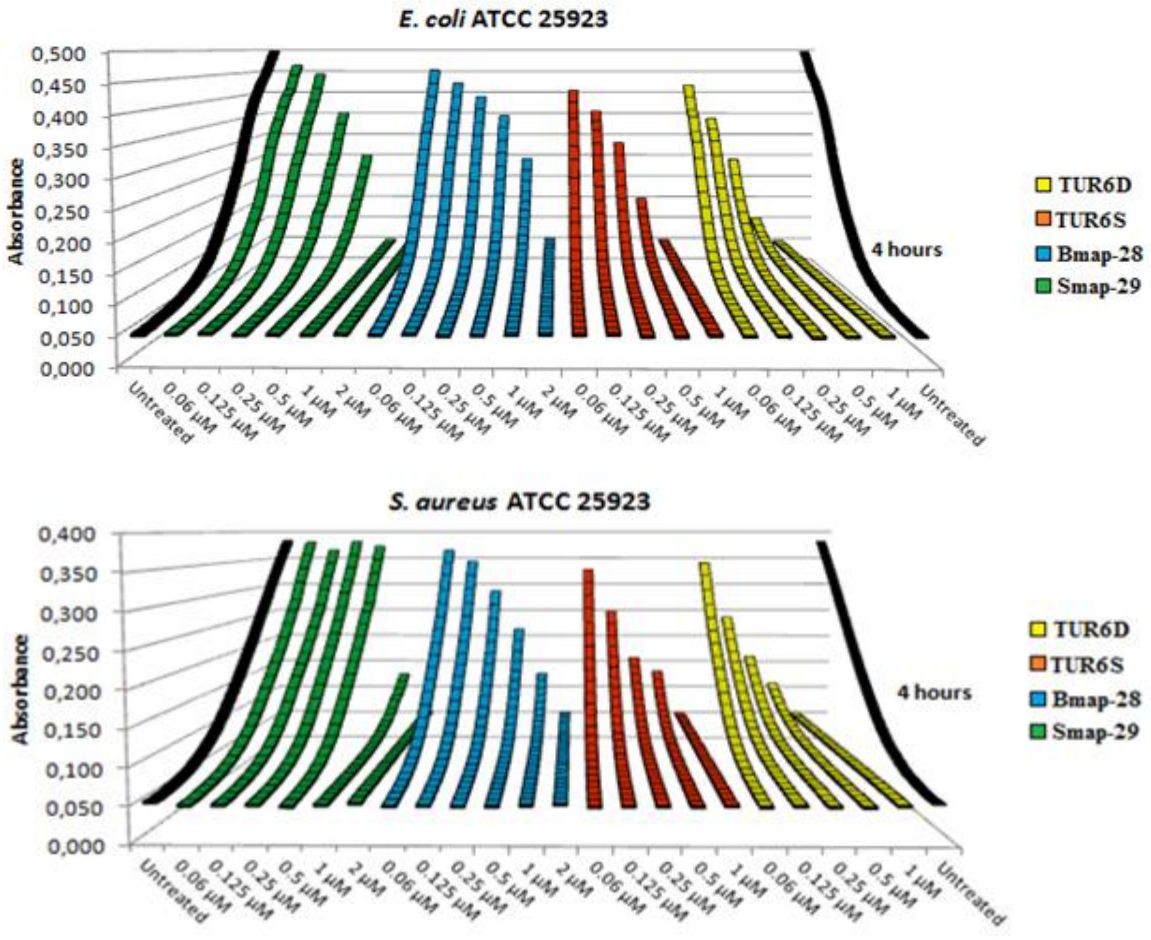

Figure 2.3.7. Growth curves for *E. coli* and *S. aureus* treated with increasing concentrations of peptide. The growth was monitored over a four-hour period. The black curves correspond to untreated bacteria (positive control). Experiments were repeated at last three times in duplicate, for each strain. Results were averaged and displayed using Excel.

These experiments were repeated several times, so obtaining the averaged growth curves with deviation. To better quantify the effect, the % inhibition was determined at an arbitrarily chosen time of 210 min. and plotted against peptide concentration, allowing determining IC^{50} values for each peptide (see **section 2.2.5**). Results are shown in **Figure 2.3.8** and IC_{50} values are listed in **Table 2.3.12**. Considering inhibition of *E. coli* ATCC 25922, it is possible to assert that growth is significantly slowed for all peptides at sub-MIC concentrations, and this is particularly evident for the dolphin orthologues, so that their IC_{50} values are in the 0.2 μM range. Curiously, the cow and sheep orthologues have a somewhat lower capacity to inhibit growth at lower concentrations, with IC_{50} values at 2-4 fold higher. It is interesting to note that the behaviour is similar towards the Gram-positive and negative bacteria.

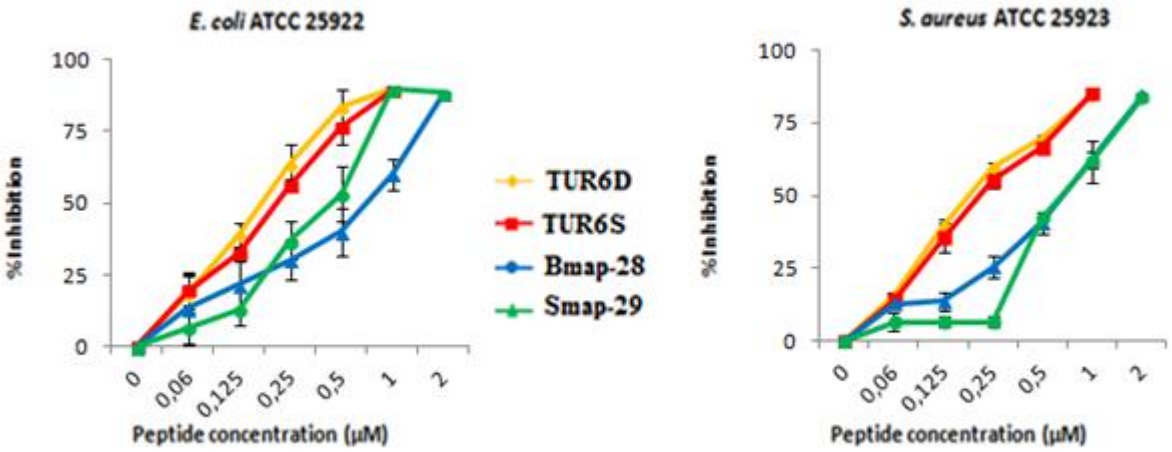

Figure 2.3.8. % inhibition of *E. coli* or *S. aureus* at increasing concentrations of TUR6 peptides and their orthologues. Values were determined in experiments repeated three times in duplicate, and the error bars reflect the calculated standard deviation. IC_{50} were determined as the concentration causing 50% inhibition and are shown in **Table 2.3.12**.

Table 2.3.12. IC_{50} values for TUR6 peptides and their orthologues with respect to the inhibition of bacterial growth for *E. coli* and *S. aureus*

	IC_{50} (μM)	
	***E.coli* ATCC 25922**	***S. aureus* ATCC 25923**
TUR6D	0.15±0.05	0.15±0.05
TUR6S	0.2±0.05	0.2±0.05
BMAP-28	0.7±0.15	0.65±0.15
SMAP-29	0.45±0.1	0.65±0.15

An explanation for the peptide's capacity to significantly inhibit growth at sub-toxic concentrations could be that these membranolytic AMPs interact very efficiently with the bacterial cytoplasmic membranes, and interfere with membrane-located processes important for growth already at quite low concentrations. However, the bacteria can somehow eventually detoxify the membrane [for example by the use of efflux pumps, (Nikaido and Takatsuka, 2009)] thus allowing recovery of normal growth. When the MIC concentration is reached, this capacity is overcome and the peptides lyse the cytoplasmic membrane, so that the bacterium is permanently incapacitated. With respect to *S. aureus* the trend seems to be quite similar, as both TUR6 peptides completely inhibit bacterial growth over 4 h, at a concentration of half the MIC, and with an IC_{50} at or below 0.2 μM. This suggests that interference with membrane bound functions is relevant also to Gram-positive bacteria.

Regarding the bovid orthologues, while BMAP-28 behaves similarly to the dolphin peptides, SMAP-29 seems to have more an all-or-nothing mechanism of inactivation, especially towards *S. aureus*, so that it significantly inhibits growth only at concentrations closer to the MIC. Taken together, these data indicate *a)* that all the peptides act via a similar (likely membranolytic) mechanism of action at higher concentration, that may be analogous for the Gram-positive and Gram-negative bacteria, *b)* they may interfere in a peptide-specific manner with membrane-bound machinery, slowing growth, with efficacy in the order TUR6S ≥ TUR6D > SMAP-29 ~BMAP-28.

To better understand if *E.coli* might be able to recover long-term growth by removing the peptide using an efflux pump, bacterial growth kinetics were carried out in the presence of TUR6D in association with an efflux pump inhibitor. The dipeptide, Phenylalanine-Arginine β-naphthylamide (*PAβN*) (MP Biomedicals) is able to inhibit the family of efflux pumps named *Resistance nodulation-cell division* (RND-type), involved in drug-resistance especially in Gram-negative strains. This was somewhat of a long shot, as it is not clear whether these types of pumps clear membrane-located AMPs, and in fact are reported not to be relevant to the human cathelicidin LL-37 (Rieg et al., 2009). However, the inhibitor was available so I felt it would be interesting to try. *PAβN* was therefore added at a concentration of 60 µM (Lomovskaya and Watkins, 2001) in bacterial growth assays with either TUR6D or BMAP-28. The PR-AMP TUR1D was used as control, as these peptides have a completely different, and non-membranolytic mechanism of action.

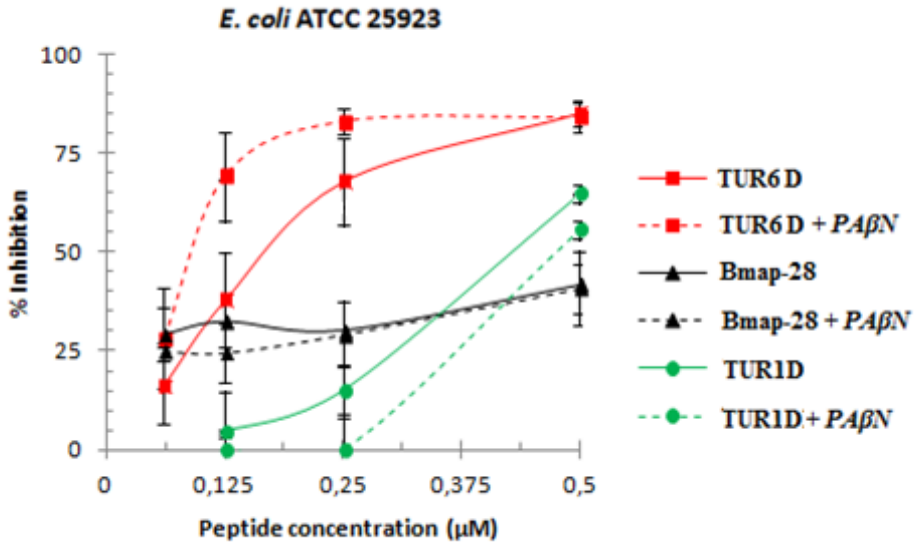

Figure 2.3.9. Percentages of inhibition of *E. coli* treated with increasing concentrations of peptide in presence of *PAβN*. The considered time is at 210 minutes. Experiments were repeated three times in duplicate.

Figure 2.3.9 shows the percentages of bacterial growth inhibition for *E. coli* ATCC 25922 after 210 minutes of treatment with different peptides in the presence of the inhibitor. An increased inhibition of the bacterial growth (i.e. inhibition at lower peptide concentration) was clearly observed when using TUR6D in association with *PAβN*, but not for the bovine

orthologue BMAP-28, or the PR-AMP TUR1D. It has been demonstrated that *PAβN* has a certain ability to permeabilize the outer membrane of *E. coli* at physiological pH at a concentration, 50 μg/ml, analogous to the one I used (Lamers et al., 2013). The increased growth inhibition by TUR6D in the presence of *PAβN* might therefore be ascribed to a loosening of the outer membrane, allowing more peptide to penetrate and therefore to have an increased effect. However, the same should apply to TUR1D, even though it acts by a different mechanism, and even more so for BMAP-28, acting by a similar mechanism. Results are consistent with a significant but reversible inhibitory effect of TUR6D on the Gram-negative bacterium, likely at the level of the bacterial membrane, at concentrations significantly lower than the MIC at which it lyses the membrane, and suggests that that the bacterium might have a certain detoxifying ability by using RND-type efflux pumps. These suppositions however have to be confirmed with more extensive testing.

2.3.8 Bacterial Growth kinetics of TUR1 orthologues

The TUR1 orthologues were also evaluated for their capacity to inhibit bacterial growth at sub-inhibitory concentrations. In this case, as they are selective for Gram-negative bacteria, assays were limited to *E. coli*, and the effect on bacterial growth kinetics was tested against the *E.coli* BW 25113 strain and its transport-deficient mutants. The growth curves are shown in **Figure 2.3.10**, while the respective % inhibition curves and calculated IC_{50} values are respectively shown in **Figure 2.3.11** and **Table 2.3.13**.

For the wild-type BW25311 strain, the TUR1D concentration at which growth is completely inhibited corresponds to the MIC value (1 μM), and slowed at 0.5 μM, but not significantly at lower concentrations. TUR1S shows a significantly lower inhibiting capacity than TUR1D, in line with its higher MIC values (8 μM). These data indicate that the bacterial inactivation mechanism requires a threshold peptide concentration, which may depend on the transport system, or interaction with the internal target(s), or both. In this respect, it is interesting that even PR39(1-18), which is not capable of long-term growth inhibition (MIC >32 μM), under these conditions shows some inhibiting capacity at 2 μM, confirming that growth kinetics assays are more sensitive than serial dilution ones.

TUR1D completely inhibits the growth of the *ΔsbmA* knock-out mutant at a somewhat higher concentrations (2 μM), but is still quite efficient at 1 μM, while the inhibiting capacity of Bac7 (1-35) seems significantly more influenced by the absence of SbmA. This is consistent

with the hypothesis that TUR1D uses SbmA but also the secondary transporter YjiL, and that both have a comparable K_M for the peptide at around 1-2 μM, while that of YjiL may be somewhat higher for Bac5(1-35). TUR1S curiously inhibits the *ΔsbmA* strain even more than the wild-type one, in line with MIC results. Both peptides seem less dependent on YjiL, as knocking it out has less effect on activity, confirming that SbmA is the primary transporter. Curiously the absence of SbmA or YjiL seem to have opposite effects on the less active PR-AMPs, as TUR1S seems to work better if SbmA is absent while PR-39(1-18) if YjiL is absent. The double knockout mutant, not surprisingly, is less subject to inhibition by all peptides. It is interesting, however, that inhibiting activity is not completely removed. Both TUR1D and Bac7(1-35) seem to be able to slow its short-term growth at 4 μM. This suggests that other mechanisms to inhibit growth may kick in at higher concentrations.

The respective role of transporters is evident also when observing growth inhibition against concentration (**Figure 2.3.11**), where TUR1D and Bac7(1-35) are seen to behave quite similarly. Considering the IC_{50} values (see also **Table 2.3.13**), it is apparent that TUR1D and Bac7 use both transporters, TUR1S may preferentially use YjiL, while PR39(1-18) preferentially uses SbmA.

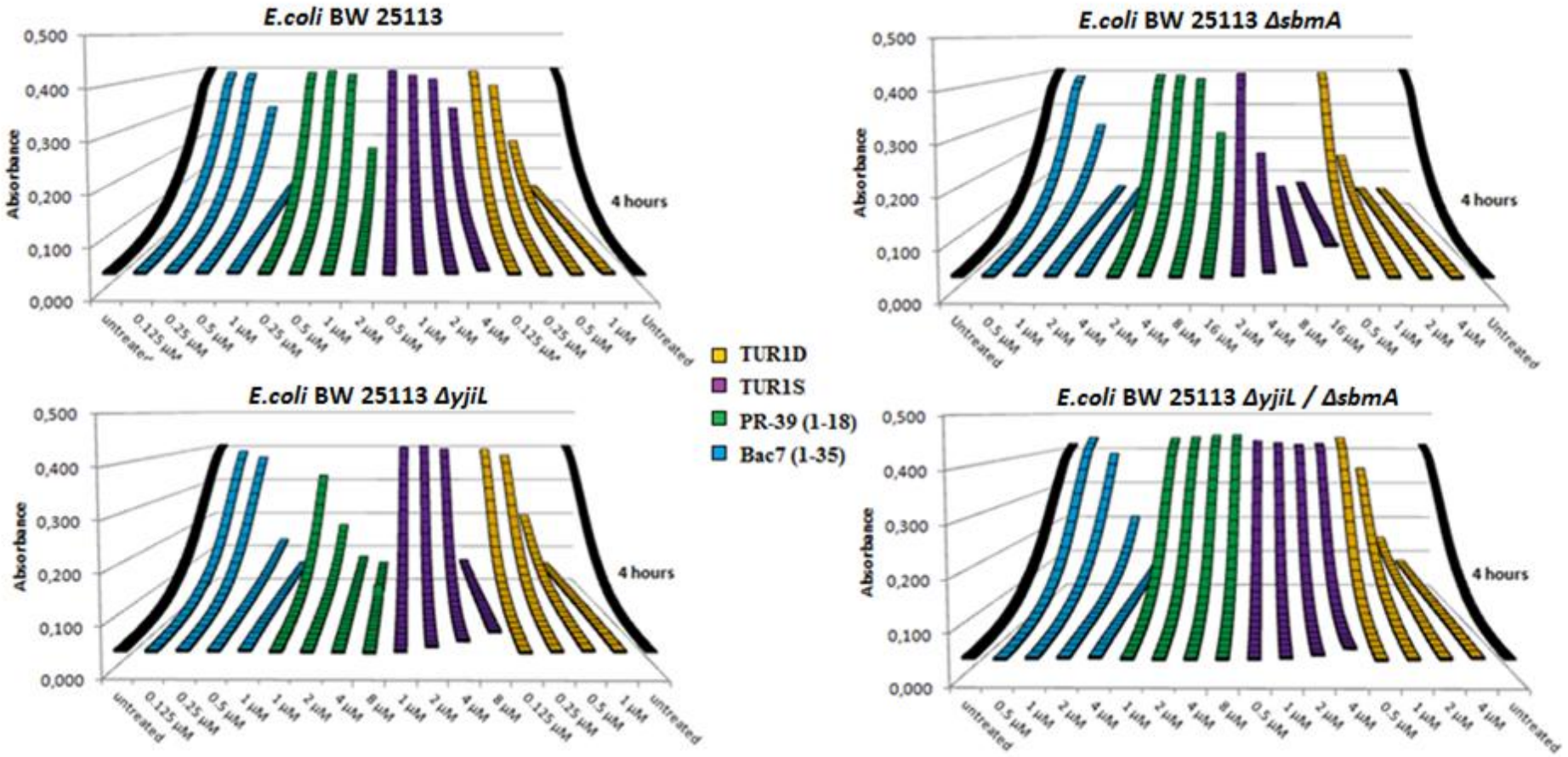

Figure 2.3.10. Growth curves of *E. coli* strains treated with increasing concentrations of peptide. The growth was monitored over four hours. The black curves correspond to untreated bacteria (positive control). Experiments were repeated three times in duplicate, for each strain.

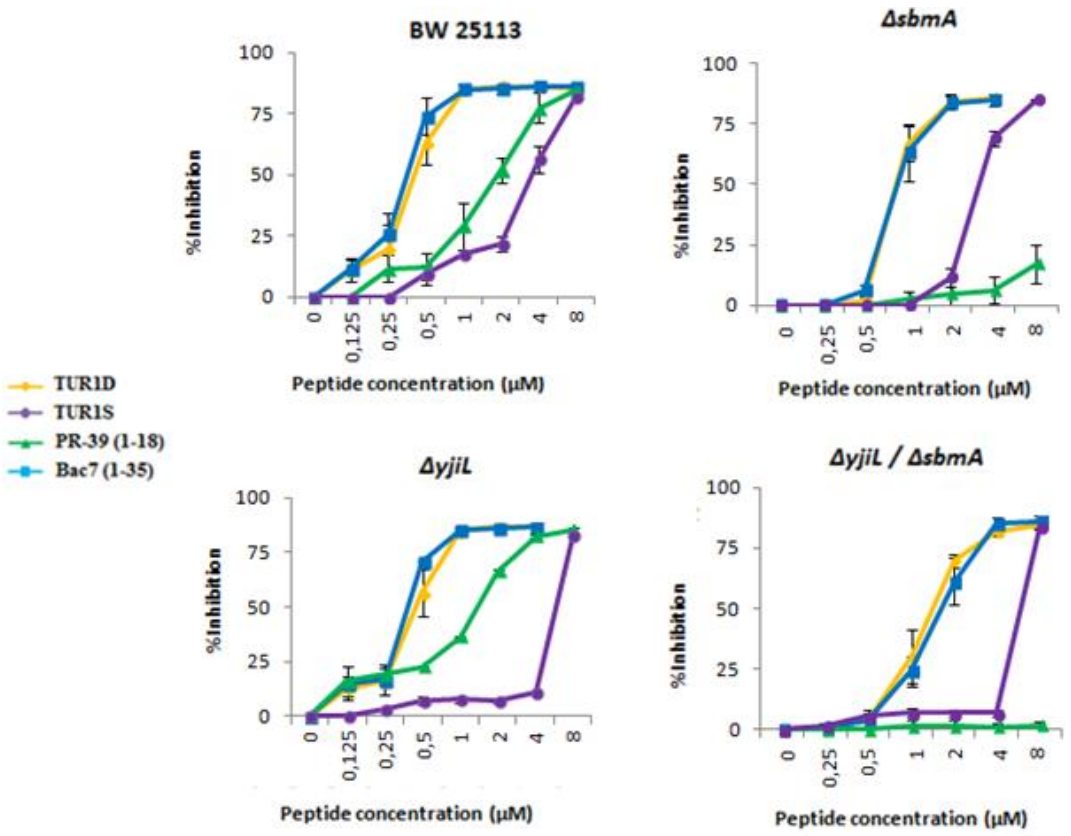

Figure 2.3.11. % growth inhibition for *E. coli* for BW 25113 and its knock-out mutants treated with increasing concentrations of PR-AMPs. Experiments were repeated three times in duplicate and the curves represent the averaged results, with SD shown as error bars.

Table 2.3.13. IC_{50} values for TUR1 peptides and their orthologues with respect to *E. Coli* BW25113 and its transporter knockout mutants.

	IC_{50} (μM)			
	E.coli **BW 25113**	***E.coli*** **BW 25113 *ΔsbmA***	***E.coli*** **BW 25113 *ΔyjiL***	***E.coli*** **BW 25113 *ΔyjiL/ΔsbmA***
TUR1D	0.4 ± 0.05	0.8 ± 0.05	0.4 ± 0.05	1.5± 0.5
TUR1S	3.5 ± 0.25	3.4 ± 0.15	6.3± 0.05	6.3± 0.05
PR-39 (1-18)	2 ± 0.25	>8	1.5± 0.05	>>8
Bac7 (1-35)	0.35 ± 0.05	0.8 ± 0.05	0.3 ± 0.05	1.7± 0.25

2.3.9 Bacterial uptake of fluorescently labelled PR-AMPs

TUR1D is a proline-rich AMP which, as shown above, has quite similar characteristics to the bovine orthologous fragment Bac7(1-35), and seems to internalize into susceptible Gram-negative bacteria through the same specific transporters. However, I felt it was necessary to confirm this by using biochemical methods. The internalization capacity of TUR1D into appropriate bacterial cells was evaluated using flow cytometry, after chemical ligation with a fluorescent probe, as described in section 2.2.4. The similarly BODIPY labeled-Bac7(1-35), well known to efficiently internalize Gram-negative bacteria (Benincasa et al., 2009), was used as positive control. The labelled peptides were added at a concentration of 0.1 μM, a concentration that is well below the lethal one, but at which Bac7 efficiently internalizes. The suspension of 10^6 CFU/ml *E.coli* BW 25113 or of its deletion mutant strains were exposed to the peptides in MH broth, for either 10 min or 30 min at 37 °C and then spun down, washed with physiological salt solution to remove extracellular and loosely surface bound peptide. To completely eliminate the signal due to residual surface-attached peptide, impermeant Trypan blue (TB) was also added to selectively quench the extracellular fluorescence, exploiting the fact that PR-AMPs cause no membrane damage at such low concentrations. This process allows a quantification of effectively internalized peptide, and results are summarized in **Figure 2.3.12.**

The mean fluorescence intensity (MFI) of *wild-type* cells after treatment with TUR1D[Cys^{33}]-BY for 10 min are comparable, but after TB quenching was somewhat less for TUR1D than that of Bac7(1-35), and reaches a comparable value at 30 min, suggesting internalization is somewhat slower for TUR1D. A more prolonged incubation time (60 min) and an increased peptide concentration did not alter these results (data not shown).

In general, it is possible to observe efficient internalization of both peptides into the wild-type strain, even at a concentration as low as 0.1 μM. Knocking out SbmA significantly decreases internalization of both peptides, while knocking out YjiL has a smaller effect at this very low peptide concentration, and this is in agreement with the MIC values (see section 2.3.5). Overall, these results demonstrate that the function of SbmA in *E. coli* as the primary transporter for the uptake of Pro-rich peptides at low concentrations, and indicate that in the SbmA-deleted strains, the internalization is strongly impaired, thus leading to a lower peptide concentration inside the cells and thereby a lower effect on bacterial viability.

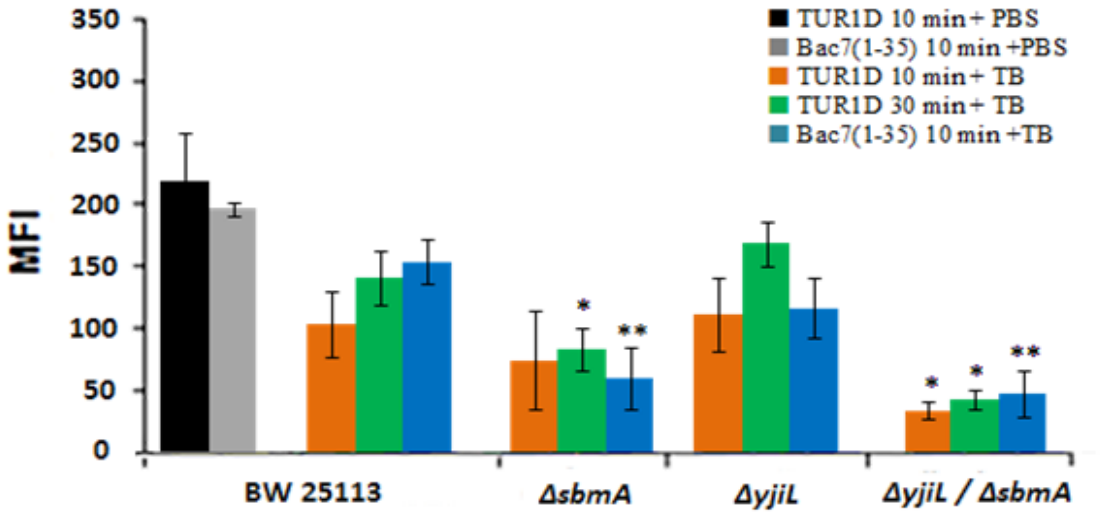

Figure 2.3.12. Flow cytometric analysis of peptide internalization. Uptake of fluorescently labelled TUR1D[Cys^{33}]-BY and Bac7(1-35)[Cys^{36}]-BY (0.1 μM) into *E. coli* BW 25113 strains (10^6 cfu/ml) after 10 min or 30 min incubation at 37°C. Green bars are total fluorescence intensity (membrane bound and internalized peptide), blue bands are fluorescence from internalized peptide after the adding of Trypan blue (TB) quencher. Data are expressed as the average of MFI (Mean Fluorescence Intensity) with standard deviation for three independent experiments. *$p \leq 0.02$ *vs* TB-treated BW25113 bacteria; **$p \leq 0.006$ *vs* TB-treated BW25113 bacteria (Student-Newman-Keuls Multiple Comparisons Test, ANOVA).

2.3.10 Flow cytometric studies of bacterial membrane permeabilization

MIC and growth inhibition assays carried out with TUR1D against *E. coli* indicated that it might use both the primary and secondary transporters YjiL the SbmA, but when both transporter component were missing antimicrobial activity was still observed, although significantly higher concentrations of peptide were required (8 μM). This raises the question as to what the killing mechanism is when both the transport systems are absent. It has been suggested that PR-AMPs, which do not permeabilize bacteria at low concentration, can switch to a membranolytic mechanism of action at significantly higher ones (Podda et al., 2006). To test if this is the case also with TUR1D, cytofluorimetric experiments were carried out with propidium iodide, which cannot enter intact bacterial cells. An *E. coli* BW 25113 suspension of 10^6 CFU /ml was incubated at 37°C with peptide for different times, in the presence of 10 μg/ml PI. Peptide concentrations corresponded to the MIC value for the *wild-type* strain (1

μM) and for the *ΔyjiL/ΔsbmA* double KO strain (8 μM), using the membranolytic TUR6D as positive control.

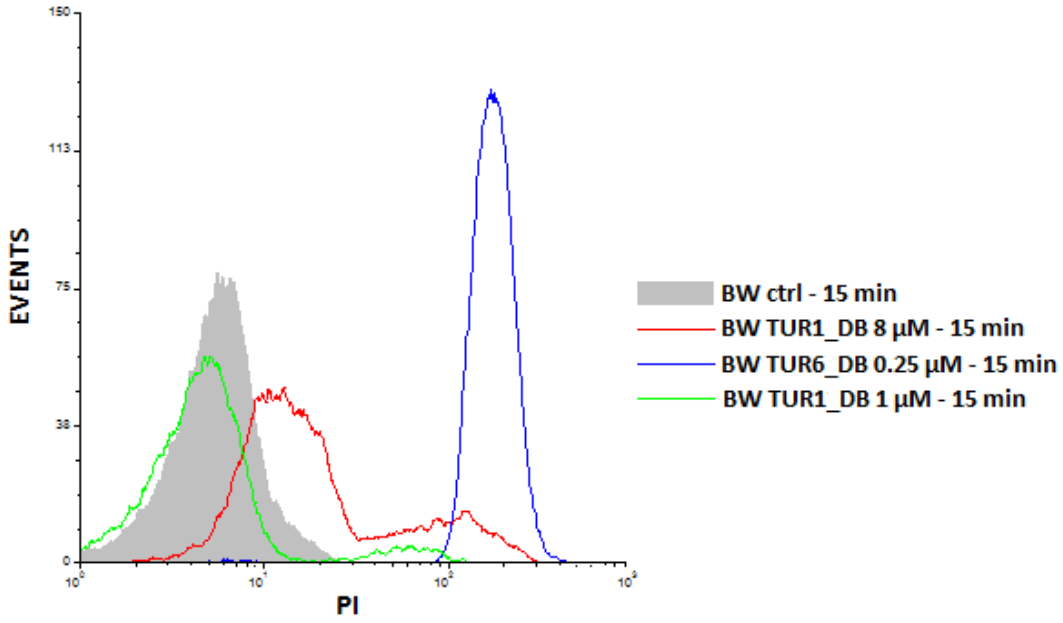

Figure 2.3.13. Effect of TUR1D on *E. coli* BW 25113 membrane integrity. Curves correspond to cells incubated for 15 min with TUR1D at 1 μM (green), 8 μM (red) and TUR6D at 0.25 μM (blue). The grey curve represents untreated cells. Each point was the mean of at least three independent evaluations.

The histograms for PI uptake are shown in **Figure 2.3.13**. As expected, TUR6D is by far the most efficient in permeabilising the *E. coli* membrane to PI, with three-fold greater number of PI positive cells already at a very low concentration (0.25 μM). TUR1D does not cause lesions to the bacterial membrane at 1 μM, even though this is sufficient to inactivate bacteria. This is consistent with a mechanism involving internalization and inactivation of an intracellular target. At 8 μM, however, it does show a shift to higher fluorescence indicating some permeabilization. It is interesting to note that two populations of cells seem to be present, the minor one shifted more closely to the completely permeabilized condition. It is difficult to say if this is due to the presence of some cells that are intrinsically more susceptible to membrane damage (e.g. at a particular stage of the cell cycle), or if this is a secondary effect deriving from dead cells losing membrane integrity.

A dual mode of action, internally acting/membranolytic, has been proposed for Bac7(1-35), depending on the peptide's concentration. At near-MIC concentrations, Bac7(1-35) rapidly killed bacteria by a non-lytic and energy dependent mechanism of action, while at higher

concentrations (≥32 μM) it showed a lytic mechanism of action (Castle et al., 1999), (Podda et al., 2006). It would appear that the dolphin ortholog also shows this behaviour, and that the switch to a lytic mechanism may become relevant at somewhat lower concentrations than Bac7. This would be in line with what I observed in the uptake assays, as TUR1D seems to have a lower internalization efficiency than Bac7(1-35), which results in a longer permanence of the peptide on the bacterial membrane outer surface, which may in turn increase its lytic activity.

2.3.11 Preliminary evaluation of cytotoxic activity on host cells.

A preliminary evaluation of the cytotoxicity of selected peptides on host cells was carried out by using the propidium iodide permeabilization assay in flow cytometry with TUR1S, 1D and 6S, and given the relatively lower toxicity of TUR1D by the MTT viability assay. These experiments were carried out in the laboratory of prof. Sabrina Pacor, at the Dept. of Life Sciences, University of Trieste.

PI permeabilization was assayed by exposing different cell lines to increasing concentrations of the peptides, in the presence of PI, and results are shown in **Table 2.3.14**. It can be seen that TUR6S and TUR1S have a significant toxicity, so that the % permeabilized cells is expected to be ~50% at the MIC values. On the other hand, TUR1D was significantly less cytotoxic against the tested cells. It was decided to test it also using the MTT assay, and given that bovine bactenecins are known to penetrate into host cells, to test if it also internalizes, using the BODIPYlated peptide. In these assays, both adhered cells and cells in suspension were used (see materials and methods section 2.2.11).

Table 2.3.14. Cytotoxicity of TUR peptides assayed by the PI permeabilization assay[a]

TUR1S (μM)	U937 cells % PI+	TUR6S (μM)	U937 cells % PI+	TUR1D (μM)	% PI+ cells MEC-1	% PI+ cells A549
0	0	0	0	0	0	0
0,4	<10	0,5	20	2.5, 5, 10	<5,n.d,n.d	<5
4	30	1	50	25,50	30,75	70,75
40	95	5	95	100	>95	>95

a) Assays were carried out at least three times per peptide, in PBS medium exposing for 30 min to the indicated concentrations of peptide and 10 μg/ml PI.

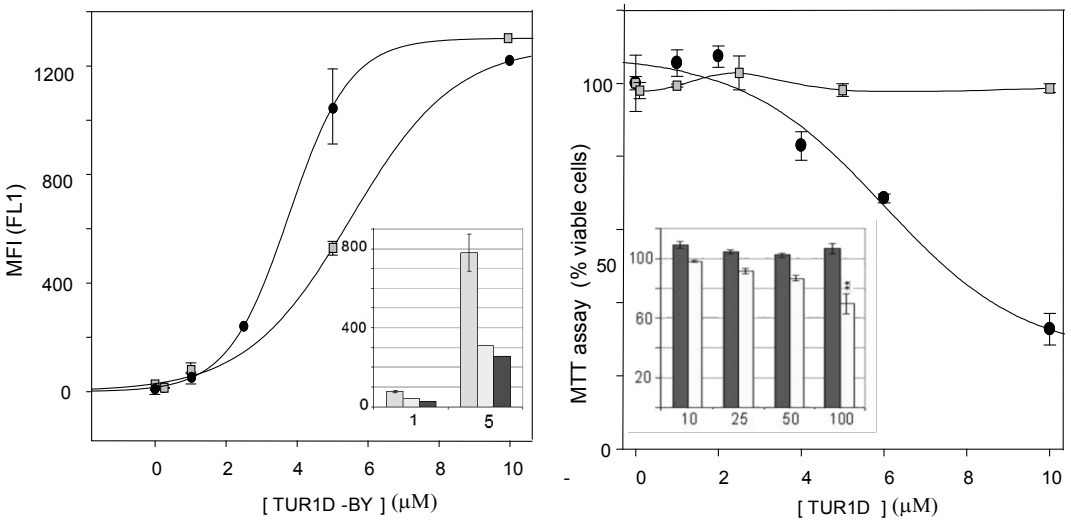

Figure 2.3.14. Effect of TUR1D on host cells. (A) Fluorescence of MEC-1 (●) and A549 (■) cells treated with TUR1D[Cys^{33}]BY for 30 min. The curves show the overall fluorescence. The inset shows the whole fluorescence of MEC-1 cells (light grey bars), the effect of washing extensively with PBS (white bars) and treating with the quencher Trypan blue (dark grey bars) at the indicated peptide concentrations. (B) MTT assay carried out on the same cells exposing to increasing peptide concentration for 24h. The inset shows the effect of significantly higher peptide concentrations on A549 cells, under the same full medium conditions (dark grey bars) or in the presence of only PBS (white bars), exposing for 1 h.

It can be seen that the BODIPYlated peptide interacts strongly with both types of cells, but in particular with MEC-1 lymphoid cells in suspension (**Figure 2.3.14A**). Washing the cells extensively with PBS more than halves the fluorescence (see inset) indicating that they adhere strongly also to the surface. However, subsequent treatment with Trypan blue does not decrease the fluorescence to any further extent, indicating it is due to internalized peptide. It is interesting that unlabelled TUR1D is more toxic to MEC-1 cells than to the adhered A459 epithelial cell line, that seem to be unaffected by peptide even at very high concentrations, as indicated by the MTT assay (**Figure 2.3.14B**). Furthermore, this is true only in the presence of medium, as in PBS alone some toxicity was observed (see inset). An explanation could be that medium has a protective effect, or that the cells are more susceptible when in stressed conditions, such as in the absence of medium. Taken together, these results indicate that a higher toxicity could correlate with a) a stronger surface interaction; b) increased internalization, and c) the metabolically more active nature of the lymphoid cells.

2.4 CONCLUSIONS

Searching in genomic databases using the sequences of known artiodactyl cathelicidins as probes revealed the presence of seven putative cathelicidins in dolphin *Tursiops truncatus*. The alignment of these sequences with the cow and pig homologues indicated that these might be more closely related to bovine ones, in accordance with the currently accepted phylogeny of Cetaceans in the super-order of *Cetartiodactyla*.

In this respect, TUR1 peptides are PR-AMPs orthologous to the bovine Bac7 and porcine PR-39, TUR2 and 3 peptides are amidated, helical peptides orthologous to bovine BMAP-27 and porcine PMAP-36, TUR4 peptides are S-S bridged and highly homologous to bovid dodecapeptides (not present in pig), and TUR6 peptides are amidated, helical orthologues of bovine BMAP-28 and ovine SMAP-29 (also not present in pig). No orthologues were found of bovine indolicidin, although one of the TUR1 peptides (TUR1S) is unusually rich in tryptophan. The most notable deviation from the artiodactyls related to the CAMP gene products (BMAP-34 and PMAP-37 in cow and pig, LL-37 in human). TUR5 is clearly orthologous, but reduced to a truncated pseudogene. A sequence corresponding closely to the canonical full peptide sequence (TUR7) is present, but seems to consist of the isolated exon 4 that is not connected to a cathelin-like domain, and it is not clear if it is expressed. If it were not, then the dolphin would be a first example of an animal without an active CAMP-related peptide. As the genomic sequences were determined at relatively low coverage, transcripts of genomic DNA were obtained and sequenced from samples of dolphin tissue, and this confirmed the correctness of the TUR5, and 7 attributed sequence. The other peptides were also essentially confirmed with some slight sequence variations.

It was possible confirm the expression of peptides using recent transcriptomics studies, that also furnished some indications as to whether expression was inducible or constitutive. TUR4 seems constitutively expressed at high levels, TUR1 seem strongly inducible, while the α-helical peptides TUR2, 3 and 6 are inducible but at lower level and only in defined periods. This could be in line with their more potent antimicrobial activity but also greater cytotoxic effects against the host cells. TUR5 and 7 were not apparently expressed, which supports the pseudogene hypothesis. An unusual aspect of the dolphin cathelicidins is the presence of one or more variants for each cathelicidin peptide, suggesting that they could have been subject to recent duplication. All the TUR1-7 peptides were also variously found in four other cetaceans, by searching the DNA databases. This confirms that the entire repertoire, including the

anomalous CAMP situation, must have been in place before divergence from land-based artiodactyls, or soon after.

I selected three sequences, showing the most molecular diversity, for chemical synthesis, and functional characterization for antimicrobial activity against a range of bacteria. In essence, I made the following observations:

ii) Pro-rich TUR1D, is selective only for susceptible Gram-negative bacteria, is not membranolytic and acts internally, in line with its bovine orthologue Bac7. Activity is however less dependent on the PR-AMP transporter SbmA (in *E. coli*), and it seems to also use the secondary YjiL transport system efficiently for internalization. This was confirmed by cytofluorimetric studies with labelled peptide that however indicated it had a slower internalization mechanism. The longer permanence on the bacterial surface may explain a somewhat greater capacity to permeabilize the bacterial membrane than Bac7, consistent with a concentration-dependent dual internalization/permeabilization mode of action with the second kicking in at relatively low concentrations (≥8 μM under these conditions).

ii) Helical TUR6S has an efficient and broad-spectrum activity, *in vitro,* covering several G-positive and -negative strains, and is capable of inhibiting short-term bacterial growth at concentrations, well under the MIC, possibly interfering with membrane-located processes. Preliminary studies indicate the bacterium somehow detoxifies the membrane until a critical concentration for lysis is reached, and I obtained intriguing indications it does this by using an efflux pump. The peptide has significant toxicity to host cells, at values comparable to the MIC, which may be correlated to the fact that it is expressed rarely and at quite low levels. One could speculate it is something like a 'last resort' cathelicidin for the dolphin, to be used only under particular infection conditions.

iii) Cyclic TUR4S showed no activity, *in vitro*, against either G+ and G- laboratory strains, or numerous other aquatic and terrestrial bacteria, even under permissive medium conditions. This was confirmed also by the more sensitive growth kinetics assays. It is possible that this is due to the lower charge (+3), which could affect the activity *in vitro*. It may have some activity against specific pathogens faced by the dolphin, *in vivo*, or more likely it may have an indirect defensive role related to immune modulation. Unfortunately, the variant I have studied does not seem to be expressed at high levels, whereas TUR4D seems to be constitutively expressed at consistently high levels. For this reason, TUR4D is now in the process of being prepared for characterization. It will be interesting to see if this peptide, with charge +4, has direct antimicrobial activity, or whether like TUR4S may have another role, such as immunomodulator.

The 1st part of my PhD thesis has contributed to the characterization of new antimicrobial peptides from the dolphin *Tursiops truncatus*, confirming in some cases an interesting antimicrobial activity with some different characteristics respect to known orthologues. This study could, therefore, lay the groundwork for research aimed to developing novel antimicrobial agents, and provides some intriguing insights into the study of the cathelicidin antimicrobial peptides in Cetaceans, in relation to those of other mammals.

Chapter 3: PRO-rich peptides as vehicles for antibiotic cargo

3.1 AIMS OF THE STUDY

Reduced antibiotic uptake due to low permeability is an important and often observed resistance mechanism in Gram-negative bacteria. Their cell wall architecture, and in particular the presence of an outer membrane, makes them intrinsically resistant to several classes of antibiotics. For those drugs that are active against them, they can acquire modifications of cell envelope components that reduce their permeability to them, or they can remove them by expulsion through efflux pumps. Aminoglycoside antibiotics, for example, are used in the treatment of a variety of Gram-negative infections, and resistant clinical isolates become impermeable to them (Ratjen et al., 2009). Tobramycin is a bactericidal aminoglycoside active against several Gram-negative bacteria, where it disrupts protein synthesis by irreversibly binding to the 70S bacterial ribosome (Vázquez-Espinosa et al., 2015). Resistant strains have developed due to alterations in membrane permeability and/or transport through the membrane and/or the presence of drug modifying enzymes (Poole, 2005).

One strategy to overcome these problems could be to conjugate tobramycin with another molecule known to be efficiently internalized in a different manner, and in this respect, Pro-rich AMPs are ideal candidates. These peptides, as seen previously, are an important subgroup of cetartiodactyl cathelicidins and have two useful characteristics in this respect: *a)* they are selective for some important Gram-negative pathogens, while non-toxic to the host (Benincasa et al., 2010), and *b)* they are efficiently internalized into the bacterial cytoplasm by known protein transporter(s). Here they can apparently inactivate different targets involved in protein synthesis and folding, including the chaperone DnaK and the bacterial ribosome (Scocchi et al., 2016).

The second part of my PhD work aimed to link tobramycin to the active and well characterized bovine PR-AMP fragment Bac7(1-35), via formation of a disulphide bond, as briefly illustrated in **Scheme I** in order to convey the antibiotic into the bacterium and then allow the release of the antibiotic in the reducing environment of the bacterial cytoplasm. This conjugate might show a mutually potentiating antimicrobial action, since the Bac7(1-35) carrier and tobramycin cargo both target the 70 S ribosome subunit.

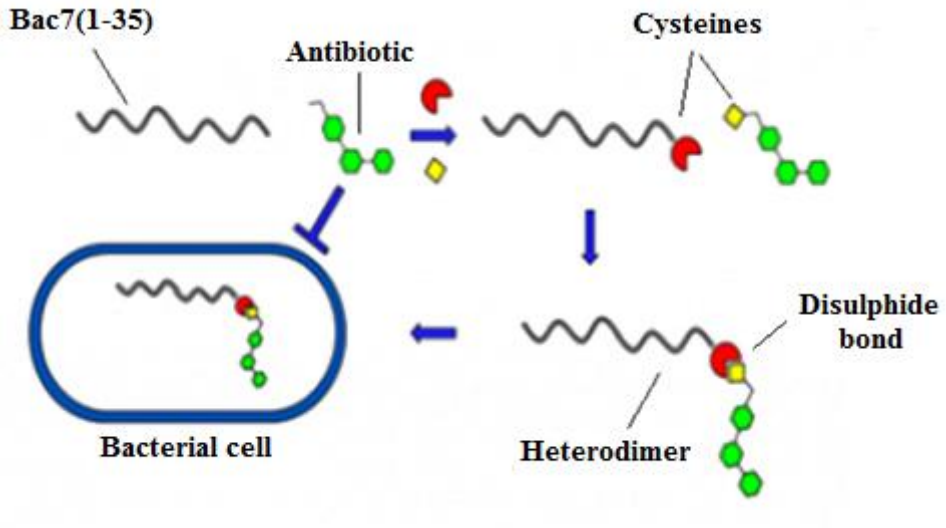

Scheme I. Assembly of an antibiotic cargo/AMP carrier system based on a modified tobramycin and an appropriately modified PR-AMP.

This part of my project was carried out in two stages:

I) Chemical modification of tobramycin, to introduce a reactive moiety that would allow linking the carrier peptide. I considered two different strategies to allow the formation of the disulphide bond:

a) acylation of the primary hydroxyl in position 6'' of the antibiotic (see Scheme II for its structure), using succinic anhydride to allow formation of a peptide bond to a cysteine residue. This would then allow disulfide bond formation with a Cys-modified carrier peptide. The advantage of this strategy is that it introduces two types of labile bonds, an ester (to succinamide) and a disulfide.

b) introduction of a sulfhydryl group in position 6'', allowing direct disulfide bond formation with the Cys-modified peptide. The advantage of this strategy is that the antibiotic is bound directly to the peptide carrier without previous addition of a bulky cysteine residue.

II) Study the efficacy of the Bac7-antibiotic conjugate(s) *in vitro* against a range of bacterial species, using standard microbiology techniques to obtain more information about the mode of action.

The approach of linking drug cargo to PR AMPs is potentially applicable to several different classes of currently available antibiotics. It would allow the use of approved molecules that are already tested for target inactivation efficacy and toxicity, which may significantly

facilitate subsequent use of the conjugate system. The only prerequisite is that the antibiotic has a functional group that is modifiable to allow linking to the carrier, but at the same time not essential for it activity.

3.2 MATERIALS and METHODS

3.2.1 Synthesis of $(Boc)_5$Tobramycin (Boc-T-OH)

First of all, in order to direct the reaction of conjugation to the position 6'' of the antibiotic and avoid undesirable side-reactions, I needed to protected the numerous reactive amine groups with di-tert-butyl dicarbonate (Boc_2O) (Michael et al., 1999). The Boc protecting group can then be removed by treatment with trifluoroacetic acid in the presence of appropriate scavengers. The reaction is shown in **Scheme II.**

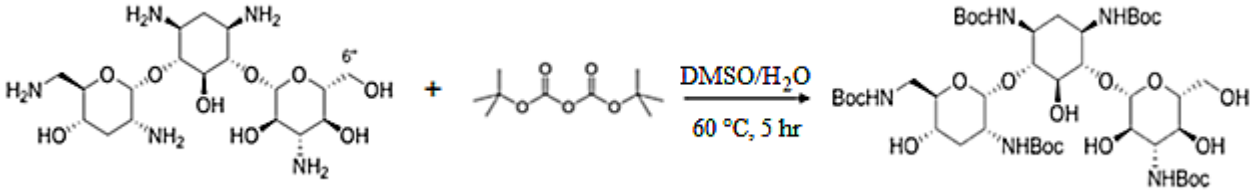

Scheme II. Boc protection of tobramycin amine groups using Boc2O

A solution of tobramycin (0.240 g, 0.500 mmol) in 10 ml aqueous DMSO (DMSO/water, v/v 6:1) was treated with di-tert-butyl dicarbonate (1.1 g, 5.0 mmol, 10 equiv.). The solution was heated at 60°C for 5 hours, and then cooled to 23°C. 5 ml 30% aqueous ammonia was then added to the mixture to stop the reaction. The precipitated was filtered, washed several times with water and dried in a desiccator. The reaction progression to the final product was m0nitored by analytical RP-HPLC (Kinetex C18, 3µm, 100 Å, 50 x 4.6 mm column from Phenomenex, USA) and ESI-MS.

3.2.2 Synthesis of $(Boc)_5$Tobramycin-Hemisuccinate (Boc-T-hS)

The first strategy to link the antibiotic to the peptide carrier required acylation of the primary hydroxyl in position 6'' of tobramycin (see **Scheme II**) by using succinic anhydride, to obtain $(Boc)_5$-tobramycin-hemisuccinate (**Scheme III**). This would allow subsequent linking to a

cysteine residue by formation of a peptide bond. The reaction was carried out according to (Rice et al., 2005), and exploits the greater reactivity of the primary hydroxyl in position 6'' with respect to the four secondary hydroxyls present on the tobramycin rings.

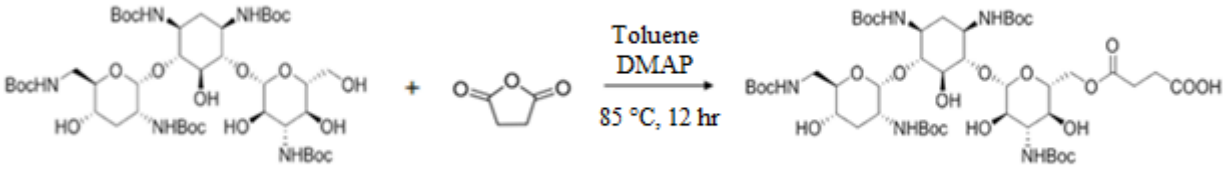

Scheme III. Introduction of an acid moiety onto the primary hydroxyl of tobramycin using succinic anhydride

$(Boc)_5$Tobramycin (0.37 g, 0.38 mmol) was dissolved in 20 ml anhydrous toluene and treated with succinic anhydride (0.058 g, 0.58 mmol, 1.5 eq.) and 4-dimethylaminopyridine (DMAP) (0.23 g, 1.9 mmol, 5 eq.) . The solution was heated at 85°C for 20 h in a paraffin oil bath, under argon flux, until the completion of the reaction (monitored by analytical RP-HPLC and ESI-MS). After cooling to room temperature, 20 ml of dichloromethane and then 40 ml of aqueous HCl (pH = 2.5) were used to separate organic and aqueous phases. A few drops of 6 M HCl was added to the aqueous phase to ensure that the all product pass to the organic layer. The combined organic layer was washed with brine, dried over Na_2SO_4 and the solvent removed on a rotary evaporator. Note that even mildly basic conditions must be avoided when storing or using the hemisuccinate or any of its products, as the ester bond is labile under those conditions.

3.2.3 Synthesis of Tobramycin(Hemisuccinate)-Cys conjugate (T-hS-Cys)

Linking of $(Boc)_5$-T-hS to cysteine was carried out as shown in **Scheme IV**. The first part of the procedure was carried out on a Biotage Initiator+ automated microwave peptide synthesizer, by coupling Fmoc-Cys(Trt)-OH (6 eq.) to Rink amide resin (0.266 g, 0.35 mmol/g. 0.1 mmol scale). After Fmoc deprotection of the resin with 20% piperidine in NMP, Fmoc-Cys(Trt)-OH/PyBop/DIPEA (1:0.98:2) in NMP were added and the reaction allowed to proceed as per the Biotage protocol. The Fmoc group was then removed by washing 3 times for 10 min with 20% piperidine solution (total 9 ml). Aliquots of the deprotection solution (100, 10 and 5 μL) were diluted with 20% piperidine and the concentration of the Fmoc group

determined spectrophotometrically at 301 nm (absorption maximum for the fulvene-piperidine adduct, ε = 7800 $M^{-1}cm^{-1}$).

The resin substitution was calculated as 0.4 mmol/g using the equation: $Rs = \frac{Abs \cdot dil \cdot vol}{\varepsilon_{FMOC} \cdot l \cdot g}$ (Abs = absorbance, dil = dilution, l = optical path in cm, g = resin grams, vol = total volume in ml, ε_{FMOC} = Fmoc molar extinction coefficient).

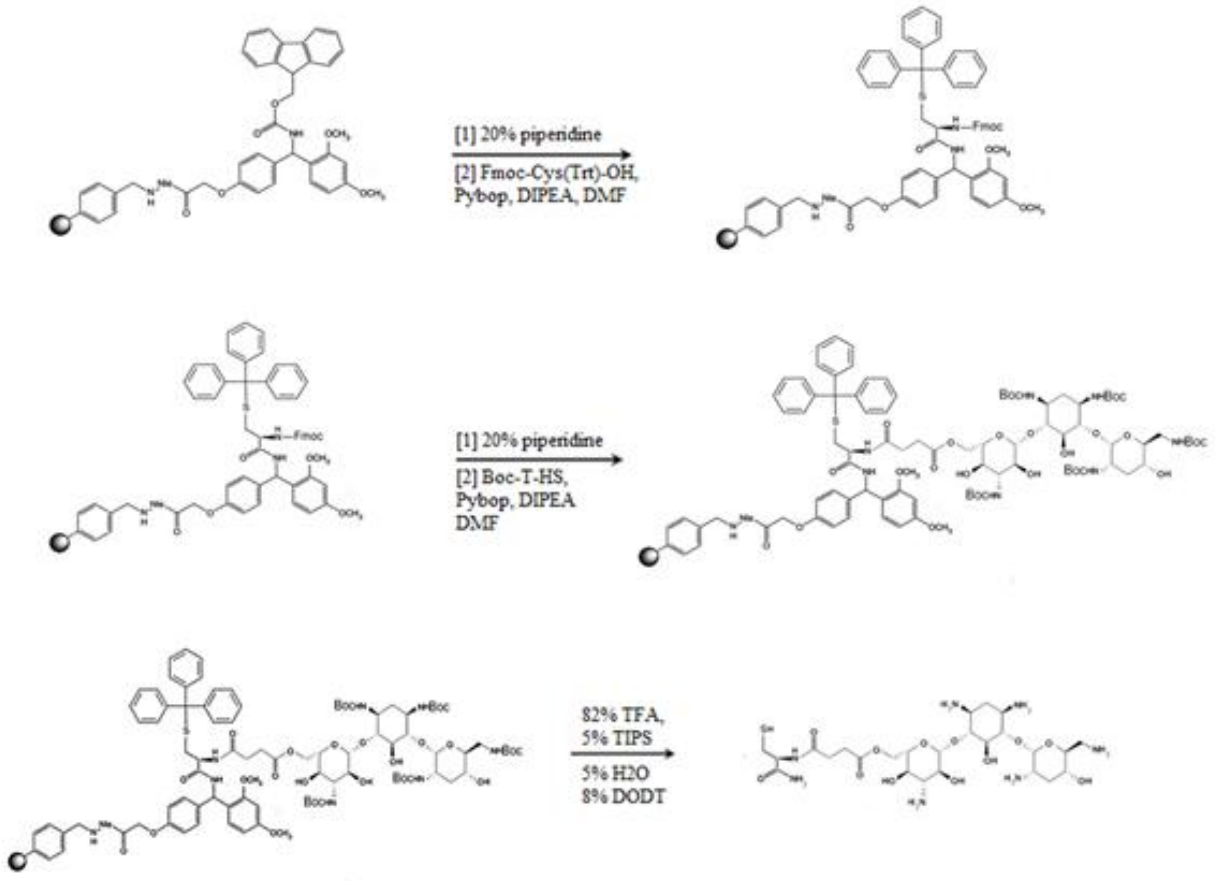

Scheme IV. Preparation of T-HS-Cys

Formation of the peptide bond to tobramycin was carried out manually by dissolving 0.17 g of $(Boc)_5$Tobramycin-Hemisuccinate (0.16 mmol) in 1.5 ml of DMF and adding 0.082 g of PyBop (0.157 mmol, 0.98 eq.) and 56 µL of DIPEA (0.314 mmol, 2 eq.). This solution was added to 0.2 g of the Cys-Rink-Amide resin (0.4 mmol/g, 0.08 mmol scale) so that T-hS was in two-fold excess. The Kaiser test carried out at the beginning of the reaction on a few grains of resin gave a dark blue colour, indicating free amino groups present on the resin. After 3 hours, the Kaiser test gave a yellow colour, indicating reaction completion. The resin was then washed

with DCM, 2-propanol and diethyl ether, and dried under an N_2 flux. The resin weight at the end of the reaction was 0.24 g, against an expected theoretical weight of 0.25 g, indicated a yield of >90%, which is good considering the steric hindrance of the tobramycin entering group.

The product was then cleaved from the resin by using a cocktail of trifluoroacetic acid (TFA), tri-isopropylsilane (TIPS), H_2O and 3,6-dioxa-1,8-octane-dithiol (DODT), (82%,5%,5%,8% v/v), also removing the Boc protecting groups. The crude material was precipitated with 20 ml cold tert-butyl methyl ether, washed, dried under N_2 flux and analysed using analytical RP-HPLC and ESI-MS.

3.2.4 Synthesis of Tobramycin-Cys-Thiopyridine (T-hS-Cys-TPy)

Tobramycin(Hemisuccinate)-Cys was pre-activated on the cysteine sulfhydryl to direct the subsequent conjugation reaction with the free sulfhydryl on the peptide carrier by formation of a heterodimeric disulfide bridge (see **Scheme V**). 0,049 g of T-hS-Cys (0.073 mmole) were suspended in 3 ml of methanol and treated with 2,2'-dithiodipyridine (0.016 g, 0.073 mmol, 1 equiv.) The solution was left for 5 hours at room temperature under agitation, until completion of the reaction (as monitored by ESI-MS). The crude product was precipitated with 20 ml cold tert-butyl methyl ether, washed, dried under N_2 flux and analysed with analytical RP-HPLC and ESI-MS.

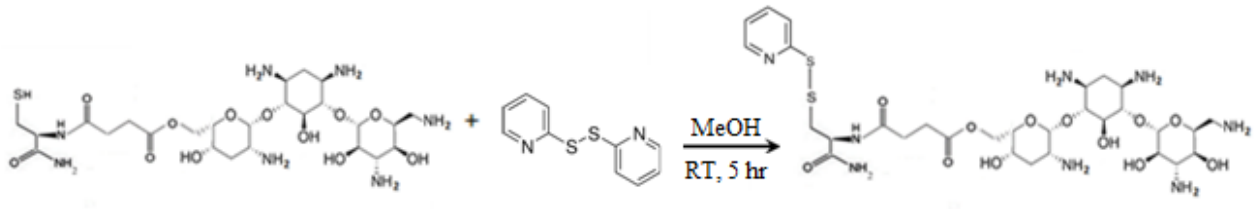

Scheme V. Preparation of T-hS-Cys -TPy

3.2.5 Synthesis of Bac7(1-35)[Cys^{36}] and Bac7(1-15)[Cys^{16}]

Carrier PR-AMPs were modified at the C-terminus, as it is reported that modification of the N-terminus affects internalization and activity (Guida et al., 2015). Both an active and an inactive fragment of the Bac7 PR-AMP were prepared. Syntheses were performed in the solid phase, using a Biotage Initiator+ automated microwave synthesizer, as previously described (see section 2.2.2).

- For preparing Bac7(1-35)[Cys^{36}] a 2-chlorotrityl chloride resin (Novabiochem, substitution ≤ 0.2 mmol/g, scale 0.1 mmol), manually preloaded with Fmoc-Cys(Trt)-OH, was used.
- For Bac7(1-15)[Cys^{16}] NovaPEG Rink Amide Resin LL (Novabiochem, substitution 0.35 mmol/g, scale 0.1 mmol) was used to produce a C-terminal amidated peptide. In this case, the C-terminal cysteine residue was introduced directly to the resin during the synthesis.

The peptides were cleaved from their resins using a cocktail of trifluoroacetic acid (TFA), thioanisole, water, 3,6-dioxa-1,8-octane-dihiol (DODT), tri-isopropylsilane (TIPS) (85%,3%,2%,8%, 2% v/v) and then precipitated and washed several times with cold tert-butyl methyl ether (TBME) and dried under nitrogen. The crude peptides were analysed by analytical RP-HPLC (Waters Symmetry 4.6 x 75 mm C18 column) and purified by preparative reverse-phase HPLC (Phenomenex Jupiter™, C18,10 µm, 90 Å, 250x21,20 mm).

3.2.6 Bac7(1-35)[Cys^{36}] alkylation with iodoacetamide

As unlabelled control peptides were required for the subsequent biological assays, the SH group on the side chain of the C-terminal cysteine residue was alkylated using 2-iodoacetamide for a small aliquot of the peptides (see **Scheme VI**). This sulfhydryl-reactive alkylating reagent prevents intermolecular dimerization of peptides during assays by disulphide bond formation. The reaction was conducted in Tris buffer 0.5 M and 2mM EDTA at pH 8.0. Iodoacetamide is unstable and light sensitive, so a 2.2 M solution was prepared immediately before use and the reaction was performed in the dark and under nitrogen, adding 1 mM peptide and 0.5 M ascorbic acid to scavenge traces of iodine. After 2 minutes, 0.5 M citric acid was added as a reaction quencher.

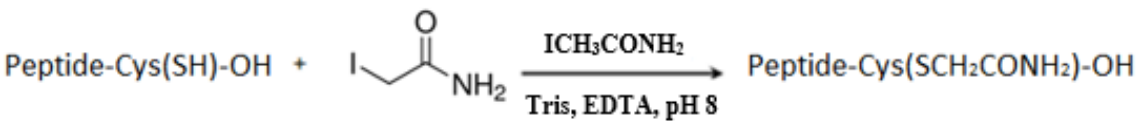

Scheme VI. Schematic representation of alkylation reaction.

The reaction mixture was then diluted with 0.05% Trifluoroacetic acid in water to a final pH of 2.5 and the peptides purified by semi-preparative RP-HPLC (Jupiter™, C18, 5 µm, 300 Å, 100x10 mm) with a linear gradient of 1→40% CH_3CN in 40 min. and 2 ml/min flowrate. Purity was confirmed by analytical RP-HPLC (Kinetex C18, 3µm, 100 Å, 50 x 4.6 mm column from Phenomenex, USA) and ESI-MS.

3.2.7 Synthesis of Tobramycin-Bac7(1-35) and Tobramycin-Bac7(1-15)

For the heterodimerization reaction (see **Scheme VII**), 2 mg of Tobramycin-Cys-Thiopyridine (0.0025 mmole) were suspended in 4 ml of 20% dimethyl sulfoxide (DMSO) in H_2O (pH = 5), and 1 eq. of Bac7(1-35)[Cys^{36}] (10.7 mg in 1 ml of H_2O) was added drop wise to the solution. The reaction mixture was then left for 24 hours at room temperature under agitation, until the completion of the reaction (monitored by RP-HPLC and ESI-MS). The heterodimer was purified by RP-HPLC on a Phenomenex semi-preparative column (Jupiter™, C18, 5 µm, 300 Å, 100x10 mm) using a 5-35% CH_3CN gradient in 50 min. with a 2 ml/min flow rate. The lyophilized heterodimer was accurately weighed and then dissolved in slightly acidic water (pH = 4.8). This was to prevent the risk of the solution becoming even slightly basic, as the hemisuccinate is unstable under those conditions. The concentration of stock solutions was determined weight, and by spectrophotometric determination of peptide bonds using ε_{214}, as well as the method of Waddle.

The same procedure was used for the synthesis of the second heterodimer Tobramycin-Bac7(1-15), using 3 mg of Tobramycin-Cys-Thiopyridine (0.004 mmole) and 1 eq. of Bac7(1-15)[Cys^{16}] (7.7 mg).

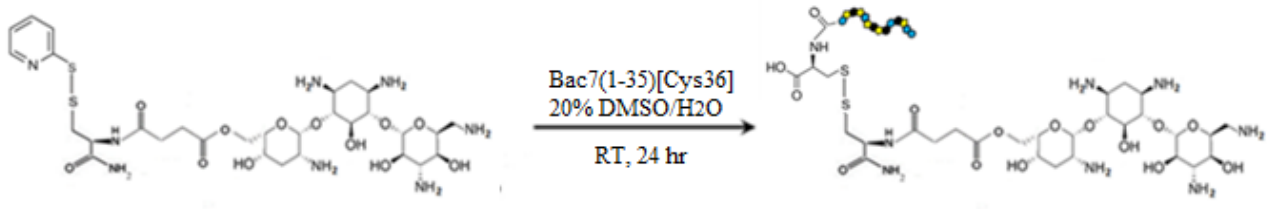

Scheme VII. Preparation of T-HS-Cys/Bac7(1-35)[Cys^{36}] heterodimer via disulphide bond formation.

3.2.8 Synthesis of $(Boc)_5$Tobramycin-OTibs (Boc-T-OTibs)

The second strategy I used to allow the formation of a disulphide bond with a modified Bac7 was to first introduce the trispropylsulfonate group (OTibs) onto position 6'' of tobramycin by reacting with trysil chloride (2,4,6-Triisopropylbenzenesulfonyl chloride, TPSCl). This would then allow linking a group bearing a thiol in this position, and then directly forming a disulfide bonds with the carrier peptide. To this end, Boc-T-OH was modified according to the method of (Michael et al., 1999). The first step was the introduction of the Tibs group as shown in **Scheme VIII.**

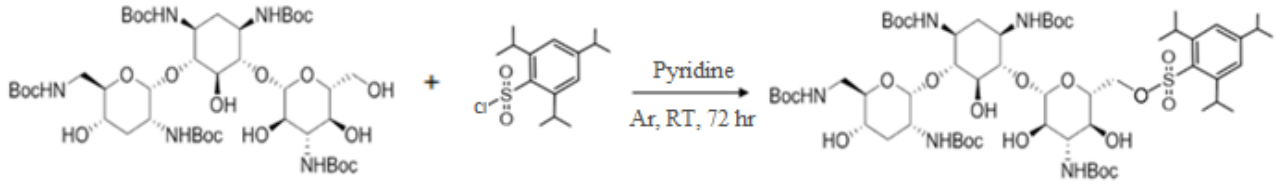

Scheme VIII. Preparation of Boc-T-OTibs

$(Boc)_5$Tobramycin (0.15 g, 0.16 mmol) was dissolved in 7 ml anhydrous pyridine in a three-necked round bottom flask and 2,4,6-Triisopropylbenzenesulfonyl chloride (TPSCl) was added (0.23 g, 1.1 mmol, 5 eq.). The solution was heated at 60°C for 72 h over a heating plate, under constant argon flux to prevent hydration, until the completion of the reaction (monitored by analytical RP-HPLC and ESI-MS). After cooling to room temperature, 250 ml of ethyl acetate and then 60 ml of water were used added and the organic and aqueous phases separated. The combined organic layer was washed with brine, dried over Na_2SO_4 and brought to dryness with a rotary evaporator.

3.2.9 Synthesis of $(Boc)_5$Tobramycin-dioxaoctanethiol (Boc-T-DOT)

The aim of this reaction was to introduce the thiol group onto position 6'' by replacing the OTibs group with dioxaoctanedithiol to form a thioether bond leaving a free sulfhydryl, as shown in **Scheme IX**

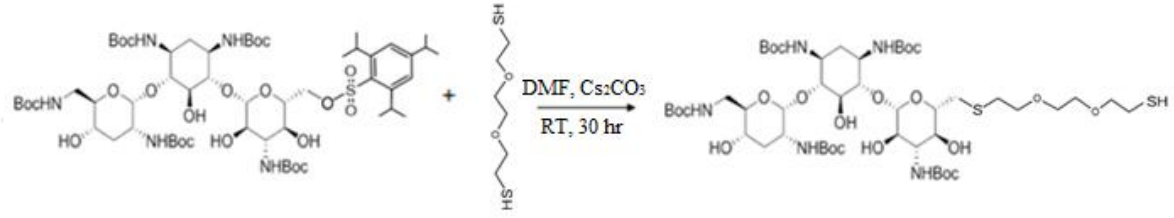

Scheme IX. Preparation of Boc-T-DOT with 2,2′-(Ethylenedioxy) diethanethiol

$(Boc)_5$Tobramycin-OTibs (0.165 g, 0.13 mmol) was dissolved in 7 ml anhydrous DMF in a three-necked round bottom flask and treated with 2,2′-(Ethylenedioxy)diethanethiol (DODT) (0.189 g, 1.04 mmol, 8 eq.) and cesium carbonate (0.075 g, 0.234 mmol, 1.8 eq.). The solution was placed at room temperature, under constant argon flux and the reaction monitored by analytical RP-HPLC and ESI-MS. After 26 hours, as it had not reached completeness another 8 eq. of thiol were added (total 16 eq.). After 36 hours, 100 ml of ethyl acetate and then 30 ml of water were added and the aqueous and organic phases separated. The combined organic layer was washed with brine, dried over Na_2SO_4 and brought to dryness with a rotary evaporator.

3.2.10 Synthesis of $(Boc)_5$Tobramycin-dioxaoctanethiol-thiopyridine (Boc-T-DOTTPy)

In order to pre-activate the (Boc)5Tobramycin-dioxaoctanethiol sulfhydryl to favour heterodimerization with Bac7, it was reacted with dithiopyridine as already discussed previously. 0.100 g (0.092 mmol) of Boc-T-DOT was reacted with 2,2'-dithiodipyridine (0.008 g, 0.036 mmol, 4 eq.) and was carried out as described in section 3.3.4. The reaction is shown in **Scheme X**

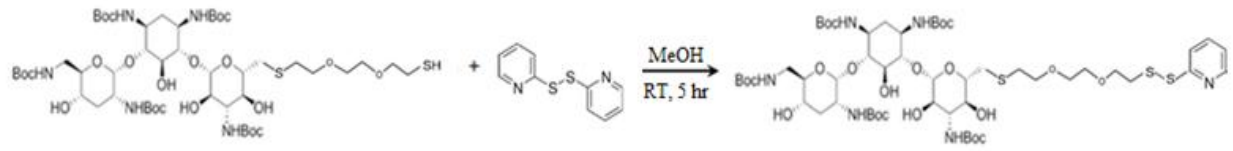

Scheme X. Preparation of Boc-T-DOTTPy

3.2.11 Antimicrobial activity assays

MIC determination and effect on bacterial growth were carried out as described in section 2.2.7. For the Tobramycin-Bac7 conjugates, as both the antibiotic and AMP carrier are antibacterial, it was necessary to consider the possibility that their activities could be neutral to each other, additive, synergic or even antagonistic. For this reason, synergy assays had to be carried out.

Synergy assays (MIC checkerboard). To assess synergistic or antagonistic effects between tobramycin and Bac7(1-35), checkerboard assays were carried out using the same sterile 96-well plates as for normal MIC assays. The set-up procedure is slightly different to the normal MIC essay (see section 2.2.7), as the plates were prepared by placing 50 μL of MH broth with the first antibacterial (32 μM of Bac7 1-35) in all the wells of the top row. To all the other wells were added 25 μL of untreated MH broth. 25 μL was then transferred to from the first to the second row and six more serial dilutions were then carried out down the rows, leaving the eighth row with 50 μL untreated MH broth. Serially diluted stock solutions were then prepared from 32 to 0.5 μM tobramycin in MH broth and 25 ml of these were added as appropriate to wells so as to have a serial dilution of the antibiotic along the columns. 25 μl of MH broth inoculated with $1*10^6$ cfu/ml bacteria were then added, and then all wells were brought to 100 μl by adding untreated medium as necessary. In this manner, wells had a bacterial load of $2.5*10^5$ cfu/ml and concentrations of antibacterials as shown in **Figure 3.2.1**.

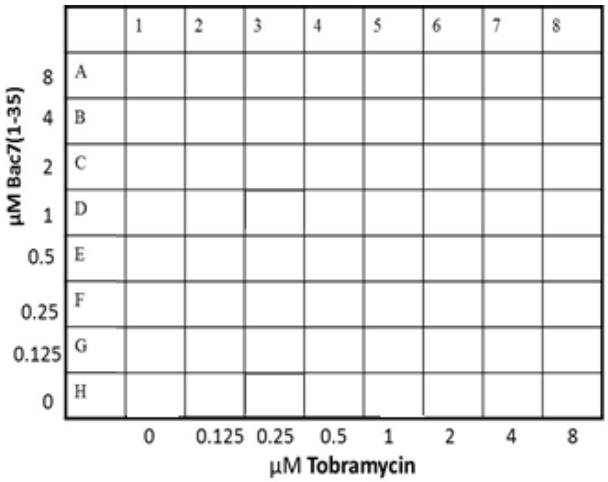

Figure 3.2.1. Scheme for the checkerboard assay. The concentration of antibacterials is given by reading the row value for Bac7(1-35) and column value for tobramycin, so that well 5E, for example, contains1 μM tobramycin and 0.5 μM Bac7(1-35) and $2.5*10^5$ cfu/ml, in a final volume of 100 μl MH broth.

Data were also analysed in terms of FIC index (Fractional Inhibitory Concentration), which is calculated with the formula:

$$FIC_A + FIC_B = (C_A/MIC_A) + (C_B/MIC_B)$$

where MIC_A and MIC_B are the MICs of component A and B alone, respectively, and C_A and C_B are respectively the concentrations of the drugs when in combination, in wells corresponding to an MIC (isoeffective combinations). A FIC value below 0.5 indicates a synergistic effect (Meletiadis et al., 2010).

3.2.12 Bacterial strains

To begin with, the antimicrobial activity of the conjugate molecules were tested in terms of minimum inhibitory concentrations (MIC) (see section 2.2.7) against several *E. coli* strains (**Table 3.3.0**), in order to get more information about the mechanism of action. When possible, it was also tested using bacterial growth kinetics assays (see section 2.2.8). Subsequently, the bacteriostatic activity was tested on a wider range of bacteria, including Gram-positive species, with particular attention to typical human pathogens and multidrug-resistant clinical isolates.

Table 3.3.0 Bacterial strains used to test tobramycin-Bac7 conjugates

Strain	Characteristics or genotype[(a)]	Reference or source
E. coli		
- BW 25113	*wild type*	Genobase
- Δ*sbmA* (JW0368)	BW25113 sbmA::Km^r mutant	Keio Collection[(b)]
- Δ*rpoS* (JW5437)	BW25113 rpoS::Km^r mutant	Keio Collection[(b)]
- Δ*hfq* (JW4130)	BW25113 hfq::Km^r mutant	Keio Collection[(b)]
- [pMAU1(*sbmA*)]	BW25113 (pUC18 *sbmA*)::Amp^r	(Mattiuzzo et al., 2007)
P. aeruginosa		
- ATCC 27853	wild type	ATCC®
- PA01	clinical isolate	Univ. Chieti[(b)]
- PA05	clinical isolate	"
- PA10	clinical isolate	"
- PA21	clinical isolate	"
- PA22	clinical isolate	"
- PA35	clinical isolate	"
A. baumannii		
- ATCC 10606	wild type	ATCC®

- 420[(c)]	clinical isolate	Univ. Trieste[(c)]
K. pneumoniae		
- ATCC 700603	wild type	ATCC®
- #4	clinical isolate	Univ. Trieste[(c)]
S. aureus ATCC 25923	wild type	ATCC®
S. epidermidis ATCC 12228	wild type	ATCC®
S. enterica ATCC 14028	wild type	ATCC®

(a) Km^r, kanamycin resistant; Amp^r, ampicillin resistant. (b) Keio Collection - Keio Collection of GenoBase (http://ecoli.aistnara.ac.jp/index.html); (c) tobramycin-resistant C.I.
(b) Kindly donated by G. Di Bonaventura, Dip I Scienze Mediche, Orali e Biotecnologiche
(c) L. Dolzani, Microbiology laboratory, Dip. Scienze della Vita

3.3 RESULTS and DISCUSSION

3.3.1 Purity check of the starting tobramycin compound

Before starting the synthetic process, the starting compound (Tobramycin, SIGMA-ALDRICH, MW = 467 g/mol) was analysed by ESI-MS and analytical RP-HPLC, in order to verify the purity. The mass spectrum is shown in **Figure 3.3.1**, and in addition to the peak corresponding to the correct structure [m/z = (m + H^+)/1 = 468.5), a second peak at 324.4 can be observed (abundance ~ 30%), that is -144 compared to that of tobramycin. This is likely due to the loss of glycosidic ring III (see **Figure 3.3.2**). This impurity varied from batch to batch, and certainly had an impact on the subsequent reaction yields.

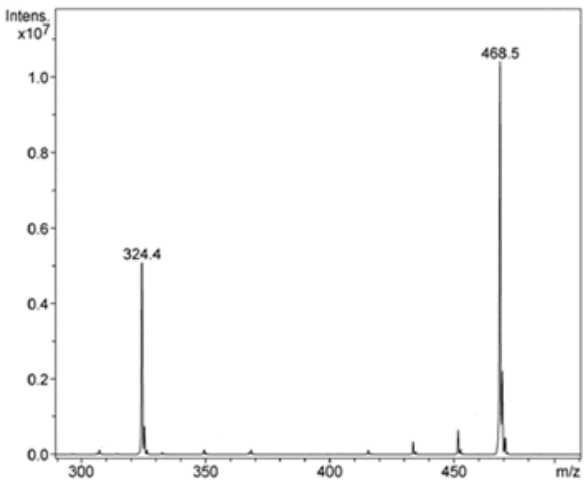

Figure 3.3.1. ESI-MS spectrum of pure tobramycin (Compound stability = 100)

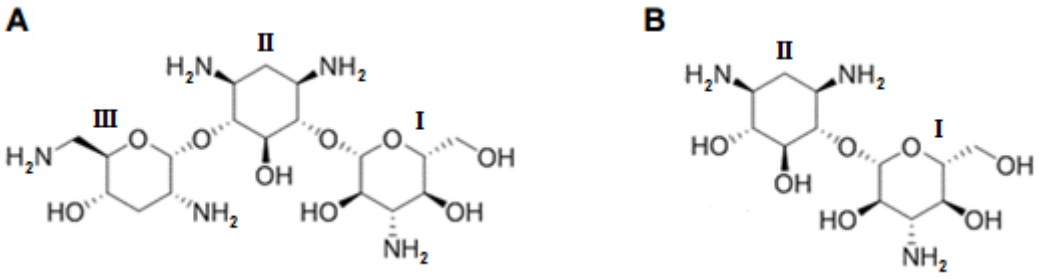

Figure 3.3.2. Molecular structure of Tobramycin (A) and likely impurity (B)

The purity was checked also by RP-HPLC, using a wavelength of 200 nm (tobramycin, unlike peptides, does not absorb at 214nm) and a gradient from 0% → 100% Solvent B (CH_3CN + 0,05 % TFA) in 40 minutes. From the chromatogram only a single peak can be observed, eluting at 30%B. Unfortunately, tobramycin and the fragment seem to elute together, so it was decided not to purify the molecule before the first reaction, as addition of Boc groups should aid separation.

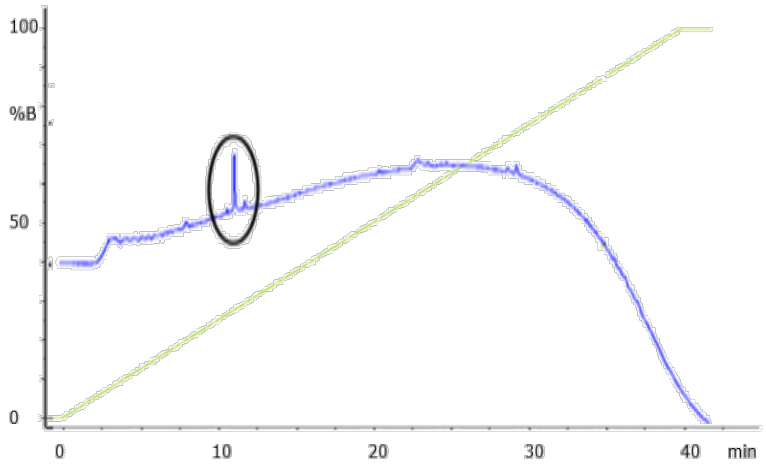

Figure 3.3.3. Analytical RP-HPLC chromatogram of pure tobramycin. Wavelength 200 nm.

3.3.2 Synthesis of $(Boc)_5$-tobramycin (Boc-T)

After performing the protection of amine groups with di-tert-butyl dicarbonate (Boc_2O), the purity of the product (**Figure 3.3.4**) was analysed by RP-HPLC and ESI-MS. The chromatogram showed a single peak with shoulder, and from the ESI-MS analysis (**Figure 4A**), two main peaks could be observed at m/z = 968.4, which corresponds to the correct product, and at m/z = 868.6, corresponding to loss of a t-Boc group (-100). It is well known that during electrospray ionization, the ion impact with the buffer gas can cause the detachment of the relatively labile protecting groups such as t-Boc, due to the collisional energy. This behaviour is, in fact, diagnostic for the presence of such groups. A low intensity peak (m/z = 912.4) between the two main ones is due to the initial detachment of an isobutene

fragment (MW = 56 g/mol), which is followed by removal of a CO_2 molecule (MW = 56 g/mol) to give the – 100 signal. As a confirmation of this process, increasing the compound stability parameter from 20 to 100 (i.e. increasing the acceleration voltage and therefore the impact energy) increased the fragmentation process, and it was possible to observe the subsequent removal of a further isobutene and t-Boc groups (**Figure 3.3.4B**).

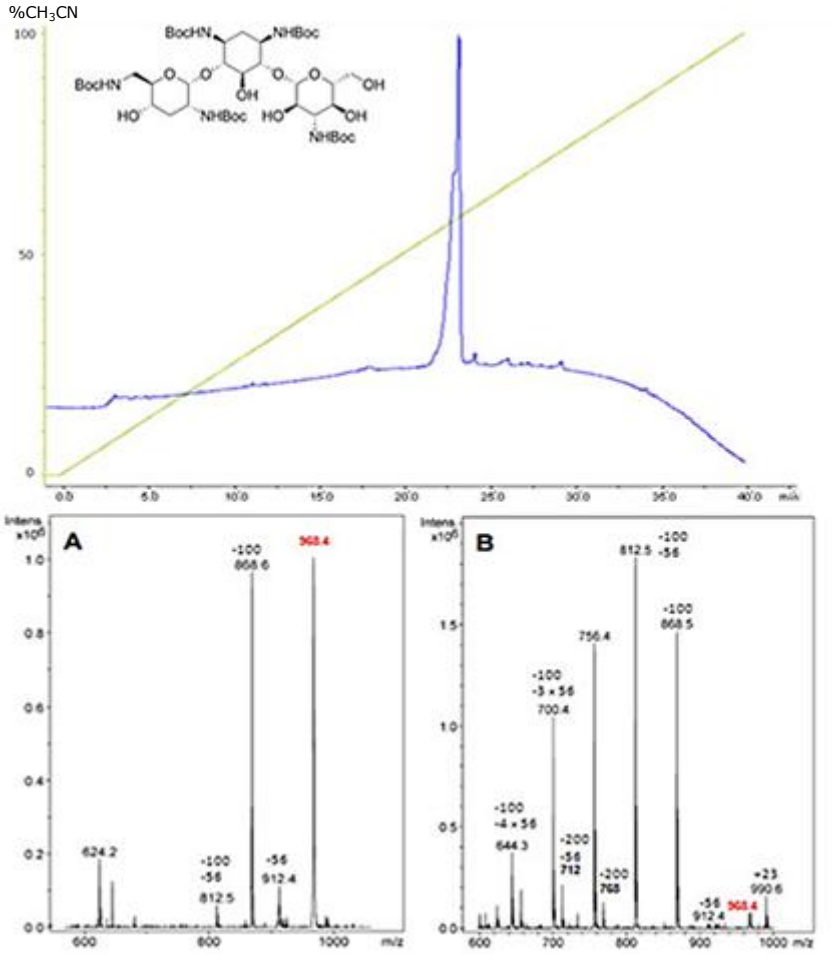

Figure 3.3.4. Structure, analytical RP-HPLC chromatogram (top) and ESI-MS spectrum (bottom) of Boc-T (MW = 967). Elution was with a 0-100 % gradient of CH_3CN + 0,05 % TFA, monitoring at 200 nm. Mass spectra were measured from aliquots of the elution peak with at compound stability of 20 A) and 100 B)

As expected, the presence of the impurity in the starting material is confirmed by the presence of a peak at m/z = 624.2 due the Boc-protected fragment lacking of the glycosidic ring III and consequent having only three Boc protecting groups. The final yield of dried product of

0.37g against a theoretical yield of 0.49g (75%), possibly reflects the presence of this impurity, but is in any case sufficiently high to continue the synthetic process.

3.3.3 Synthesis of $(Boc)_5$Tobramycin-Hemisuccinate (Boc-T-HS)

After the reaction of $(Boc)_5$Tobramycin with succinic anhydride, the purity of the product was again tested by analytical RP-HPLC and ESI-MS (see **Figure 3.3.5**). In this case it was possible to use monitoring wavelengths at both 200 and 214 nm and the chromatogram showed three main peaks, where the circled elution peak corresponds to $(Boc)_5$Tobramycin-hemisuccinate, which elutes at 58%B. The first peak (54% B) corresponds to the unreacted succinic anhydride, present in excess, as also indicated by the absorbance at 214 nm; the third peak (60% B) corresponds to a secondary reaction. This step had two significantly complicating factors; *a)* the unreacted succinic anhydride elutes at the same %B as the starting compound $(Boc)_5$Tobramycin, and *b)* succinic anhydride has the same MW as tBOC, which together with mass fragmentation made it difficult to evaluate the presence of unreacted material.

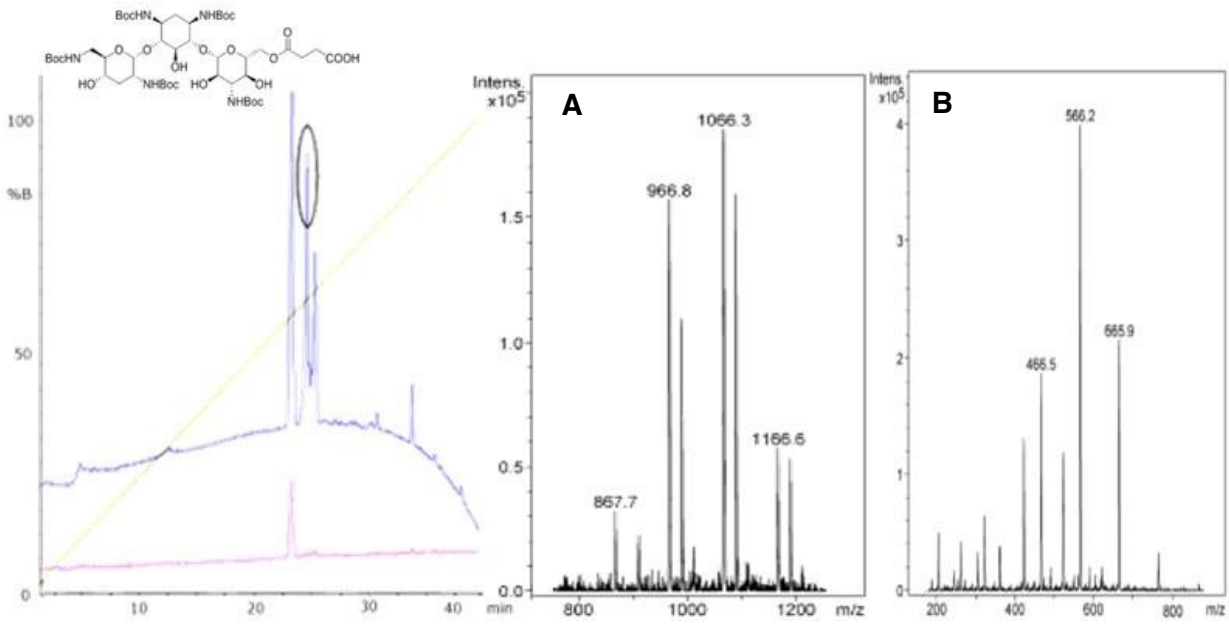

Figure 3.3.5. Structure, analytical RP-HPLC chromatogram (left) and ESI-MS spectrum of (A) Boc-T-hS (MW = 1066) and (B) T-hS (MW = 566). Elution was with a 0-100 % gradient of CH_3CN + 0,05 % TFA (0.8 ml/min), monitoring at 200 (blue) and 214 nm (magenta). Mass spectra were measured from aliquots of the elution peak at compound stability of 100.

The ESI-MS analysis of the crude material showed a high intensity peak at m/z = 1066.3 (**Figure 3.3.5A**), corresponding to the desired product $(Boc)_5$Tobramycin-hemisuccinate, and a lower peak at m/z = 1166.6, likely corresponding to a second hemisuccinate linked to a secondary hydroxyl group (+100). This unfortunately means that these hydroxyl groups are not completely unreactive under the reaction conditions used. Another intense peak at m/z = 966.8 could correspond to the starting material, or to the Boc-T-HS product lacking a t-Boc group due to the ESI-MS fragmentation (-100), or both possibilities. For this reason, a small amount of crude material was deprotected with 95% aqueous TFA to remove all t-Boc groups, and analysed by ESI-MS. As can be seen in **Figure 3.3.5B** the main peak at m/z = 566.2 corresponds to the correct Tobramycin-hemisuccinate product, while a medium intensity peak at m/z = 466.5 corresponds to not reacted starting compound. The peak at m/z = 665.9 again confirms a significant presence of the secondary product with two hemisuccinate groups. It is also important to note that the three main peaks be coupled with satellite peaks corresponding to (+23), as the acid groups carry Na^+ ions with them.

The final yield of dried crude product of 0.30 g against a theoretical yield of 0.40 g (75%), reflects the presence of unreacted material (tobramycin fragment and double hemisuccinate), but again was considered sufficiently high to continue the synthetic process. For the subsequent reaction with the cysteine residue, it was decided to proceed using the crude product in order to reduce excessive loss of material in a purification step. In this respect, the starting material should not react, and the secondary product with double-hemisuccinate should be readily purified subsequently by RP-HPLC.

3.3.4 Synthesis of Tobramycin(Hemisuccinate)-Cys (T-HS-Cys)

To conjugate the modified tobramycin to the antimicrobial peptide by a disulfide bridge, it was necessary first to introduce a cysteine residue by formation of an amide bond, to obtain Tobramycin(Hemisuccinate)-Cys. This would allow disulfide bond formation with the C-terminal cysteine residue on the peptide. The reaction was carried out in the solid phase, with microwave assistance, then removing the product from the resin and simultaneously deprotecting the t-Boc groups. The correct structure of the crude product verified via ESI-MS (**Figure 3.3.6**).

The ESI-MS spectrum shows a high intensity peak with m/z = 670.4 corresponding to Tobramycin(hemisuccinate)-Cys. The presence of the fragment impurity is confirmed by a

peak at m/z = 526.2 corresponding to the lack of the glycosidic ring III (-144). The product otherwise appears relatively pure. The yield of dried crude product of 49 mg against a theoretical yield of 53 mg (>90%), indicates efficient coupling of the antibiotic to the Cys residue.

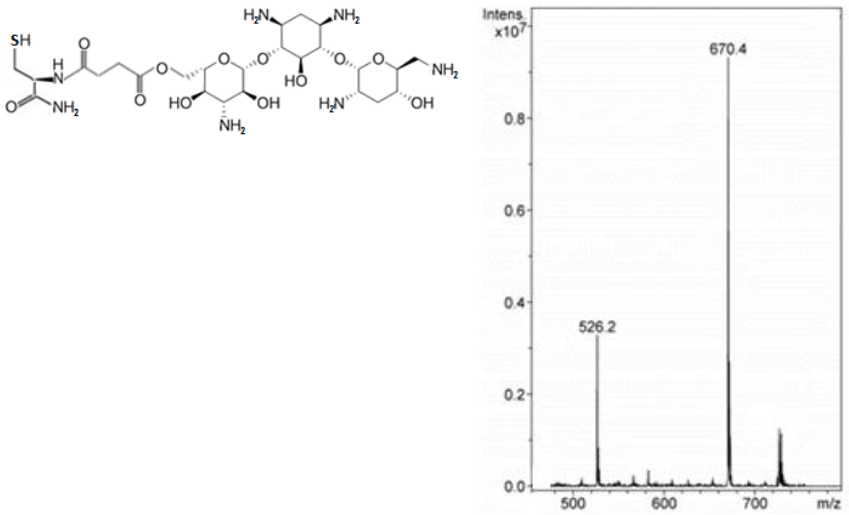

Figure 3.3.6. Structure of T-HS-Cys (MW = 670) and ESI-MS spectrum of crude product. Compound stability = 100.

3.3.5 Synthesis of Tobramycin-Cys-Thiopyridine (T-hS-Cys-TPy)

To direct coupling of the antibiotic to the peptide carrier, and avoid homo-dimer formation (or dimerization of the peptide carrier), the sulfhydryl group of Tobramycin-hS-Cys was pre-activated with 2,2'-dithiodipyridine. This reaction was relatively straightforward, and the ESI-MS spectrum with main peak at m/z = 779.4 confirmed the presence of tobramycin-hS-Cys-thiopyridine, as well as the related product lacking the glycosidic ring III (m/z = 635.3) (see **Figure 3.3.7**). The yield of dried crude product of 40 mg against an expected theoretical yield of 57 mg (~70%), indicates some loss of material in this step, but it is in any case acceptable, considering that a significantly higher loss could occur through homodimer formation, which would also complicate purification.

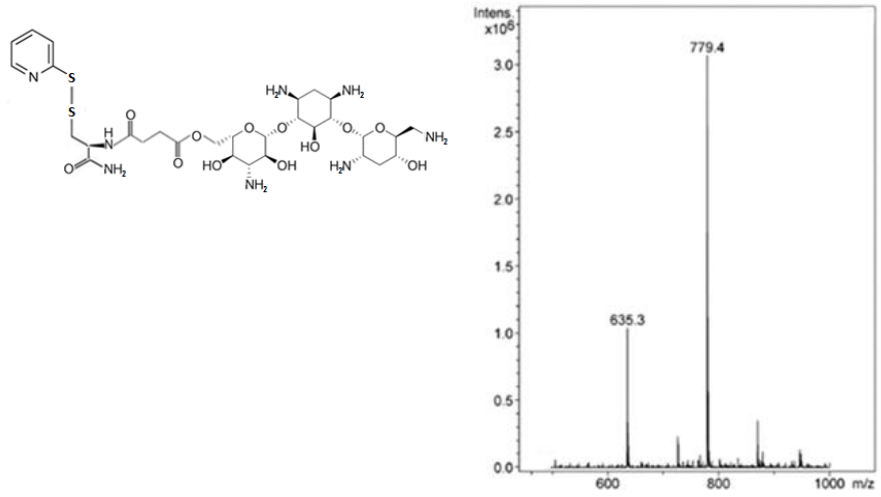

Figure 3.3.7. Structure of T-hS-Cys-TPy (MW = 779) and ESI-MS spectrum. Compound stability = 100.

3.3.6 Synthesis of Bac7(1-35)[Cys^{36}] and Bac7(1-15)[Cys^{16}]

The SPPS of Bac7(1-35)[Cys^{36}] was straightforward and produced high quality peptide, as confirmed by ESI-MS analysis (**Figure 3.3.8**), with a single peak at m/z = 4310.7 corresponding to the correct structure. The yield was significantly lower than expected (~ 30%), but given the high quality of the peptide was likely due to overestimation of resin substitution (it was more like 0.1 mmol/g than 0.35 mmol/g). The high quality of the crude final product is important, as it allows proceeding with the dimerization reaction without a prior RP-HPLC purification step, which can cause losses of up to 50%. This more than made up for the relatively low yield.

For the shorter Bac7(1-15)[Cys^{16}], it was decided to produce a C-terminal amidated peptide, remove the C-terminal negative charge. In this case the synthesis proceeded with a yield of crude material >90%. The ESI-MS spectrum (**Figure 3.3.9A)** shows a main peak with m/z = 2022.3 corresponding to the correct Bac7(1-15)[Cys^{16}] structure and the purity was also confirmed by analytical RP-HPLC.

A small amount of the Bac7 crude peptides were alkylated using 2-iodoacetamide, in order to block the reactive SH groups the C-terminal cysteine residue, for use as controls, preventing intermolecular dimerization during assays. The reaction was confirmed by ESI-MS (see

Figures 3.3.10 and **3.3.11**) and alkylated peptides purified by preparative RP-HPLC in good yields.

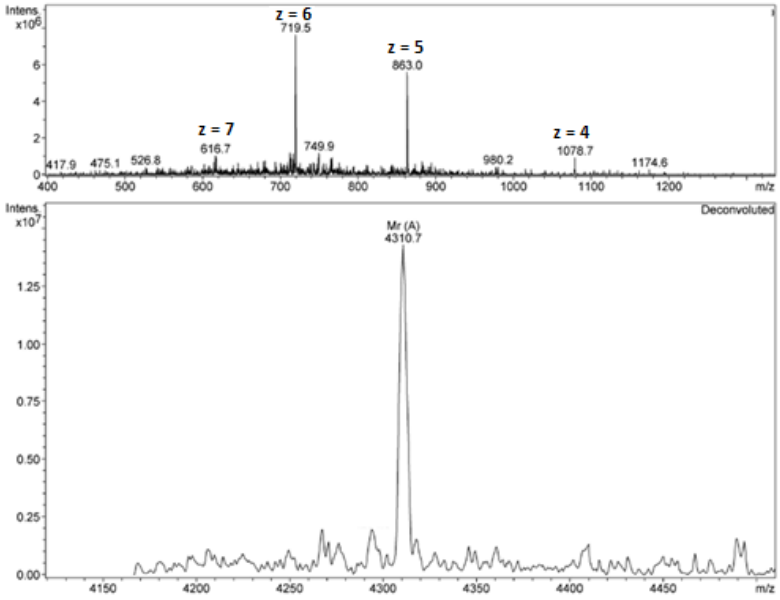

Figure 3.3.8. Mass spectrum of Bac7(1-35)[Cys^{36}]. Top: ESI-MS spectrum of crude material at Compound stability = 100. Below: reconstructed spectrum based on m/z peaks.

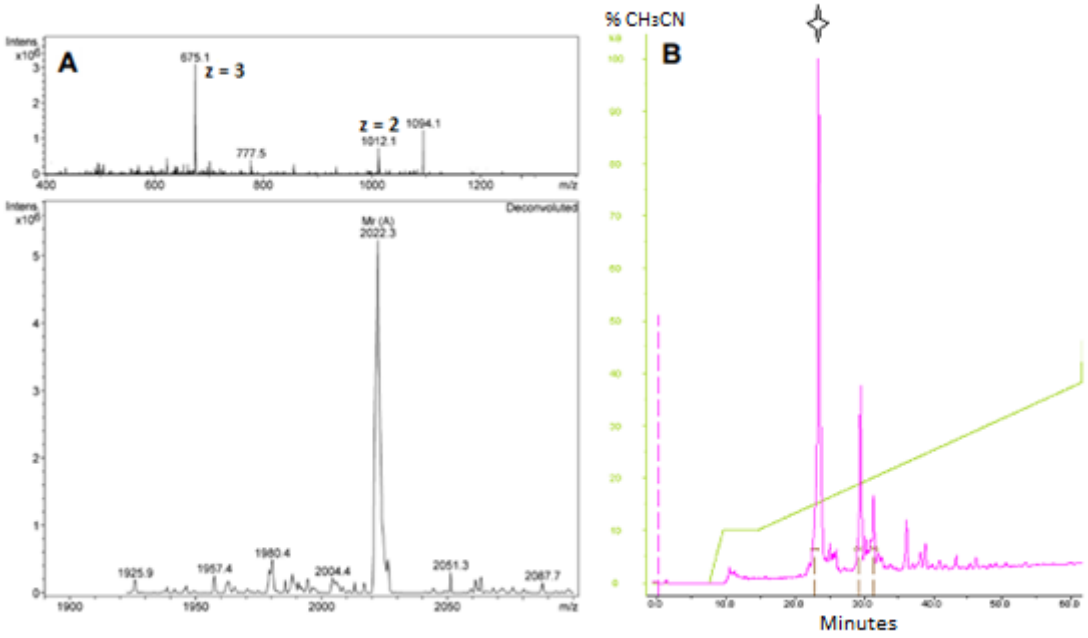

Figure 3.3.9. Analysis of Bac7(1-15)[Cys^{16}]: A) ESI-MS spectrum of crude material at Compound stability = 100. The reconstructed spectrum based on m/z peaks is shown below. **B)** analytical RP-HPLC chromatogram of crude material (wavelength at 214 nm, flow 0.8 ml/min, 10-40% CH_3CN in 40 min).

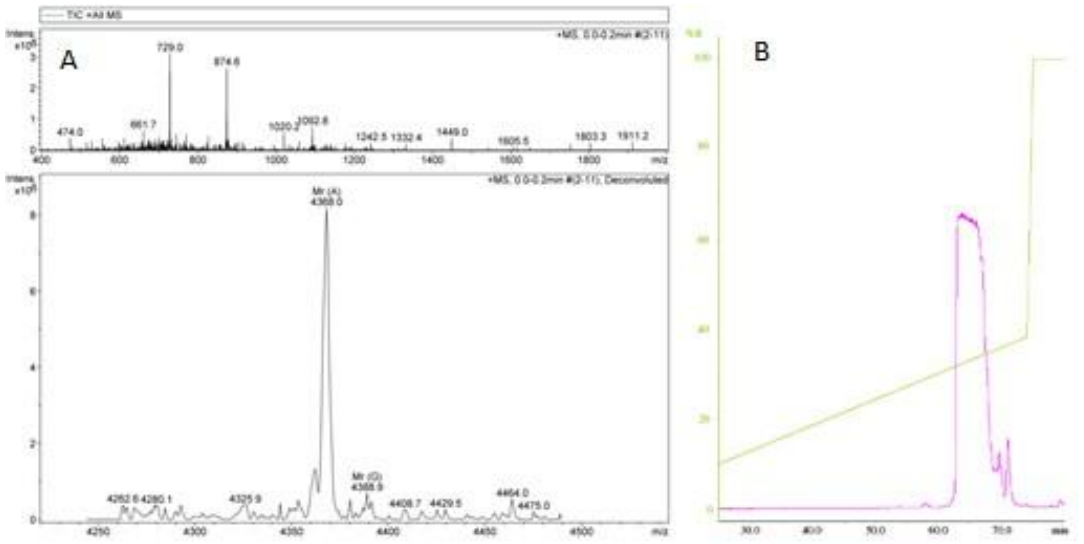

Figure 3.3.10. Mass spectra and preparative RP-HPLC of (Bac7(1-35)[Cys^{36}]-ALK (MW = 4368). A) ESI-MS spectrum at Compound stability = 100); below: spectrum reconstructed based on m/z peaks. **B)** preparative RP-HPLC chromatogram (wavelength at 214 nm, flow 8 ml/min, 10-40% CH_3CN in 40 min).

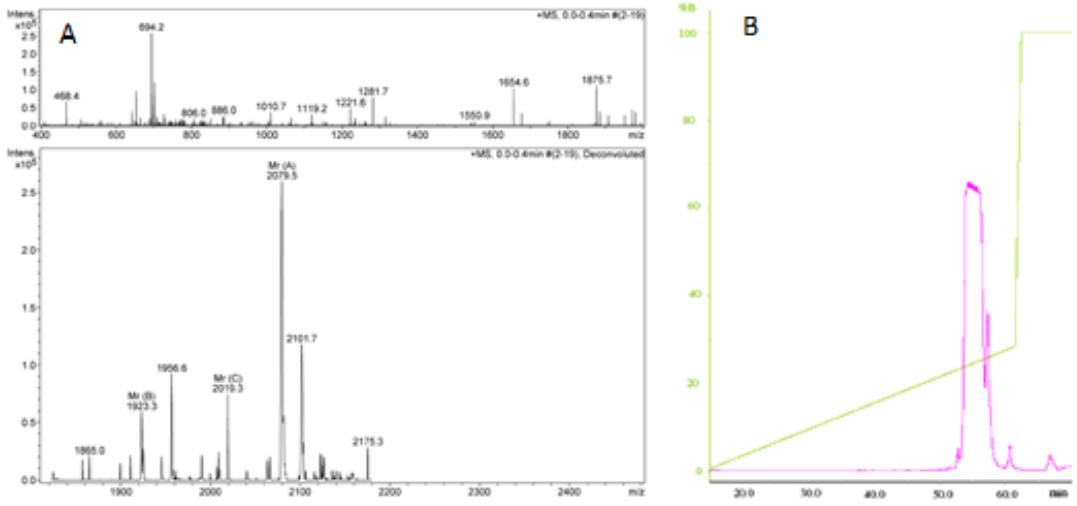

Figure 3.3.11. Mass spectra and preparative RP-HPLC of Bac7(1-15)[Cys^{16}]-ALK (MW=2079): **A)** ESI-MS spectrum at Compound stability = 100; below: spectrum reconstructed based on m/z peaks. **B)** preparative RP-HPLC chromatogram (wavelength at 214 nm, flow 8 ml/min, 0-35% CH_3CN in 50 min).

3.3.7 Synthesis of Tobramycin-Bac7(1-35) and Tobramycin-Bac7(1-15)

The last step in the synthetic process was to conjugate Tobramycin-Cys-Thiopyridine with the antimicrobial peptides modified with cysteine. The reaction was carried out with small quantities of antibiotic and peptide, at relatively high dilution and was monitored by analytical RP-HPLC, by taking small aliquots of the reaction solution, and determining the molecular weight of collected peaks with ESI-MS (see **Figure 3.3.12**). After two hours two main chromatographic peaks could be observed, circled in black and red on the chromatograms, corresponding respectively to the desired hetero-dimer Tobramycin-Bac7(1-35), and the unreacted Bac7(1-35)[Cys^{36}]. The second peak significantly decreased after 4 hours but the reaction reached completion only after 24 hours, indicating it is rather slow. This is likely because a 1:1 ratio of antibiotic and peptide were used to avoid peptide dimerization. The chromatograms showed some secondary peaks, so that the product was purified by preparative RP-HPLC (**Figure 3.3.13**). The collected peak (highlighted in black) was confirmed by ESI-MS to correspond to the correct heterodimer (m/z = 4977.3), which was collected with good purity, although the yield of pure product was relatively low, due to both the dimerization and purification steps (~20%).

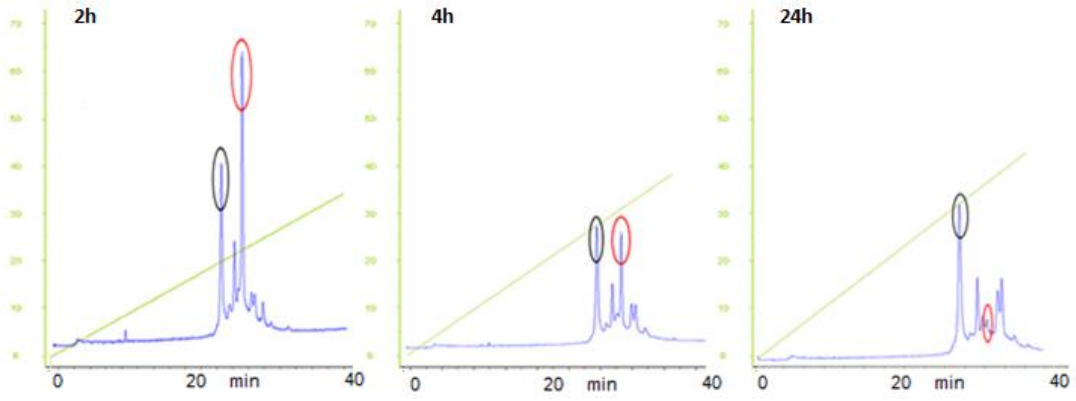

Figure 3.3.12. Analytical RP-HPLC chromatograms of Tobramycin-Bac7(1-35) ligation time course (wavelength at 200 nm, flow 0.8 ml/min, 0-35% CH_3CN in 40 min).

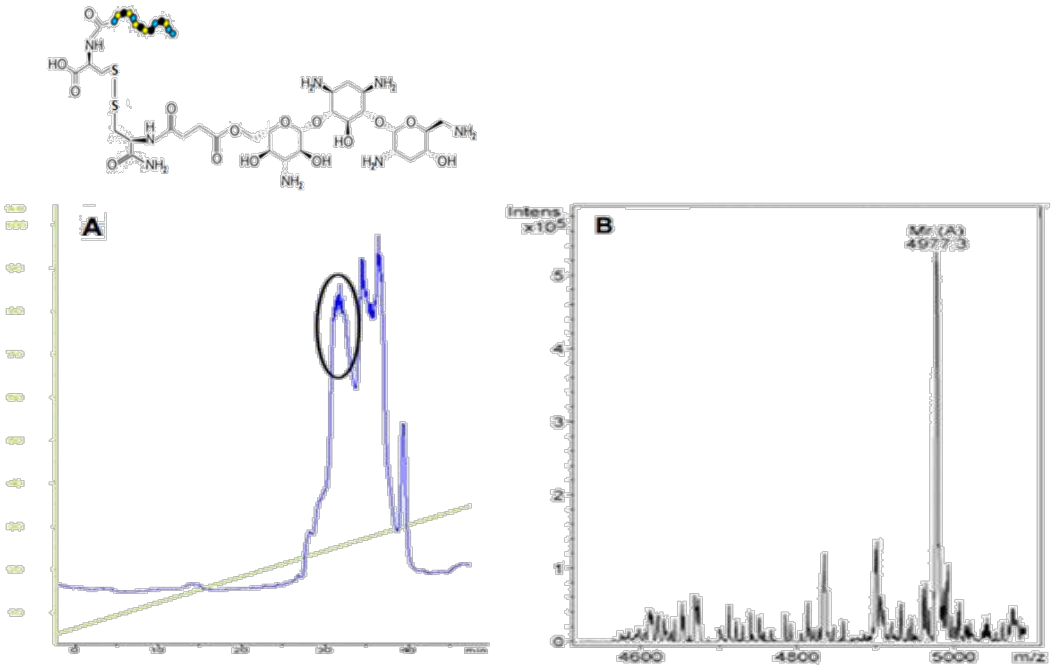

Figure 3.3.13. Tobramycin-Bac7(1-35) heterodimerization: A) preparative RP-HPLC chromatogram (wavelength at 200 nm, flow 8 ml/min, 0-35% CH_3CN in 50 min); **B)** ESI-MS spectrum at Compound stability = 100.

The same procedure was performed for Tobramycin-Bac7(1-15). In this case, however, after two hours three main peaks were present, highlighted in black, red and green in **Figure 3.3.14**, corresponding respectively to the complete heterodimer, the unreacted Bac7(1-15)[Cys^{16}] and [Bac7(1-15)Cys^{16}]$_2$ homo-dimer. This peak progressively decreases in intensity compared to the heterodimer, indicating a relatively quick process of homodimerization over which heterodimerization with Tobramycin-hS-Cys-TPy then prevails. After 24h, purification by preparative RP-HPLC followed by mass spectrometric analysis of collected fractions (**Figure 3.3.15**) confirmed a main peak (black circle) corresponding to the correct heterodimer, and significant other peaks corresponding to unreacted peptide (red circle), and Bac7 homodimer (green). In retrospect, the introduction of C-terminal amidation, by removing charge reduced electrostatic repulsion between peptide C-termini, and may have favoured homodimeric disulfide formation. It may be better to avoid it in future. It likely contributed to the low yield of ~12%.

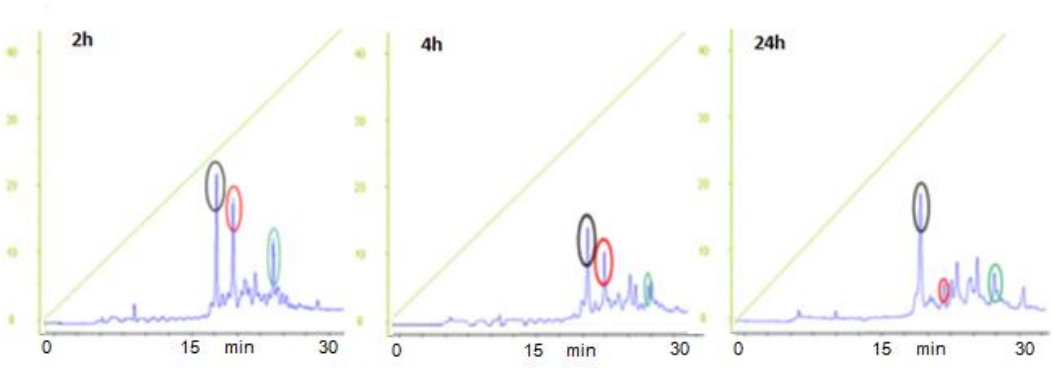

Figure 3.3.14. Analytical RP-HPLC chromatograms of Tobramycin-Bac7(1-15) ligation time course (wavelength at 200 nm, flow 0.8 ml/min, 0-40% CH_3CN in 30 min).

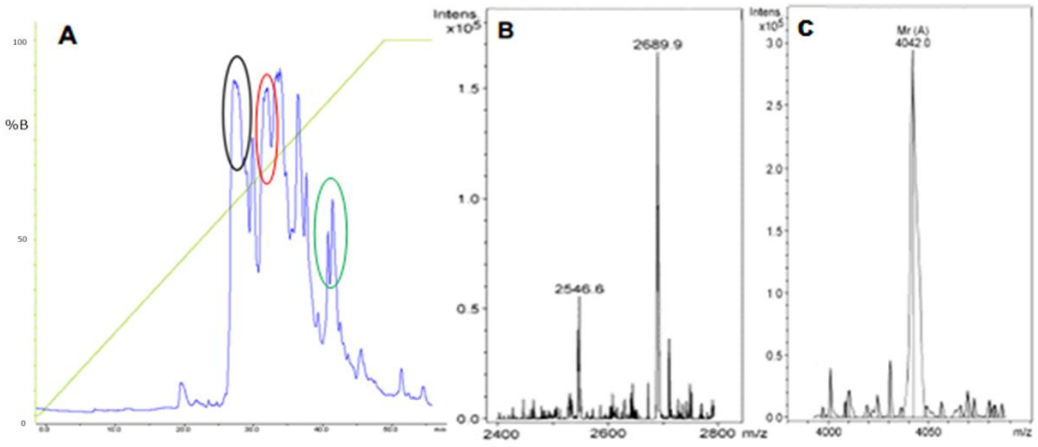

Figure 3.3.15. Tobramycin-Bac7(1-15) heterodimerization: A) preparative RP-HPLC chromatogram (wavelength at 200 nm, flow 8 ml/min, 0-100% CH_3CN in 50 min). **B)** Tobramycin-Bac7(1-15) ESI-MS spectrum; **C)** [Bac7(1-15)Cys^{16}]$_2$ ESI-MS spectrum. Compound stability = 100

3.3.8 Overall reaction analysis

The synthesis of the tobramycin-peptide conjugate by disulfide formation through Cys residues requires several steps, some of which with low synthetic yields **(see Table 3.3.1)**, so the overall yield was also low. However, it was possible to collect several milligrams of pure conjugates, sufficient for preliminary functional assays and proof of principle. It is likely that the process can be significantly improved. In particular, it is necessary to improve the

antibiotic-to-peptide conjugation step. Possibly a better activator than thiopyridine can be found that can be used to prepared pre-activated antibiotic in greater yield, and allow a faster and more complete heterodimerization, reducing the amount of unreacted peptide and peptide homodimer. In this respect, avoiding peptide amidation at the C-terminal may also possibly help.

Table 3.3.1. Synthesis of Tobramycin-peptide conjugates by the hemisuccinate-Cys strategy

Product	MW (g/mol)	Expected weight (g)	Actual weight (g)	% Yield
Boc-T	967	0.488	0.367	75 %
Boc-T-hS	1067	0.405	0.303	75 %
T-hS-Cys	670	0.053	0.049	92 %
T-hS-Cys-TPy	779	0.057	0.040	70 %
T-hS-Cys-Bac7(1-35) -Cys	4978	0.0124	0.0026	21 %
T-hS-Cys-Bac7(1-15) -Cys	2689	0.012	0.0015	12.5 %

3.3.9 Synthesis of $(Boc)_5$Tobramycin-OTibs (Boc-T-OTibs)

The second strategy I attempted to synthesize the heterodimer was to introduce a sulphide group in place of the primary hydroxyl of tobramycin, to allow direct S-S bond formation Bac7(1-35)[Cys^{36}]. For this reason, a trisyl chloride (Tibs) group was first used to pre-activate position 6" of $(Boc)_5$Tobramycin (see **Figure 3.3.16** and section 3.3.1). The considerable steric hindrance of the activator has the advantage of avoiding its addition to less reactive hydroxyl secondary hydroxyl groups.

The reaction solution was monitored by ESI-MS over three days but an m/z peak corresponding to the desired molecule (MW = 1230) was not observed (see **Figure 3.3.17A**). However, signals corresponding to loss of 1 to 5 Boc protecting groups could be observed. Furthermore, after extraction and drying, a signal with reduced intensity at m/z = 1253.4 could correspond to the desired with the addition of a Na^+ ion (+23) (**Figure 3.3.17B**). Taken

together with the low intensity of the signal corresponding to unreacted **Boc-T** these m/z signals are a good indication that the reaction went substantially to completion, and a yield of >90% was estimated from the weight of crude product

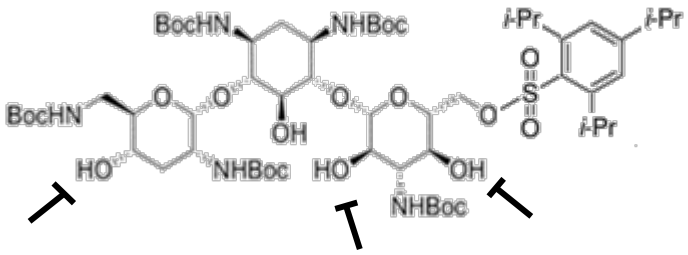

Figure 3.3.16. Molecular structure of Boc-T-OTibs and its reactive and unreactive hydroxyl groups.

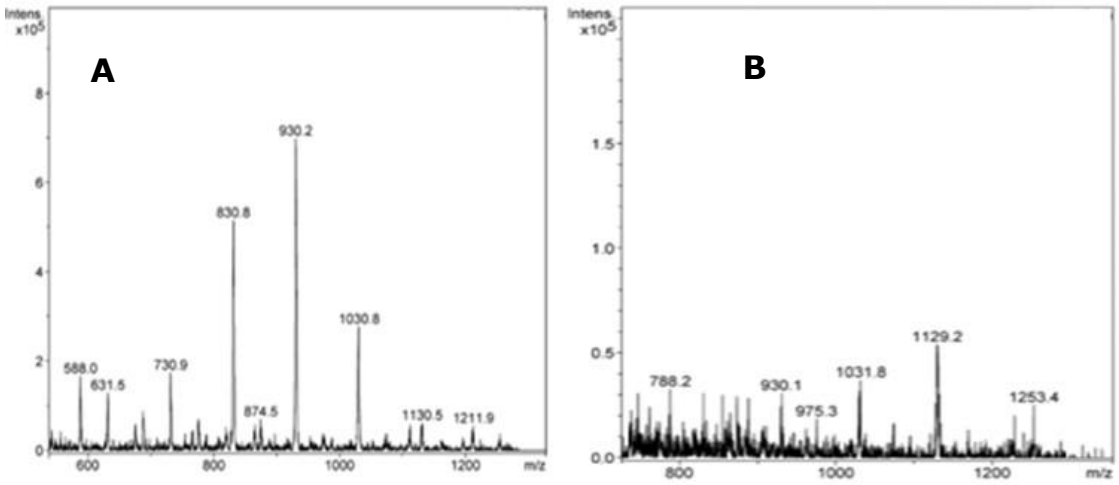

Figure 3.3.17. ESI-MS spectrum reaction solution (A) and extracted, dried crude product (B) solution. Compound stability = 100.

3.3.10 Synthesis of (Boc) $_5$Tobramycin-dioxaoctanethiol (Boc-T-DOT)

The subsequent reaction with DODT was difficult to monitor with ESI-MS due to an apparently low molecular ionization of the product. Despite the reduced intensity, it was possible to perform analysis only for the crude material. As the reaction did not proceed to completion, the excess of DODT was increased. After 36 hours, The ESI-MS spectra (**Figure 3.3.18**) showed mainly a signal m/z = 1130.7, which corresponds to the correct Boc-T-DOT product (MW =

1131). Unfortunately, the DOT adduct has the same molecular weight as the unreacted starting material with one Boc group missing through fragmentation (as part of the series seen in **Figure 3.3.18A**), and the weak signal at m/z = 1253.7, corresponding to the sodium adduct of the starting compound; indicated starting material was indeed still present. For this reason, a small amount of crude material was deprotected and analysed by ESI-MS revealing a signal at m/z = 731.0 (**Figure 3.3.18B**), which corresponded to tobramycin-OTibs, indicating that the reaction was not successful. It was repeated under several different conditions, but in all cases has proved to be a critical step in this synthetic strategy. Subsequent studies have indicated a likely reason for the lack of correct product is the strong tendency of DODT to form a linear and cyclic multimers that make the ESI-MS spectra rather dirty. A DODT multimer may also form on the DOT group of Boc-T-DOT, making it difficult to isolate the product. The reaction is now being reconsidered in this light to improve the yield.

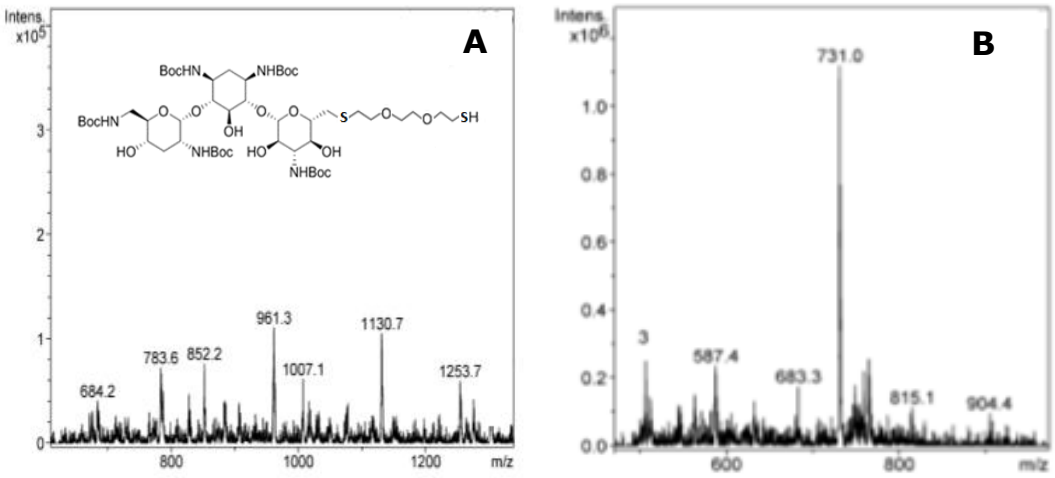

Figure 3.3.18. ESI-MS spectrum of the reaction mixture for the Boc-T-OTibs + DODT reaction, after extraction and drying before (A) and after (B) deprotection from Boc groups. The correct structure of the reaction product (see inset) has MW = 1131, the starting material Boc-T-OTibs has MW = 1230. Their respective deprotected MW are 731 and 631. The ESI-MS spectra were taken with CS = 100.

3.3.11 Antibiotic/peptide Heterodimer and Peptide carrier quantification

Before starting the functional assays, all synthesized molecules were quantificated comparing the theoretical concentration obtained by weighing, with that obtained by measuring the absorbance at 214 nm and for peptides by the Waddel method. In table are indicated the molar extinction coefficients for the peptides, calculated according to those reported in literature (Kuipers and Gruppen, 2007). The measurments provided a final concentration as the arithmetic mean, with a relatively low error.

Table 3.3.2. Table of concentration values (mM) obtained after quantification.

a) Concentration	Molecule	[Wt] [(a)]	ε_{214} ($M^{-1}cm^{-1}$)	[214]	[Wad]	[Final]
	T-Bac7(1-35)	2.6	90500	2.8[(b)]	2.6	2.7± 0.1
	T-Bac(1-15)	3.2	33000	3.5[(b)]	3.6	3.4± 0.2
	Bac7(1-35)[Cys^{36}@]	3.15	89500	3.1[(c)]	3.2	3.15± 0.05
	Bac7(1-15)[Cys^{16}@]	3.5	33000	3.0[(c)]	2.9	3.1± 0.3

(a) Quantification by: [Wt] = by weight; [214] = by absorption at 214nm; [Wad] = by the Waddle 214nm/220nm absorption method; [Final] = average concentration with error.
(b)Tobramycin does not absorb at 214nm, only the peptide bond to Cys and S-S bond were considered.
(c) For the alkylated Cys (indicated by @) the absorption was considered to be similar to that of Met.

3.3.12 Synergy assays (MIC checkerboard)

Since both tobramycin and Bac7(1-35) peptide target the 70S ribosome subunit (Vázquez-Espinosa et al., 2015), (Mardirossian et al., 2014), the single components of the T-Bac7(1-35) conjugate were tested together in order to evaluate any synergistic, additive or antagonist effect of the molecules. This was evaluated in terms of a checkerboard MIC assay, by treating *E. coli* BW 25113 simultaneously with Bac7(1-35) and tobramycin in different combinations, as shown schematically in **Figure 3.3.19**.

The checkerboard experiment clearly indicated that the two components did not affect each other's efficacy, as confirmed by the calculated Fractional Inhibitory Concentration (FIC) value = 1. A synergic effect would have required FIC ≤ 0.5, and an additive effect 1 > FIC > 0.5. Therefore the Bac7(1-35) and tobramycin seem to be indifferent to each other's action, as individual molecules, if co-administered to susceptible bacteria.

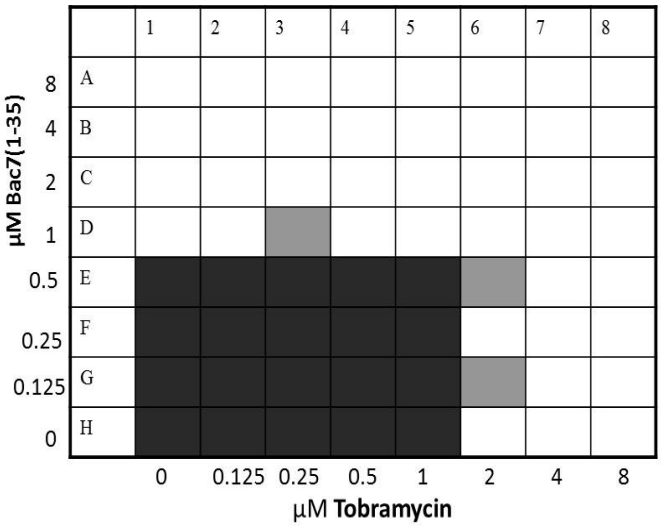

Figure 3.3.19. Schematic representation of the checkerboard MIC assay using Bac7(1-35) and tobramycin against *E. coli* BW 25113: Black boxes indicate bacterial growth; white boxes indicate complete growth inhibition. Grey boxes indicate some turbidity but no deposit on the bottom of wells

3.3.13 Activity of T-Bac7(n) against *E.coli* strains

The bacteriostatic activity (MIC) of the T-Bac7(1-35) conjugate was determined against *E.coli* BW25311 and its *ΔsbmA* mutant devoid of the SbmA transporter, in order to gain information about the possible internalization of the conjugate (**Table 3.3.3**). T-Bac7(1-15) was assayed in parallel, since free Bac7(1-15) is a fragment that is thought to penetrate into susceptible bacteria but has a lower intrinsic antimicrobial activity (Guida et al., 2015). It was hoped this would allow isolating the antibacterial contribution of tobramycin from that of the peptide carrier.

Results were somewhat surprising. MIC values confirm that the alkylated Bac7(1-15)[Cys^{16}] PR-AMP was inactive against E.coli BW 25113 and consequently also against the deletion mutant. Alkylated Bac7(1-35)[Cys^{36}] instead has the same activity as Bac7(1-35). When the SbmA transporter was missing, activity was reduced for the peptide carrier, Bac7(1-35)[Cys^{36}@] (MIC 2→8 µM), but surprisingly also for the antibiotic cargo Tobramycin, which showed a fourfold decrease in activity (MIC 4→16µM). On the other hand, the conjugate not only improved its activity against the *wt E.coli* BW25311, but substantially

maintained it in the absence of SbmA. Furthermore, the conjugate with the inactive Bac7(1-15), also showed a significant activity.

Table 3.3.3. MIC values for antibiotic/PR-AMP conjugates against *E. coli* and its SbmA deletion mutant, compared to those of the free antibiotic and PR-AMPs.

	MIC (μM) [(a)]	
	***E.coli* BW 25113 (*w.t.*)**	***E.coli* BW 25113 *ΔsbmA***
Tobramycin (T)	4	16
T-Cys – Cys^{36}-Bac7(1-35)	1	2
Bac7(1-35)[Cys^{36}@][(b)]	2	8
T-Cys – Cys^{16}-Bac(1-15)	4	4
Bac7(1-15)[Cys^{16}@][(c)]	>32	>32

(a) Experiments were repeated three times in triplicate, inoculating 2.5x10^5 CFU/ml bacteria in 100% MH broth at 37 ° C for 20 hours. MIC values were visually evaluated as the lowest concentration at which bacterial growth was inhibited (no turbidity/deposit on bottom of well); (b) @ indicates that the Cys side-chain on the peptide was acetylated; (c) C-terminal Cys residue on the peptide was both side-chain acetylated and amidated.

This raises some interesting questions. The significant increase in MIC for tobramycin on its own, in absence of transporter could have two different explanations: *i)* SbmA is not only capable of PR-AMP internalization, but also of internalizing the antibiotic, a very different molecule. This would be consistent with reports showing that SbmA transports molecules as different as PR-AMPs, bleomycin and microcins (Yorgey et al., 1994), (Salomón and Farías, 1995), (LeVier et al., 2000). *ii)* Production of the *ΔsbmA* deletion mutant for the Keio library requires introduction of an antibiotic-resistance-determining cassette (Km^R) for kanamycin, aminoglycoside, so this could make the strain resistant also to tobramycin. Somehow, conjugation of the antibiotic to the PR-AMP would allow it to evade this resistance mechanism, and the conjugate could enter in sufficient quantity by the other transporter to allow a good activity.

The second question concerns the appreciable activity of the tobramycin conjugate with inactive Bac7(1-15)[Cys^{16}]. For the *w.t*. strain, a simple explanation would be that the peptide is internalizing with its antibiotic cargo, and as the conjugate's activity is the same as that of the free antibiotic, the carrier has no effect on its own but also no effect on the antibiotic's activity. It is more difficult to explain the activity on the transporter deletion mutant, unless it is the same as for point *ii)* above.

To test a possible role of the mutant's antibiotics resistant cassette on the activity of Tobramycin, the MIC was evaluated against the *E.coli* BW 25113 *ΔrpoS* and *E.coli* BW 25113 *Δhfq* Keio collection strains, chosen at random. Like *ΔsbmA,* these mutants have the antibiotic-resistance for kanamycin (Km^{r}) but they are knocked-out for genes that are not involved in PR-AMP internalization. To test for a possible role of the SbmA transporter in tobramycin internalization, activity was tested against BW25113[pMAU1(*sbmA*)], a particular *E. coli* Δ*sbmA* clone that was transformed with an exogenous plasmid (pUC18) carrying a copy of the wild-type *sbmA* gene (pMAU1). This complementation should restore the normal internalization mechanism (Mattiuzzo et al., 2007).

As shown in **Table 3.3.4**, MIC values for all three mutants are the same as for the *wild-type* strain, indicating that the decreased activity of tobramycin in *E. coli* Δ*sbmA* is not given by its resistance to kanamycin and strengthening the hypothesis that SbmA plays a role in antibiotic transport. Without it, internalization of tobramycin is significantly decreased, reducing its activity. A higher level of internalization would be restored by re-introducing the SbmA gene on a plasmid, as is in fact observed. These results confirm that a functional SbmA is relevant for not only internalization of PR-AMPs, but also for tobramycin, and possibly other antibiotics. This is an unexpected and quite interesting result.

Taken together, these data provide another important item of information concerning the conjugate's stability in the extracellular medium; the heterodimer was stable in bulk solution, as on separating the single components would be expected to show a lower antimicrobial activity against the *E. coli* Δ*sbmA* deletion mutant. This is indirect evidence of extracellular stability and supports the hypothesis that tobramycin is internalised into the bacterial cytoplasm by the conjugate.

Table 3.3.4. MIC values for Tobramycin against selected *E.coli* BW 25113 deletion mutant strains

	MIC (μM) [(a)]		
	BW 25113 *ΔrpoS*	**BW 25113 *Δhfq***	**BW 25113 *ΔsbmA* [pMAU1(*sbmA*)]**
Tobramycin	4	4	4

(a) Experiments were repeated three times in triplicate and the values were obtained using micro-dilution, inoculating 2.5 * 10^5 CFU / ml in 100% MH broth and maintaining the plates at 37 ° C for 20 hours. The MIC values were evaluated by visually determining the lowest concentration at which bacterial growth was inhibited.

3.3.14 Bacterial Growth kinetics

The antimicrobial activity of T-Bac7(1-35) was evaluated also by monitoring its effect on bacterial growth kinetics, at sub-MIC concentrations, using *E.coli* BW25311 and its *ΔsbmA* mutant. For the *wild-type* strain, the concentration at which growth is completely inhibited over a 4 hour period, 1 μM, corresponds to the MIC value, whereas growth is not significantly slowed at sub-MIC concentrations. For T-Bac7(1-15), growth is inhibited at 2 μM, which is half of the MIC value, and tobramycin on its own also shows inhibiting activity, over this period, at sub-MIC concentrations. Unconjugated Bac7(1-35)[Cys^{36}@] also inhibits growth only at its MIC value against the *w.t*. strain, but is quite active at only 2 μM against the transporter-deficient mutant, inhibiting growth over a four hour period. This short-term inhibiting capacity is even more marked for the Bac7(1-15)[Cys^{16}@] fragment, that bocks growth of both *w.t* and mutant strains at 4 μM, which is well below the MIC of >32 μM. It may be an indication that the peptide enters the bacterium and interacts with its target sufficiently to temporarily inhibit its growth, but is cleared on the longer term.

The deletion of the SbmA transporter resulted in a decreased capacity of the peptides, antibiotic and antibiotic-peptide conjugates to inhibit growth, confirming its role in the internalization of all three types of molecules. However, activity was not abrogated, but shifted to a 2-fold higher concentration, consistent with an alternative, less efficient, means of internalization.

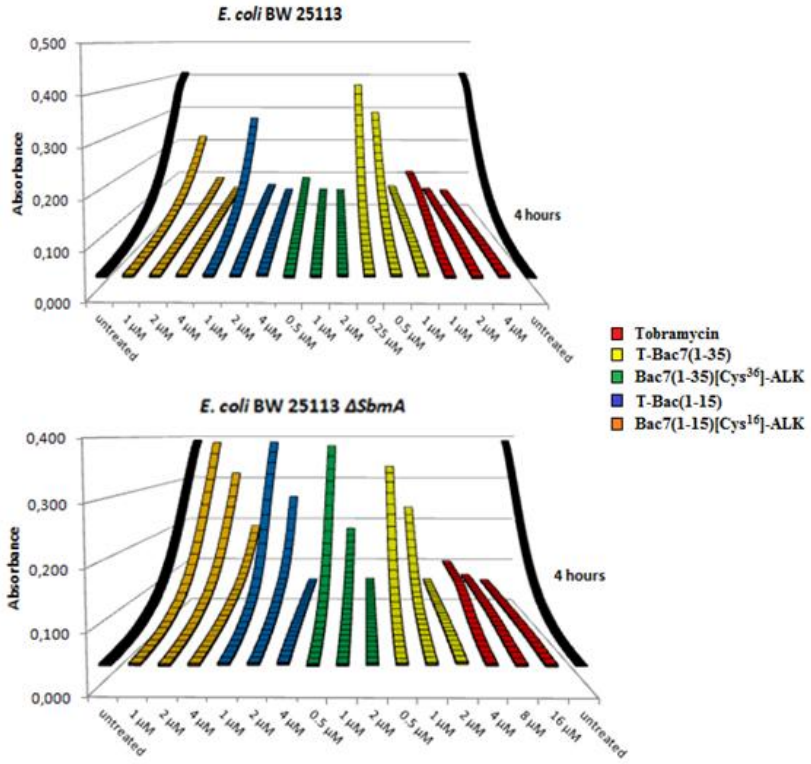

Figure 3.3.20. Growth curves for *E. coli* strains treated with increasing concentrations of antibiotic, PR-AMP and antibiotic-peptide conjugate. Growth was monitored over four hours. The black curves correspond to untreated bacteria (positive control). Experiments were repeated three times in duplicate, for each strain.

3.3.15 Investigating the potential of the Tobramycin/PR-AMP conjugate against other bacterial strains

After investigating the mechanism of action of the conjugate with respect to the susceptible bacterium *E. coli*, it was decided extend testing to a wider range of bacterial strains, with particular attention to Gram-negative *P. aeruginosa*, *K. pneumoniae* and *A. baumannii*. These are responsible for severe infections due to the increasing incidence of drug-resistance. For each of the pathogens the activity of T-Bac conjugates was evaluated in terms of MIC, using both a reference strain and clinical isolates collected in various hospitals in Italy from patients with epidemiologically unrelated infections. The aim was to assess whether T-Bac7(1-35) could indicate a promising strategy for novel antimicrobial therapies, and understand how the molecule's efficacy varied according to the intrinsic characteristics of each strain. In this

respect, while *K. pneumoniae* and *A. baumannii* express homologues of the SbmA PR-AMP transporter, *P. aeruginosa* does not. Consequently, the susceptibility of this bacterium to PR-AMPs is quite variable among different strains (Runti et al., 2013). Furthermore, two Gram-positive strains were also tested, *S. aureus* and *S. epidermidis*, that are intrinsically resistant to PR-AMPs.

The activity of the conjugates, carrier peptides and antibiotic against a *Pseudomonas aeruginosa* ATCC reference strains and several isolates collected from cystic fibrosis patients with lung disease, are shown in **Table 3.3.5**. Bac7(1-35) was not active against the reference strain, but showed an appreciable activity against some of the clinical isolates. Conversely, tobramycin was active against the reference strain and a subset of clinical isolates that only partly overlaps with those susceptible to the peptide. T -Bac7(1-35) conjugate is quite active against all strains, as indicated by the MIC values of 1-4 μM. It is apparent that conjugation intrinsically favours activity, as the T-Bac7(1-15) conjugate also has an appreciable activity against all strains, even though the carrier peptide is by itself inactive. While the structural or functional factors in *Pseudomonas* that makes the different strains more or less susceptible to the antibiotic are not known, it appears that the carrier peptides efficiently convey the antibiotic cargo to the bacterial cell surface, where it can then somehow penetrate to the cytoplasm to exert its antibacterial activity, escaping resistance mechanisms.

Only three of the *P. aeruginosa* isolates tested in this study were resistant to tobramycin, so it is necessary continue testing T-Bac7(1-35) against other clinical isolates, and try to understand the acquired mechanisms of resistance in these strains to understand how the conjugate evades them. Several possible mechanisms have been proposed, including reduced permeability, inactivating enzymes and efflux pumps (Poole, 2005). It is important to gain this insight, as it has been demonstrated that tobramycin therapy is often associated with a trend towards higher MICs and resistance among *P. aeruginosa* isolates and that long term tobramycin therapy could be a risk factor for the development of multi-drug resistant *strains* (Merlo et al., 2007). Moreover, the increased prevalence of aminoglycoside resistance in cystic fibrosis and the speed at which resistance to tobramycin is developed may be due to the fact that sub-lethal concentrations of tobramycin induce mutagenesis in *P. aeruginosa in vitro* (Nair et al., 2013). The strategy of conjugating tobramycin to PR-AMPS may possibly reverse this trend in some cases.

The conjugated molecules were then used for a further characterization of their *in vitro* antimicrobial activity against a panel of Gram-negative and Gram-positive bacteria, including

a tobramycin-resistant *Acinetobacter baumannii* clinical isolate (AB 420). Looking the table, T-Bac7(1-35) have a broad-spectrum activity against both Gram-negative and Gram-positive microorganisms. Gram-positive species are significantly more sensitive to tobramycin respect to Gram-negative but, as expected, they are quite resistant to Bac7.

Table 3.3.5. MIC values for antibiotic/PR-AMP conjugates against *P. aeruginosa strains*, compared to those of the free antibiotic and PR-AMPs.

	MIC (μM) [(a)]						
	***P. a* ATCC 27853**	**PA01**	**PA05**	**PA10**	**PA21**	**PA22**	**PA35**
Tobramycin	1	1	2	>32	>32	0.5	>32
T-Bac7(1-35)	1	1	1	2	2	1	1
Bac7(1-35)[Cys^{36}@]	32	16	4	>32	>32	4	1
T-Bac(1-15)	4	2	2	4	4	1	4
Bac7(1-15)[Cys^{16}@]	>32	>32	>32	>32	>32	>32	32

Table 3.3.6. MIC values for antibiotic/PR-AMP conjugates against *Gram-negative and Gram-positive bacterial strains*, **compared to those of the free antibiotic and PR-AMPs.**

	MIC (μM) [(a)]						
	Gram negative					**Gram positive**	
	A. baumannii		***K. pneumoniae***		***S. enteritidis***	***S. aureus***	***S. epidermidis***
	ATCC 10606	**AB420**	**ATCC 700603**	**KP#4**	**ATCC 14028**	**ATCC 25923**	**ATCC 12228**
Tobramycin	4	>32	16	16	8	0.5	0.5
T-Bac7(1-35)	2	4	4	4	1	2	1
Bac7(1-35)[Cys^{36}@]	2	2	2	4	1	>32	32
T-Bac(1-15)	2	>32	>32	>32	4	>32	1
Bac7(1-15)[Cys^{16}@]	16	32	16	32	32	>32	>32

(a) Experiments were repeated three times in triplicate and the values were obtained using micro-dilution, inoculating 2.5 * 10^5 CFU / ml in 100% Mueller-Hinton broth and maintaining the plates at 37 ° C for 20 hours. The MIC values were then evaluated by observing the turbidity of the lowest concentration at which bacterial growth was inhibited.

3.4 CONCLUSIONS

Reduced antibiotic uptake is an important and frequently observed resistance mechanism in Gram-negative bacteria. The presence of an outer membrane and the modifications they can acquire in their envelope components makes some intrinsically resistant to several classes of antibiotics. Tobramycin is an aminoglycoside antibiotic often used in the treatment of Gram-negative infections, acting intracellularly by irreversibly binding to bacterial ribosomes and disrupting protein synthesis, but it is subject to resistance development by alterations in permeability or transport.

The aim of this part of my PhD work was to design an efficient delivery system capable of internalizing tobramycin into bacteria and possibly overcome these resistance mechanisms. The idea was to conjugate it with another molecule known to be efficiently internalized in a different way. In this respect the PR-AMP Bac7(1-35) was an ideal candidate, given its capacity to efficiently internalize into Gram-negative pathogens without disrupting the bacterial membrane, and its lack of toxicity in animal models. Moreover, it targets the 70 S ribosome subunit like the antibiotic, so that the conjugate might show a mutually potentiated antimicrobial action.

I linked the antibiotic to the peptide by using a disulphide bond, which should be stable in the extracellular medium but spontaneously cleave in the reducing conditions of the bacterial cytoplasm, releasing the cargo molecule. This required protecting all the antibiotics reactive groups except for a primary hydroxyl moiety, which could then be acylated with succinic anhydride, to allow linking to a cysteine residue by an amide bond. This would then allow formation of a disulphide bond with a Cys-modified Bac7. A second, potentially simpler strategy for directly introducing a sulfhydryl group onto the primary hydroxyl was tried, but was not successful.

Before testing the activity of the antibiotic/PR-AMP conjugate, I evaluated if the two components had a synergistic effect by using a MIC checkerboard assay, and I found that they do not, but are rather indifferent one to the other. I then attempted to gain some information about how the conjugate acted by testing its antimicrobial activity against different *E.coli* strains, one of which lacked the principal PR-AMP transport system, SbmA. Unexpectedly I found that SbmA is important also for internalization of tobramycin. Nonetheless, the conjugate was quite active against an SbmA knockout mutant, suggesting it could use an

alternative transport system. Moreover, this gave me useful information about the conjugate's stability in the extracellular medium.

I then tested the conjugate against a large variety of bacteria, with particular attention to human pathogens and multidrug-resistant clinical isolates, in order to obtain further information for possible biomedical applications. Interestingly, the most promising results were observed against some *P. aeruginosa* clinical isolates, as the conjugate molecule displayed an improved antimicrobial activity compared to the single components. It appears that, despite the drug-resistance mechanism of some strains, Bac7 can somehow convey the antibiotic to and/or into the bacteria, and evading them. Furthermore, the tobramycin/Bac7 conjugate was also surprisingly active against Gram-positive pathogens that are not susceptible to the carrier peptide.

The approach of linking drug cargo to PR-AMPs is potentially applicable to other classes of currently available antibiotics, as long as they have reactive moieties that permit linking, and that can be modified without affecting the antibiotic's activity. This would allow the use of molecules that are already approved as drugs for efficacy and toxicity, and may significantly reduce times for development of these modified compounds to be used in the clinic.

In conclusion, this research project opens the possibility of chemical optimization and production of new hybrid antimicrobial molecules obtained via conjugation of a known antibiotic with PR-AMPs. These constructs should be capable of efficiently penetrating into Gram-negative bacteria species that normally represent challenging targets for many currently available antibiotics. The project produced some important preliminary and intermediate results, which will set the basis for subsequent mode-of-action, efficacy and toxicity studies in *in vitro* and animal models of infection, and may help in the recruitment of commercial partners necessary to further develop these new antimicrobials. My hope is that I may have contributed to solving the looming bacterial antibiotic resistance problem and reducing the increasing risk of uncontrolled spread of bacterial infections.

4. REFERENCES

Ageitos, J.M., Sánchez-Pérez, A., Calo-Mata, P., and Villa, T.G. (2016). Antimicrobial peptides (AMPs): Ancient compounds that represent novel weapons in the fight against bacteria. Biochem. Pharmacol.

Agerberth, B., Lee, J.Y., Bergman, T., Carlquist, M., Boman, H.G., Mutt, V., and Jörnvall, H. (1991). Amino acid sequence of PR-39. Isolation from pig intestine of a new member of the family of proline-arginine-rich antibacterial peptides. Eur. J. Biochem. *202*, 849–854.

Agerberth, B., Gunne, H., Odeberg, J., Kogner, P., Boman, H.G., and Gudmundsson, G.H. (1995). FALL-39, a putative human peptide antibiotic, is cysteine-free and expressed in bone marrow and testis. Proc. Natl. Acad. Sci. U. S. A. *92*, 195–199.

Andreu, D., and Rivas, L. (1998). Animal antimicrobial peptides: an overview. Biopolymers *47*, 415–433.

Antcheva, N., Morgera, F., Creatti, L., Vaccari, L., Pag, U., Pacor, S., Shai, Y., Sahl, H.-G., and Tossi, A. (2009). Artificial beta-defensin based on a minimal defensin template. Biochem. J. *421*, 435–447.

Arguello, J.R., Fan, C., Wang, W., and Long, M. (2007). Origination of chimeric genes through DNA-level recombination. Genome Dyn. *3*, 131–146.

Atherton, E., and Sheppard, R. (1989). Solid phase peptide synthesis: a practical approach. , Oxford, (Oxford: IRL Press).

Bals, R. (2000). Epithelial antimicrobial peptides in host defense against infection. Respir. Res. *1*, 141–150.

Baquero, F. (2001). Low-level antibacterial resistance: a gateway to clinical resistance. Drug Resist. Updat. Rev. Comment. Antimicrob. Anticancer Chemother. *4*, 93–105.

Benincasa, M., Skerlavaj, B., Gennaro, R., Pellegrini, A., and Zanetti, M. (2003). In vitro and in vivo antimicrobial activity of two alpha-helical cathelicidin peptides and of their synthetic analogs. Peptides *24*, 1723–1731.

Benincasa, M., Scocchi, M., Podda, E., Skerlavaj, B., Dolzani, L., and Gennaro, R. (2004). Antimicrobial activity of Bac7 fragments against drug-resistant clinical isolates. Peptides *25*, 2055–2061.

Benincasa, M., Scocchi, M., Pacor, S., Tossi, A., Nobili, D., Basaglia, G., Busetti, M., and Gennaro, R. (2006). Fungicidal activity of five cathelicidin peptides against clinically isolated yeasts. J. Antimicrob. Chemother. *58*, 950–959.

Benincasa, M., Pacor, S., Gennaro, R., and Scocchi, M. (2009). Rapid and Reliable Detection of Antimicrobial Peptide Penetration into Gram-Negative Bacteria Based on Fluorescence Quenching. Antimicrob. Agents Chemother. *53*, 3501–3504.

Benincasa, M., Pelillo, C., Zorzet, S., Garrovo, C., Biffi, S., Gennaro, R., and Scocchi, M. (2010). The proline-rich peptide Bac7(1-35) reduces mortality from Salmonella typhimurium in a mouse model of infection. BMC Microbiol. *10*, 178.

Boman, H.G., Agerberth, B., and Boman, A. (1993). Mechanisms of action on Escherichia coli of cecropin P1 and PR-39, two antibacterial peptides from pig intestine. Infect. Immun. *61*, 2978–2984.

Brogden, K.A. (2005). Antimicrobial peptides: pore formers or metabolic inhibitors in bacteria? Nat. Rev. Microbiol. *3*, 238–250.

Bulet, P., Dimarcq, J.L., Hetru, C., Lagueux, M., Charlet, M., Hegy, G., Van Dorsselaer, A., and Hoffmann, J.A. (1993). A novel inducible antibacterial peptide of Drosophila carries an O-glycosylated substitution. J. Biol. Chem. *268*, 14893–14897.

Cai, S., Li, Y., Wang, K., Cen, Y., Lu, H., Dong, B., Chen, Y., and Kong, J. (2016). Pathogenic Effects of Biofilm on Pseudomonas Aeruginosa Pulmonary Infection and Its Relationship to Cytokines. Med. Sci. Monit. Int. Med. J. Exp. Clin. Res. *22*, 4869–4874.

Casteels, P., Ampe, C., Riviere, L., Van Damme, J., Elicone, C., Fleming, M., Jacobs, F., and Tempst, P. (1990). Isolation and characterization of abaecin, a major antibacterial response peptide in the honeybee (Apis mellifera). Eur. J. Biochem. *187*, 381–386.

Castle, M., Nazarian, A., Yi, S.S., and Tempst, P. (1999). Lethal effects of apidaecin on Escherichia coli involve sequential molecular interactions with diverse targets. J. Biol. Chem. *274*, 32555–32564.

Cederlund, A., Gudmundsson, G.H., and Agerberth, B. (2011). Antimicrobial peptides important in innate immunity. FEBS J. *278*, 3942–3951.

Chan, Y.R., and Gallo, R.L. (1998). PR-39, a syndecan-inducing antimicrobial peptide, binds and affects p130(Cas). J. Biol. Chem. *273*, 28978–28985.

Chen, J., Guan, S.-M., Sun, W., and Fu, H. (2016). Melittin, the Major Pain-Producing Substance of Bee Venom. Neurosci. Bull. *32*, 265–272.

Cheng, Y., Prickett, M.D., Gutowska, W., Kuo, R., Belov, K., and Burt, D.W. (2015). Evolution of the avian β-defensin and cathelicidin genes. BMC Evol. Biol. *15*, 188.

Chesnokova, L.S., Slepenkov, S.V., and Witt, S.N. (2004). The insect antimicrobial peptide, L-pyrrhocoricin, binds to and stimulates the ATPase activity of both wild-type and lidless DnaK. FEBS Lett. *565*, 65–69.

Choi, K.-Y., Chow, L.N.Y., and Mookherjee, N. (2012). Cationic host defence peptides: multifaceted role in immune modulation and inflammation. J. Innate Immun. *4*, 361–370.

Christensen, B., Fink, J., Merrifield, R.B., and Mauzerall, D. (1988). Channel-forming properties of cecropins and related model compounds incorporated into planar lipid membranes. Proc. Natl. Acad. Sci. U. S. A. *85*, 5072–5076.

Coccia, C., Rinaldi, A.C., Luca, V., Barra, D., Bozzi, A., Di Giulio, A., Veerman, E.C.I., and Mangoni, M.L. (2011). Membrane interaction and antibacterial properties of two mildly

cationic peptide diastereomers, bombinins H2 and H4, isolated from Bombina skin. Eur. Biophys. J. EBJ *40*, 577–588.

Cole, A.M., Weis, P., and Diamond, G. (1997). Isolation and Characterization of Pleurocidin, an Antimicrobial Peptide in the Skin Secretions of Winter Flounder. J. Biol. Chem. *272*, 12008–12013.

Cole, A.M., Darouiche, R.O., Legarda, D., Connell, N., and Diamond, G. (2000). Characterization of a Fish Antimicrobial Peptide: Gene Expression, Subcellular Localization, and Spectrum of Activity. Antimicrob. Agents Chemother. *44*, 2039–2045.

Daley, D.O., Rapp, M., Granseth, E., Melén, K., Drew, D., and von Heijne, G. (2005). Global topology analysis of the Escherichia coli inner membrane proteome. Science *308*, 1321–1323.

Delcaru, C., Alexandru, I., Podgoreanu, P., Grosu, M., Stavropoulos, E., Chifiriuc, M.C., and Lazar, V. (2016). Microbial Biofilms in Urinary Tract Infections and Prostatitis: Etiology, Pathogenicity, and Combating strategies. Pathog. Basel Switz. *5*.

D'Este, F., Benincasa, M., Cannone, G., Furlan, M., Scarsini, M., Volpatti, D., Gennaro, R., Tossi, A., Skerlavaj, B., and Scocchi, M. (2016). Antimicrobial and host cell-directed activities of Gly/Ser-rich peptides from salmonid cathelicidins. Fish Shellfish Immunol. *59*, 456–468.

Dufourcq, J., and Faucon, J.F. (1977). Intrinsic fluorescence study of lipid-protein interactions in membrane models. Binding of melittin, an amphipathic peptide, to phospholipid vesicles. Biochim. Biophys. Acta *467*, 1–11.

Elgharably, H., Hussain, S.T., Shrestha, N.K., Blackstone, E.H., and Pettersson, G.B. (2016). Current Hypotheses in Cardiac Surgery: Biofilm in Infective Endocarditis. Semin. Thorac. Cardiovasc. Surg. *28*, 56–59.

Fellermann, K., and Stange, E.F. (2001). Defensins -- innate immunity at the epithelial frontier. Eur. J. Gastroenterol. Hepatol. *13*, 771–776.

Fernandez, D.I., Le Brun, A.P., Whitwell, T.C., Sani, M.-A., James, M., and Separovic, F. (2012). The antimicrobial peptide aurein 1.2 disrupts model membranes via the carpet mechanism. Phys. Chem. Chem. Phys. PCCP *14*, 15739–15751.

Fernández, L., Breidenstein, E.B.M., and Hancock, R.E.W. (2011). Creeping baselines and adaptive resistance to antibiotics. Drug Resist. Updat. Rev. Comment. Antimicrob. Anticancer Chemother. *14*, 1–21.

Foote, A.D., Liu, Y., Thomas, G.W.C., Vinař, T., Alföldi, J., Deng, J., Dugan, S., van Elk, C.E., Hunter, M.E., Joshi, V., et al. (2015). Convergent evolution of the genomes of marine mammals. Nat. Genet. *47*, 272–275.

Frank, R.W., Gennaro, R., Schneider, K., Przybylski, M., and Romeo, D. (1990). Amino acid sequences of two proline-rich bactenecins. Antimicrobial peptides of bovine neutrophils. J. Biol. Chem. *265*, 18871–18874.

Froy, O., and Gurevitz, M. (2003). Arthropod and mollusk defensins--evolution by exon-shuffling. Trends Genet. TIG *19*, 684–687.

Gasink, L.B., Edelstein, P.H., Lautenbach, E., Synnestvedt, M., and Fishman, N.O. (2009). Risk factors and clinical impact of Klebsiella pneumoniae carbapenemase-producing K. pneumoniae. Infect. Control Hosp. Epidemiol. *30*, 1180–1185.

Gennaro, R., Skerlavaj, B., and Romeo, D. (1989). Purification, composition, and activity of two bactenecins, antibacterial peptides of bovine neutrophils. Infect. Immun. *57*, 3142–3146.

Gennaro, R., Zanetti, M., Benincasa, M., Podda, E., and Miani, M. (2002). Pro-rich antimicrobial peptides from animals: structure, biological functions and mechanism of action. Curr. Pharm. Des. *8*, 763–778.

Ghiselli, R., Giacometti, A., Cirioni, O., Circo, R., Mocchegiani, F., Skerlavaj, B., D'Amato, G., Scalise, G., Zanetti, M., and Saba, V. (2003). Neutralization of endotoxin in vitro and in vivo by Bac7(1-35), a proline-rich antibacterial peptide. Shock Augusta Ga *19*, 577–581.

Giangaspero, A., Sandri, L., and Tossi, A. (2001). Amphipathic α helical antimicrobial peptides. Eur. J. Biochem. *268*, 5589–5600.

Glazebrook, J., Ichige, A., and Walker, G.C. (1993). A Rhizobium meliloti homolog of the Escherichia coli peptide-antibiotic transport protein SbmA is essential for bacteroid development. Genes Dev. *7*, 1485–1497.

Guida, F., Benincasa, M., Zahariev, S., Scocchi, M., Berti, F., Gennaro, R., and Tossi, A. (2015). Effect of size and N-terminal residue characteristics on bacterial cell penetration and antibacterial activity of the proline-rich peptide Bac7. J. Med. Chem. *58*, 1195–1204.

Hale, J.D.F., and Hancock, R.E.W. (2007). Alternative mechanisms of action of cationic antimicrobial peptides on bacteria. Expert Rev. Anti Infect. Ther. *5*, 951–959.

Hancock, R.E., and Diamond, G. (2000). The role of cationic antimicrobial peptides in innate host defences. Trends Microbiol. *8*, 402–410.

Hancock, R.E.W., Brown, K.L., and Mookherjee, N. (2006). Host defence peptides from invertebrates--emerging antimicrobial strategies. Immunobiology *211*, 315–322.

Hao, X., Yang, H., Wei, L., Yang, S., Zhu, W., Ma, D., Yu, H., and Lai, R. (2012). Amphibian cathelicidin fills the evolutionary gap of cathelicidin in vertebrate. Amino Acids *43*, 677–685.

Harwig, S.S., Kokryakov, V.N., Swiderek, K.M., Aleshina, G.M., Zhao, C., and Lehrer, R.I. (1995). Prophenin-1, an exceptionally proline-rich antimicrobial peptide from porcine leukocytes. FEBS Lett. *362*, 65–69.

Huang, H.J., Ross, C.R., and Blecha, F. (1997). Chemoattractant properties of PR-39, a neutrophil antibacterial peptide. J. Leukoc. Biol. *61*, 624–629.

Huttner, K.M., Lambeth, M.R., Burkin, H.R., Burkin, D.J., and Broad, T.E. (1998). Localization and genomic organization of sheep antimicrobial peptide genes. Gene *206*, 85–91.

Janeway, C.A. (2001). How the immune system protects the host from infection. Microbes Infect. *3*, 1167–1171.

Janeway, C.A., and Medzhitov, R. (2002). Innate immune recognition. Annu. Rev. Immunol. *20*, 197–216.

Kanwar, I.L., Sah, A.K., and Suresh, P.K. (2016). Biofilm-mediated Antibiotic-resistant Oral Bacterial. Curr. Pharm. Des.

Kavanagh, K., and Dowd, S. (2004). Histatins: antimicrobial peptides with therapeutic potential. J. Pharm. Pharmacol. *56*, 285–289.

Kharami, A., Bibi, Z., Nielsen, H., Høiby, N., and Döring, G. (1989). Effect of Pseudomonas aeruginosa rhamnolipid on human neutrophil and monocyte function. APMIS Acta Pathol. Microbiol. Immunol. Scand. *97*, 1068–1072.

Kokryakov, V.N., Harwig, S.S., Panyutich, E.A., Shevchenko, A.A., Aleshina, G.M., Shamova, O.V., Korneva, H.A., and Lehrer, R.I. (1993). Protegrins: leukocyte antimicrobial peptides that combine features of corticostatic defensins and tachyplesins. FEBS Lett. *327*, 231–236.

Kragol, G., Lovas, S., Varadi, G., Condie, B.A., Hoffmann, R., and Otvos, L. (2001). The antibacterial peptide pyrrhocoricin inhibits the ATPase actions of DnaK and prevents chaperone-assisted protein folding. Biochemistry (Mosc.) *40*, 3016–3026.

Krizsan, A., Volke, D., Weinert, S., Sträter, N., Knappe, D., and Hoffmann, R. (2014). Insect-derived proline-rich antimicrobial peptides kill bacteria by inhibiting bacterial protein translation at the 70S ribosome. Angew. Chem. Int. Ed Engl. *53*, 12236–12239.

Krizsan, A., Knappe, D., and Hoffmann, R. (2015). Influence of the yjiL-mdtM Gene Cluster on the Antibacterial Activity of Proline-Rich Antimicrobial Peptides Overcoming Escherichia coli Resistance Induced by the Missing SbmA Transporter System. Antimicrob. Agents Chemother. *59*, 5992–5998.

Kuipers, B.J.H., and Gruppen, H. (2007). Prediction of molar extinction coefficients of proteins and peptides using UV absorption of the constituent amino acids at 214 nm to enable quantitative reverse phase high-performance liquid chromatography-mass spectrometry analysis. J. Agric. Food Chem. *55*, 5445–5451.

Lai, Y., and Gallo, R.L. (2009). AMPed up immunity: how antimicrobial peptides have multiple roles in immune defense. Trends Immunol. *30*, 131–141.

Lamers, R.P., Cavallari, J.F., and Burrows, L.L. (2013). The efflux inhibitor phenylalanine-arginine beta-naphthylamide (PAβN) permeabilizes the outer membrane of gram-negative bacteria. PloS One *8*, e60666.

Larrick, J.W., Hirata, M., Shimomoura, Y., Yoshida, M., Zheng, H., Zhong, J., and Wright, S.C. (1993). Antimicrobial activity of rabbit CAP18-derived peptides. Antimicrob. Agents Chemother. *37*, 2534–2539.

Laviña, M., Pugsley, A.P., and Moreno, F. (1986). Identification, mapping, cloning and characterization of a gene (sbmA) required for microcin B17 action on Escherichia coli K12. J. Gen. Microbiol. *132*, 1685–1693.

Lee, J.Y., Yang, S.-T., Lee, S.K., Jung, H.H., Shin, S.Y., Hahm, K.-S., and Kim, J.I. (2008). Salt-resistant homodimeric bactenecin, a cathelicidin-derived antimicrobial peptide. FEBS J. *275*, 3911–3920.

Lehrer, R.I. (2007). Multispecific myeloid defensins. Curr. Opin. Hematol. *14*, 16–21.

LeVier, K., Phillips, R.W., Grippe, V.K., Roop, R.M., and Walker, G.C. (2000). Similar requirements of a plant symbiont and a mammalian pathogen for prolonged intracellular survival. Science *287*, 2492–2493.

Liebscher, M., and Roujeinikova, A. (2009). Allosteric Coupling between the Lid and Interdomain Linker in DnaK Revealed by Inhibitor Binding Studies. J. Bacteriol. *191*, 1456–1462.

Lindblad-Toh, K., Garber, M., Zuk, O., Lin, M.F., Parker, B.J., Washietl, S., Kheradpour, P., Ernst, J., Jordan, G., Mauceli, E., et al. (2011). A high-resolution map of human evolutionary constraint using 29 mammals. Nature *478*, 476–482.

Lomovskaya, O., and Watkins, W. (2001). Inhibition of efflux pumps as a novel approach to combat drug resistance in bacteria. J. Mol. Microbiol. Biotechnol. *3*, 225–236.

Mamishi, S., Moradkhani, S., Mahmoudi, S., Hosseinpour-Sadeghi, R., and Pourakbari, B. (2014). Penicillin-Resistant trend of Streptococcus pneumoniae in Asia: A systematic review. Iran. J. Microbiol. *6*, 198–210.

Mancia, A., Lundqvist, M.L., Romano, T.A., Peden-Adams, M.M., Fair, P.A., Kindy, M.S., Ellis, B.C., Gattoni-Celli, S., McKillen, D.J., Trent, H.F., et al. (2007). A dolphin peripheral blood leukocyte cDNA microarray for studies of immune function and stress reactions. Dev. Comp. Immunol. *31*, 520–529.

Mangoni, M.L. (2011). Host-defense peptides: from biology to therapeutic strategies. Cell. Mol. Life Sci. CMLS *68*, 2157–2159.

Mardirossian, M., Grzela, R., Giglione, C., Meinnel, T., Gennaro, R., Mergaert, P., and Scocchi, M. (2014). The host antimicrobial peptide Bac71-35 binds to bacterial ribosomal proteins and inhibits protein synthesis. Chem. Biol. *21*, 1639–1647.

Marlow, V.L., Haag, A.F., Kobayashi, H., Fletcher, V., Scocchi, M., Walker, G.C., and Ferguson, G.P. (2009). Essential role for the BacA protein in the uptake of a truncated eukaryotic peptide in Sinorhizobium meliloti. J. Bacteriol. *191*, 1519–1527.

Mattiuzzo, M., Bandiera, A., Gennaro, R., Benincasa, M., Pacor, S., Antcheva, N., and Scocchi, M. (2007). Role of the Escherichia coli SbmA in the antimicrobial activity of proline-rich peptides. Mol. Microbiol. *66*, 151–163.

Matzinger, P. (2002). The Danger Model: A Renewed Sense of Self. Science *296*, 301–305.

McConnell, M.J., Actis, L., and Pachón, J. (2013). Acinetobacter baumannii: human infections, factors contributing to pathogenesis and animal models. FEMS Microbiol. Rev. *37*, 130–155.

Medzhitov, R. (2007). Recognition of microorganisms and activation of the immune response. Nature *449*, 819–826.

Meletiadis, J., Pournaras, S., Roilides, E., and Walsh, T.J. (2010). Defining fractional inhibitory concentration index cutoffs for additive interactions based on self-drug additive combinations, Monte Carlo simulation analysis, and in vitro-in vivo correlation data for antifungal drug combinations against Aspergillus fumigatus. Antimicrob. Agents Chemother. *54*, 602–609.

Merlo, C.A., Boyle, M.P., Diener-West, M., Marshall, B.C., Goss, C.H., and Lechtzin, N. (2007). Incidence and risk factors for multiple antibiotic-resistant Pseudomonas aeruginosa in cystic fibrosis. Chest *132*, 562–568.

Michael, K., Wang, H., and Tor, Y. (1999). Enhanced RNA binding of dimerized aminoglycosides. Bioorg. Med. Chem. *7*, 1361–1371.

Mookherjee, N., and Hancock, R.E.W. (2007). Cationic host defence peptides: innate immune regulatory peptides as a novel approach for treating infections. Cell. Mol. Life Sci. CMLS *64*, 922–933.

Morey, J.S., Neely, M.G., Lunardi, D., Anderson, P.E., Schwacke, L.H., Campbell, M., and Van Dolah, F.M. (2016). RNA-Seq analysis of seasonal and individual variation in blood transcriptomes of healthy managed bottlenose dolphins. BMC Genomics *17*, 720.

Morikawa, N., Hagiwara, K., and Nakajima, T. (1992). Brevinin-1 and -2, unique antimicrobial peptides from the skin of the frog, Rana brevipoda porsa. Biochem. Biophys. Res. Commun. *189*, 184–190.

Mylonakis, E., Podsiadlowski, L., Muhammed, M., and Vilcinskas, A. (2016). Diversity, evolution and medical applications of insect antimicrobial peptides. Philos. Trans. R. Soc. Lond. B. Biol. Sci. *371*.

Nair, C.G., Chao, C., Ryall, B., and Williams, H.D. (2013). Sub-lethal concentrations of antibiotics increase mutation frequency in the cystic fibrosis pathogen Pseudomonas aeruginosa. Lett. Appl. Microbiol. *56*, 149–154.

Nakamura, T., Furunaka, H., Miyata, T., Tokunaga, F., Muta, T., Iwanaga, S., Niwa, M., Takao, T., and Shimonishi, Y. (1988). Tachyplesin, a class of antimicrobial peptide from the hemocytes of the horseshoe crab (Tachypleus tridentatus). Isolation and chemical structure. J. Biol. Chem. *263*, 16709–16713.

Nikaido, H., and Takatsuka, Y. (2009). Mechanisms of RND multidrug efflux pumps. Biochim. Biophys. Acta *1794*, 769–781.

Nikaido, M., Rooney, A.P., and Okada, N. (1999). Phylogenetic relationships among cetartiodactyls based on insertions of short and long interpersed elements: Hippopotamuses are the closest extant relatives of whales. Proc. Natl. Acad. Sci. U. S. A. *96*, 10261–10266.

Oren, Z., and Shai, Y. (1998). Mode of action of linear amphipathic alpha-helical antimicrobial peptides. Biopolymers *47*, 451–463.

Otvos, L., O, I., Rogers, M.E., Consolvo, P.J., Condie, B.A., Lovas, S., Bulet, P., and Blaszczyk-Thurin, M. (2000). Interaction between heat shock proteins and antimicrobial peptides. Biochemistry (Mosc.) *39*, 14150–14159.

Park, C.B., Yi, K.S., Matsuzaki, K., Kim, M.S., and Kim, S.C. (2000). Structure-activity analysis of buforin II, a histone H2A-derived antimicrobial peptide: the proline hinge is responsible for the cell-penetrating ability of buforin II. Proc. Natl. Acad. Sci. U. S. A. *97*, 8245–8250.

Podda, E., Benincasa, M., Pacor, S., Micali, F., Mattiuzzo, M., Gennaro, R., and Scocchi, M. (2006). Dual mode of action of Bac7, a proline-rich antibacterial peptide. Biochim. Biophys. Acta *1760*, 1732–1740.

Pompilio, A., Crocetta, V., Scocchi, M., Pomponio, S., Di Vincenzo, V., Mardirossian, M., Gherardi, G., Fiscarelli, E., Dicuonzo, G., Gennaro, R., et al. (2012). Potential novel therapeutic strategies in cystic fibrosis: antimicrobial and anti-biofilm activity of natural and designed α-helical peptides against Staphylococcus aureus, Pseudomonas aeruginosa, and Stenotrophomonas maltophilia. BMC Microbiol. *12*, 145.

Poole, K. (2005). Aminoglycoside resistance in Pseudomonas aeruginosa. Antimicrob. Agents Chemother. *49*, 479–487.

Pränting, M., Negrea, A., Rhen, M., and Andersson, D.I. (2008). Mechanism and fitness costs of PR-39 resistance in Salmonella enterica serovar Typhimurium LT2. Antimicrob. Agents Chemother. *52*, 2734–2741.

Price, S.A., Bininda-Emonds, O.R.P., and Gittleman, J.L. (2005). A complete phylogeny of the whales, dolphins and even-toed hoofed mammals (Cetartiodactyla). Biol. Rev. Camb. Philos. Soc. *80*, 445–473.

Purrello, S.M., Garau, J., Giamarellos, E., Mazzei, T., Pea, F., Soriano, A., and Stefani, S. (2016). Methicillin-resistant Staphylococcus aureus infections: A review of the currently available treatment options. J. Glob. Antimicrob. Resist. *7*, 178–186.

Qian, S., Wang, W., Yang, L., and Huang, H.W. (2008). Structure of transmembrane pore induced by Bax-derived peptide: evidence for lipidic pores. Proc. Natl. Acad. Sci. U. S. A. *105*, 17379–17383.

Ratjen, F., Brockhaus, F., and Angyalosi, G. (2009). Aminoglycoside therapy against Pseudomonas aeruginosa in cystic fibrosis: a review. J. Cyst. Fibros. Off. J. Eur. Cyst. Fibros. Soc. *8*, 361–369.

Rice, A., Liu, Y., Michaelis, M.L., Himes, R.H., Georg, G.I., and Audus, K.L. (2005). Chemical modification of paclitaxel (Taxol) reduces P-glycoprotein interactions and increases permeation across the blood-brain barrier in vitro and in situ. J. Med. Chem. *48*, 832–838.

Rieg, S., Huth, A., Kalbacher, H., and Kern, W.V. (2009). Resistance against antimicrobial peptides is independent of Escherichia coli AcrAB, Pseudomonas aeruginosa MexAB and Staphylococcus aureus NorA efflux pumps. Int. J. Antimicrob. Agents *33*, 174–176.

Risso, A., Zanetti, M., and Gennaro, R. (1998). Cytotoxicity and apoptosis mediated by two peptides of innate immunity. Cell. Immunol. *189*, 107–115.

Romeo, D., Skerlavaj, B., Bolognesi, M., and Gennaro, R. (1988). Structure and bactericidal activity of an antibiotic dodecapeptide purified from bovine neutrophils. J. Biol. Chem. *263*, 9573–9575.

Runti, G., Lopez Ruiz, M. del C., Stoilova, T., Hussain, R., Jennions, M., Choudhury, H.G., Benincasa, M., Gennaro, R., Beis, K., and Scocchi, M. (2013). Functional characterization of SbmA, a bacterial inner membrane transporter required for importing the antimicrobial peptide Bac7(1-35). J. Bacteriol. *195*, 5343–5351.

Rus, H., Cudrici, C., and Niculescu, F. (2005). The role of the complement system in innate immunity. Immunol. Res. *33*, 103–112.

Salomón, R.A., and Farías, R.N. (1995). The peptide antibiotic microcin 25 is imported through the TonB pathway and the SbmA protein. J. Bacteriol. *177*, 3323–3325.

Sang, Y., Ortega, M.T., Rune, K., Xiau, W., Zhang, G., Soulages, J.L., Lushington, G.H., Fang, J., Williams, T.D., Blecha, F., et al. (2007). Canine cathelicidin (K9CATH). Dev. Comp. Immunol. *31*, 1278–1296.

Sawa, T., Shimizu, M., Moriyama, K., and Wiener-Kronish, J.P. (2014). Association between Pseudomonas aeruginosa type III secretion, antibiotic resistance, and clinical outcome: a review. Crit. Care Lond. Engl. *18*, 668.

Scocchi, M., Skerlavaj, B., Romeo, D., and Gennaro, R. (1992). Proteolytic cleavage by neutrophil elastase converts inactive storage proforms to antibacterial bactenecins. Eur. J. Biochem. *209*, 589–595.

Scocchi, M., Romeo, D., and Zanetti, M. (1994). Molecular cloning of Bac7, a proline- and arginine-rich antimicrobial peptide from bovine neutrophils. FEBS Lett. *352*, 197–200.

Scocchi, M., Wang, S., Gennaro, R., and Zanetti, M. (1998). Cloning and analysis of a transcript derived from two contiguous genes of the cathelicidin family. Biochim. Biophys. Acta *1398*, 393–396.

Scocchi, M., Mattiuzzo, M., Benincasa, M., Antcheva, N., Tossi, A., and Gennaro, R. (2008). Investigating the mode of action of proline-rich antimicrobial peptides using a genetic approach: a tool to identify new bacterial targets amenable to the design of novel antibiotics. Methods Mol. Biol. Clifton NJ *494*, 161–176.

Scocchi, M., Pallavicini, A., Salgaro, R., Bociek, K., and Gennaro, R. (2009). The salmonid cathelicidins: a gene family with highly varied C-terminal antimicrobial domains. Comp. Biochem. Physiol. B Biochem. Mol. Biol. *152*, 376–381.

Scocchi, M., Lüthy, C., Decarli, P., Mignogna, G., Christen, P., and Gennaro, R. (2009). The Proline-rich Antibacterial Peptide Bac7 Binds to and Inhibits in vitro the Molecular Chaperone DnaK. Int. J. Pept. Res. Ther. *15*, 147–155.

Scocchi, M., Tossi, A., and Gennaro, R. (2011). Proline-rich antimicrobial peptides: converging to a non-lytic mechanism of action. Cell. Mol. Life Sci. CMLS *68*, 2317–2330.

Scocchi, M., Mardirossian, M., Runti, G., and Benincasa, M. (2016). Non-Membrane Permeabilizing Modes of Action of Antimicrobial Peptides on Bacteria. Curr. Top. Med. Chem. *16*, 76–88.

Seefeldt, A.C., Nguyen, F., Antunes, S., Pérébaskine, N., Graf, M., Arenz, S., Inampudi, K.K., Douat, C., Guichard, G., Wilson, D.N., et al. (2015). The proline-rich antimicrobial

peptide Onc112 inhibits translation by blocking and destabilizing the initiation complex. Nat. Struct. Mol. Biol. *22*, 470–475.

Selsted, M.E., Novotny, M.J., Morris, W.L., Tang, Y.Q., Smith, W., and Cullor, J.S. (1992). Indolicidin, a novel bactericidal tridecapeptide amide from neutrophils. J. Biol. Chem. *267*, 4292–4295.

Shamova, O., Brogden, K.A., Zhao, C., Nguyen, T., Kokryakov, V.N., and Lehrer, R.I. (1999). Purification and Properties of Proline-Rich Antimicrobial Peptides from Sheep and Goat Leukocytes. Infect. Immun. *67*, 4106–4111.

Simunić, J., Petrov, D., Bouceba, T., Kamech, N., Benincasa, M., and Juretić, D. (2014). Trichoplaxin — A new membrane-active antimicrobial peptide from placozoan cDNA. Biochim. Biophys. Acta BBA - Biomembr. *1838*, 1430–1438.

Skerlavaj, B., Gennaro, R., Bagella, L., Merluzzi, L., Risso, A., and Zanetti, M. (1996). Biological Characterization of Two Novel Cathelicidin-derived Peptides and Identification of Structural Requirements for Their Antimicrobial and Cell Lytic Activities. J. Biol. Chem. *271*, 28375–28381.

Skerlavaj, B., Benincasa, M., Risso, A., Zanetti, M., and Gennaro, R. (1999). SMAP-29: a potent antibacterial and antifungal peptide from sheep leukocytes. FEBS Lett. *463*, 58–62.

Skerlavaj, B., Scocchi, M., Gennaro, R., Risso, A., and Zanetti, M. (2001). Structural and functional analysis of horse cathelicidin peptides. Antimicrob. Agents Chemother. *45*, 715–722.

Steiner, H., Hultmark, D., Engström, A., Bennich, H., and Boman, H.G. (2009). Sequence and specificity of two antibacterial proteins involved in insect immunity. Nature 292: 246-248. 1981. J. Immunol. Baltim. Md 1950 *182*, 6635–6637.

Storici, P., Scocchi, M., Tossi, A., Gennaro, R., and Zanetti, M. (1994). Chemical synthesis and biological activity of a novel antibacterial peptide deduced from a pig myeloid cDNA. FEBS Lett. *337*, 303–307.

Tang, Y.Q., Yuan, J., Osapay, G., Osapay, K., Tran, D., Miller, C.J., Ouellette, A.J., and Selsted, M.E. (1999). A cyclic antimicrobial peptide produced in primate leukocytes by the ligation of two truncated alpha-defensins. Science *286*, 498–502.

Tomasinsig, L., and Zanetti, M. (2005). The cathelicidins--structure, function and evolution. Curr. Protein Pept. Sci. *6*, 23–34.

Tomasinsig, L., Skerlavaj, B., Papo, N., Giabbai, B., Shai, Y., and Zanetti, M. (2006). Mechanistic and Functional Studies of the Interaction of a Proline-rich Antimicrobial Peptide with Mammalian Cells. J. Biol. Chem. *281*, 383–391.

Tomasinsig, L., De Conti, G., Skerlavaj, B., Piccinini, R., Mazzilli, M., D'Este, F., Tossi, A., and Zanetti, M. (2010). Broad-spectrum activity against bacterial mastitis pathogens and activation of mammary epithelial cells support a protective role of neutrophil cathelicidins in bovine mastitis. Infect. Immun. *78*, 1781–1788.

Top, J., Willems, R., and Bonten, M. (2008). Emergence of CC17 Enterococcus faecium: from commensal to hospital-adapted pathogen. FEMS Immunol. Med. Microbiol. *52*, 297–308.

Tossi, A., Sandri, L., and Giangaspero, A. (2000). Amphipathic, alpha-helical antimicrobial peptides. Biopolymers *55*, 4–30.

Tossi, A., D'Este, F., Skerlavaj, B., and Gennaro, R. (2017). Structural and Functional Diversity of Cathelicidins. In Antimicrobial Peptides, Discovery, Design and Novel Therapeutic Strategies, Wang, ed. (GABI Press), p. (in press).

Uzzell, T., Stolzenberg, E.D., Shinnar, A.E., and Zasloff, M. (2003). Hagfish intestinal antimicrobial peptides are ancient cathelicidins. Peptides *24*, 1655–1667.

Vázquez-Espinosa, E., Girón, R.M., Gómez-Punter, R.M., García-Castillo, E., Valenzuela, C., Cisneros, C., Zamora, E., García-Pérez, F.J., and Ancochea, J. (2015). Long-term safety and efficacy of tobramycin in the management of cystic fibrosis. Ther. Clin. Risk Manag. *11*, 407–415.

Waddell, W.J. (1956). A simple ultraviolet spectrophotometric method for the determination of protein. J. Lab. Clin. Med. *48*, 311–314.

Wang, Y., Hong, J., Liu, X., Yang, H., Liu, R., Wu, J., Wang, A., Lin, D., and Lai, R. (2008). Snake cathelicidin from Bungarus fasciatus is a potent peptide antibiotics. PloS One *3*, e3217.

Xhindoli, D., Pacor, S., Benincasa, M., Scocchi, M., Gennaro, R., and Tossi, A. (2016). The human cathelicidin LL-37--A pore-forming antibacterial peptide and host-cell modulator. Biochim. Biophys. Acta *1858*, 546–566.

Yacoub, H.A., Elazzazy, A.M., Mahmoud, M.M., Baeshen, M.N., Al-Maghrabi, O.A., Alkarim, S., Ahmed, E.S., Almehdar, H.A., and Uversky, V.N. (2016). Chicken cathelicidins as potent intrinsically disordered biocides with antimicrobial activity against infectious pathogens. Dev. Comp. Immunol. *65*, 8–24.

Yang, L., Harroun, T.A., Weiss, T.M., Ding, L., and Huang, H.W. (2001). Barrel-stave model or toroidal model? A case study on melittin pores. Biophys. J. *81*, 1475–1485.

Yeaman, M.R., and Yount, N.Y. (2007). Unifying themes in host defence effector polypeptides. Nat. Rev. Microbiol. *5*, 727–740.

Yorgey, P., Lee, J., Kördel, J., Vivas, E., Warner, P., Jebaratnam, D., and Kolter, R. (1994). Posttranslational modifications in microcin B17 define an additional class of DNA gyrase inhibitor. Proc. Natl. Acad. Sci. U. S. A. *91*, 4519–4523.

Zanetti, M. (2005). The role of cathelicidins in the innate host defenses of mammals. Curr. Issues Mol. Biol. *7*, 179–196.

Zanetti, M., Gennaro, R., and Romeo, D. (1995). Cathelicidins: a novel protein family with a common proregion and a variable C-terminal antimicrobial domain. FEBS Lett. *374*, 1–5.

Zanetti, M., Gennaro, R., Scocchi, M., and Skerlavaj, B. (2000). Structure and biology of cathelicidins. Adv. Exp. Med. Biol. *479*, 203–218.

Zarember, K.A., Katz, S.S., Tack, B.F., Doukhan, L., Weiss, J., and Elsbach, P. (2002). Host Defense Functions of Proteolytically Processed and Parent (Unprocessed) Cathelicidins of Rabbit Granulocytes. Infect. Immun. *70*, 569–576.

Zasloff, M. (1987). Magainins, a class of antimicrobial peptides from Xenopus skin: isolation, characterization of two active forms, and partial cDNA sequence of a precursor. Proc. Natl. Acad. Sci. U. S. A. *84*, 5449–5453.

Zasloff, M. (2002). Antimicrobial peptides of multicellular organisms. Nature *415*, 389–395.

Zasloff, M. (2011). Observations on the remarkable (and mysterious) wound-healing process of the bottlenose dolphin. J. Invest. Dermatol. *131*, 2503–2505.

Zhang, H., Xia, X., Han, F., Jiang, Q., Rong, Y., Song, D., and Wang, Y. (2015). Cathelicidin-BF, a Novel Antimicrobial Peptide from Bungarus fasciatus, Attenuates Disease in a Dextran Sulfate Sodium Model of Colitis. Mol. Pharm. *12*, 1648–1661.

Zhao, H., Gan, T.-X., Liu, X.-D., Jin, Y., Lee, W.-H., Shen, J.-H., and Zhang, Y. (2008). Identification and characterization of novel reptile cathelicidins from elapid snakes. Peptides *29*, 1685–1691.

Zhu, S. (2008). Discovery of six families of fungal defensin-like peptides provides insights into origin and evolution of the CSalphabeta defensins. Mol. Immunol. *45*, 828–838.